FLIP-THROUGH EFFECT AND BENDING OF PVDF SHALLOW SPHERICAL PIEZO-ELECTRICAL SWITCHES

by

JOSHUA MICHAEL SZULCZEWSKI, P.E.

A dissertation submitted to the

Graduate School – New Brunswick

Rutgers, the State University of New Jersey

in partial fulfillment of the requirements

for the degree of

Doctor of Philosophy

Graduate Program in Civil and Environmental Engineering

written under the direction of

Professor Yook-Kong Yong, P.E.

and approved by

_____

_____

_____

_____

New Brunswick, New Jersey

May 2016

ABSTRACT OF THE DISSERTATION

FLIP-THROUGH EFFECT AND BENDING OF PVDF SHALLOW SPHERICAL PIEZO-ELECTRICAL SWITCHES

By: JOSHUA MICHAEL SZULCZEWSKI, P.E.

Dissertation Director:

Dr. Yook-Kong Yong, P.E.

The use of piezo-electrical devices is becoming more widespread. The principle of such devices was discovered to aid in the study of radiation. The piezo-device was found to give off an electrical charge when it was depressed. A year later, researchers also realized that not only could this device give off electrical charge, but also, if an electric charge was released into it, that it would turn that electrical charge into mechanical work.

There is also study of a phenomenon called the flip effect. This effect occurs when a structure is created by fusing two materials together. For the remainder of this thesis we will use the term *bi-material* to describe such a structure. The flip-effect occurs when a solid structure is heated (or freeze) whereby energy is either added or removed. As a result, the structure becomes

unstable in its current configuration and transitions to a new stable state. This happens because there is internal moment within the structure that gives it rigidity.

This thesis looks at the equations that are related to energy for what causes the structure to become unstable and then flip to the other side. Another aspect that was looked at was how COMSOL models also demonstrate that such a structure can be created. The energy equations are related to theses COMSOL models. From the model information a structure is then built from manufactured parts.

When the researcher was looking for materials to experiment piezo-electrical polymers were found. These polymers are quite new and not widely utilized at present. They have been primarily used in speaker systems. Previously, speaker systems were made of quartz, paper, or other types of vibrating materials. These polymers were selected as a basis for this thesis since they are exceptionally flexible and easy to mold.

Experiments have been conducted with piezo-polymers, with results that are similar to the COMSOL and the derived equations. It was found that a fairly reliable switch can be created using the polymers; however, there are questions of cost and design constraints that have to be looked at on a case-by-case basis.

Dedication

Dedicated to all those

people great and small

who helped me complete

my advanced degrees

Table of Contents

List of Figures

List of Variables Used in Thesis

β = angle of the normal of the shallow shell

t_p = thickness of plastic layer

t_m = thickness of piezo-layer

t_t = total thickness of shell

R = radius of hemisphere

r = radius of disk

u,v,w = deflections in X, Y, and Z directions respectively

ϵ_x = strain in X direction

ϵ_y = strain in Y direction

ϵ_{RR} = strain in radius direction

$\epsilon_{\theta\theta}$ = strain in angle direction

$\gamma_{r\theta}$ = shear stress in angle direction

E = average elastic modulus

α = average coefficient of expansion

V = voltage

ω = change in temperature

T_f = temperature final

T_i = temperature initial

ν = Poisson's ratio

Q = element of the stiffness matrix

d = dielectric constant

f = stress function

κ = curvature element

Θ = angle on disk

ϵ_X = differential with respect to how many variables

$\overline{\epsilon_{RR}}$ = strain in radius direction with curvature correction to it (same for the other strain and shearing)

a = distance from north pole to origin

σ_{rr} = stress in radial direction

$\sigma_{\Theta\Theta}$ = stress in angular direction

$\gamma_{\Theta r}$ = shear stress throughout

F_{rr} = force in radial direction

$F_{\Theta\Theta}$ = force in angular direction

$F_{\Theta r}$ = force in shear direction

M_{rr} = moment in radial direction

$M_{\Theta\Theta}$ = moment in angular direction

$M_{\Theta r}$ = Moment in shear direction

N_{0r} = critical buckling load

q = outside pressure (assumed 0 for rest of thesis)

List of Equations

Chapter 1

Introduction

The original conception of this thesis was inspired by the problem of how to make a piezo-electric element change shape and hold that shape for an indefinite amount of time. Most piezo-electric elements that have thus far been created do not hold their shape for an extended amount of time. The main function of a piezo-electric element is to give off an electric charge when its shape is changed, and then to return to its original shape. This application is mostly used in push buttons where one depresses a button: an electrical signal is then sent off to a controller. This application will be explained in more detail in the Background Information section below.

What was then thought of if it is possible to get a piezo-electrical element to change its shape. The next question was how to get the element to hold that shape.

1. Piezo-electrical button operation

A piezo-electrical button is a button activated either by human intervention or by a lever that pushes it. First, the lever applies a force to the piezo-electrical button. Due to the force of the lever on the piezo-electrical button, the button becomes depressed. The depression of the button causes the piezo-electrical element to change shape. When the button changes shape, it builds an electrical potential in it due to this reshaping. Once the element begins to return to the original shape, a charge is released via an electrode connected to a system that then allows the charge to travel throughout it and execute whatever task the button was designed for. This charge also travels to a device that is hooked up to the system in order to monitor this charge. Once this charge reaches the

device's controller, it then activates whatever device(s) the controller is hooked up to. See figure 3-1 below for a more complete description.

A piezo-electrical device can also work in the opposite direction whereby an electrical charge is introduced into the system instead. This electrical charge goes through a wire that is hooked up to the piezo-device, resulting in the reshaping of the piezo-device. This reshaping is mechanical energy that is released to a lever that then activates whatever it was designed to activate.

A substitute for the lever is a change in temperature. The change in temperature causes the element to be reshaped due to the resulting expansion or contraction. When the element is reshaped, it stores electricity that, at a certain point, will be released to the outside, whereupon the element returns to its original shape.

In summary, a piezo-electrical element is used to either convert electrical energy into mechanical energy or vice versa.

2. Why the piezo-button is important for this thesis

The piezo-button is important for this thesis because of the fact it can be reshaped. One of the things that has not yet been studied is whether a piezo-element can hold its own prime shape when it is activated. The prime shape is the shape that a piezo-electric element takes on when a charge is introduced into it. This means that, given an amount of electricity or heatflux/cooling flux that is introduced to the system, the system then is activated and changes shape.

3. Piezo-polymer versus piezo-ceramic

Information obtained from sellers of piezo-electric products indicates that these products come in either a film shape or a ceramic shape. The film is a very thin element that is easily bendable. The ceramic is very rigid and does not allow for much bending of the element. A film element can be bent very far using very little force, while the ceramic only bends less than half of one millimeter for every 100 millimeters of length. The ceramic disks are very rigid and do not move much. This information indicates that the element to be preferred is the piezo-electrical polymer film.

4. Applications

Two applications were examined for this thesis. One application was the tiny electrical switches that power up and power down electronic devices such as televisions and computers. The research proved that a tiny switch would be capable of replacing the current plunger design used for many devices. It would take up roughly a third of the space that is now used by on and off plungers for such devices. The other application that was examined was for an electric transformer switch.

5. Next Steps

To improve this switch application further, it will be necessary to look into different available materials and to investigate others that might not be on the market yet. This thesis surveyed what was on the market today; however, new materials are continuously being invented, and some potentially effective materials are not yet being manufactured in large quantities.

Chapter 2

Background Information

This section contains useful background information from various resources consisting of journal articles and earlier works. It also contains information on the original developers of the phenomenon. This section also surveys piezo-products currently being produced and touches upon some of their applications. Lastly, an overview of the current state of the industry is provided.

A. Earlier Works

This first section describes preliminary work that preceded the first piezo-experiments were done and the formulation of the equations. One of the first researchers was John Harrison, an 18th century English clockmaker who developed the first bi-material strips used primarily for temperature control in clocks. Pierre Curie is also mentioned, as he was the first to discover the piezo-electric effect. Unfortunately, not much info is available on this event, and sources are very vague, as this was Curie's earliest work and was conducted when he was only 21. While he is credited with this discovery, most works mention only his later experiments with radioactivity, the primary focus of his career. Later, in his absence, his wife and daughter continued this work. Sometime later in Japan, two scientists working in collaboration, Fukada and Kawai, ([31]) found that Curie's piezo-electric effect in quartz also translated into organic materials, being first discovered in bone. ([31]) The investigations were continued by medical researchers, who found certain other crystalline organics displaying piezo-qualities. ([33]) The above info on previous

work in the field leads to the present day lab set-up to test this switch on. Now the thesis moves into the literature search on piezo-electric switches.

1. Bi-material Strips

To understand piezo-electric elements and in the focus of this dissertation, an understanding of bi-metallic strips and how they work as the predecessor to piezo-electric sheets and strips is essential. As all piezo-electric products are bi-material objects, they are very similar to bi-metallic strips, the earliest-known invention of metallic strips made of two metals.

The bi-metallic strips are strips made of two different materials. "The principle behind a bi-metallic strip thermometer relies on the fact that different metals expand at different rates as they warm up**.** By bonding two different metals together, you can make a simple electric controller that can withstand fairly high temperatures." (Bewoor, 2009, [2]). How the bi-metallic strip works is similar to the piezo-electrical strip. However, instead of temperature, the piezo-electrical strip will react to electrical charge or voltage.

2. John Harrison

The first bi-metallic strip was developed in the early 1700's to solve the problem of changes in temperature. In the design of a clock "H3," John Harrison included "a bi-metallic strip, to compensate the balance spring for the effects of changes in temperature." (Betts, 2012, [1]) This invention was part of a larger study by the clockmaker into how to make an accurate clock that did not lose time. The bi-metallic strip was used to compensate for temperature changes that would slow or speed the clock up. This was precisely what

the first bi-metallic strip was developed for. Eventually, such strips would also be used for heating and cooling elements.

The reason why it was clock H3 is that two earlier clocks had been developed for other reasons. John Harrison was faced with the problem of developing a clock that kept the same time to reflect it at a different location relative to the suns position on the globe at the end of a ship's voyage from where it started. The following excerpt sets the stage for his earliest efforts: "Harrison made this clock [H1] in an effort to provide a reliable means of measuring longitude (the east-west position). An inability to calculate longitude had been the cause of many disasters at sea, prompting the British government to launch the Longitude Prize in 1714. There would be a reward of £20,000 – several million in today's money – for the person who solved the problem. While some attempted astronomical solutions, Harrison, a clockmaker by trade, was sure that an accurate timekeeper was the key to the problem." (Roberts, 2014, [12]) This states that if a clock were to show 9 a.m. in England, the same clock would show 9 a.m. in North America consistent to where 9 a.m. would be for that location. Harrison's clock had to be "programmed" to lose an hour for every 15 degrees of longitude traversed by ship heading West. His first two clocks H1 and H2 were used to start on this problem. The bi-metallic strips were used later to compensate for summer and winter differences in a pendulum clock.

The balance spring element of a clock is the "… extremely thin, coiled spring that controls the swings, or oscillations, of the balance. The inner end of the hairspring is attached to the balance staff and the outer end to a stud on the balance cock. The spring's elasticity ensures that the balance swings back and forth at a regular rate."(WatchTime,

2015, [50]) The balance wheel performs the same operation that a pendulum does in a grandfather's clock. See Figure 2-1 below for an example of a balance spring.

Figure 2-1: Balance spring example (Angle, 2013, [44])

John Harrison also developed the pendulum that we have today. I am not going to get deeply into this, as while the pendulum is bi-metallic, the surfaces of the two metal components are not bonded together. Such a configuration is not relevant to this thesis, as this work specifically looks at cases where two materials that are bonded or melded together in a single piece.

This leads us to this fundamental engineering and physics fact: If these following conditions are met: two different ductile materials are bonded together with two different coefficients of temperature expansion, the composite object not being insulated from the external environment, and if the melting temperature of one of those materials is not exceeded, the end result is an object that can change shape when the temperature in the external environment changes. This is an undergraduate freshman Physics problem. In

fact, one can consult any freshman Physics text ([43]) for the methodology behind how and why this phenomenon works.

John Harrison gave us a bi-material strip. However, in order for the researcher to be able to study the piezo-electric effect where a material turns mechanical deformation into electrical charge and vice versa, the next area this work touches upon is how piezo-electrics were developed from the earliest form of quartz to modern day carbon- and silicon-based piezo-electric products. The next inventor that must be covered to understand piezo-electrics and how they finally developed is Pierre Curie.

3. Pierre Curie

Pierre Curie was the scientist responsible for discovering piezo-electric effects. "By the time Pierre was 21 and Jacques 24, the brothers had discovered the piezo-electric effect (from the Greek word meaning 'to press'). The Curie brothers had found that when pressure is applied to certain crystals, they generate electrical voltage. Reciprocally, when placed in an electric field these same crystals become compressed. Recognizing the connection between the two phenomena helped Pierre to develop pioneering ideas about the fundamental role of symmetry in the laws of physics." (American Institutes of Physics, 2015, [14]) Basically, here was the science of piezo-electricity discovered; however, Pierre Curie did not go far into the science of piezo-electricity. All he knew was that, if certain crystals were pressed, they would release an electric current. He used this phenomenon in his research on radioactivity.

What is not well known is that the Curies were really helped along by the mathematician Gabriel Lippman. ([14]) Lippman stated that piezo-objects could be

operated with electricity as well. “The following year, mathematician Gabriel Lippman demonstrated that there should be a converse piezo-electric effect, whereby applying an electric field to a crystal should cause that material to deform in response. The brothers rushed to test Lippman’s theory, and their experiments showed the mathematician was correct. Piezo-electricity could indeed work in the other direction [electrical to mechanical work].” (Anonymous, 2014, [14]) So therefore, the focus of this dissertation is actually the reverse of the piezo-electric effect, since the researcher is discussing putting an electric charge through the piezo-element to get it to deform, buckle, and flip to the first mode. This is very important as the switch is going to absorb an electrical charge and then react accordingly. See Figure 2-2 below for more clarification.

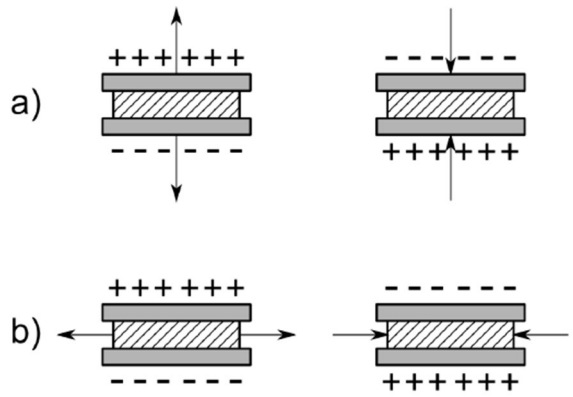

Figure 2-2: The piezo-electric effect is shown above; mechanical tension or compression on a piezo-electric object will induce a current depending type of stress and direction. (Lam, 2015, [19])

An additional factor that Curie found is called the Curie point. While this mostly has to do with magnetism, it does also have relevance to piezo-electronic elements, since they have an elemental structure similar to that of magnets. This point is defined as “[the]

temperature at which certain magnetic materials undergo a sharp change in their magnetic properties. In the case of rocks and minerals, remnant magnetism appears below the Curie point—about 570° C (1,060° F). (Encyclopedia Britannica, 2015, [29]) This will be a very important concept for this thesis, because it imposes a design limitation on piezo-materials that will be presented later on. If a piezo-material goes beyond the Curie point, the piezo-electric properties are gone as well. This is because at that temperature point the atoms become misaligned and no longer act as a magnetic pole.

The next discovery relevant to our current material did not happen until after World War II. The hypothesis was developed that, since at the time there were crystalline structures (quartz) that displayed piezo-electrical functions, that there might be other matrix-like structures similar to crystalline structures that also display piezo-electrical properties. Further, if such structures did exist, what were the piezo-electric constants and how did they compare to the inorganic materials already discovered?

B. Later Works

1. Organic versus Inorganic

After the piezo-electric breakthrough with Curie, the piezo-effect became widely known. However, up until after World War II, the phenomenon was mainly connected with inorganic, crystalline solids. One of the piezo-electric requirements was that atoms had to be in a solid crystal matrix. However, when the possibility of growing inorganic crystals attracted the attention of researchers, a different hypothesis was formed: could materials other than inorganic crystals could hold a piezo-electric effect? There are organic materials that have a crystalline structure like the quartz crystals that were examined by Curie, but they had other elements in them besides silicone and carbon and were not good at holding a charge.

One early piece of research (Fukada [32]) that is expanded by later research (Kawai) (ref#35) is about studying piezo-electrics in organic materials. What Fukada did is the following. "The piezo-electric effect of bone has been observed similarly to the case of wood or ramie. The specimens were cut out from the femur of man and ox, and dried completely by heating. The piezo-electric constants were measured by three different experiments, that is, measurements of the static direct effect, the dynamic direct effect and the dynamic converse effect. The piezo-electric effect appears only when the shearing force is applied to the collagen fibres to make them slip past each other. The magnitude of piezo-electric constant depends on the angle between the applied pressure and the axis of the bone. The maximum value of piezo-electric constant amounts to 6×10^{-9} c.g.s. e.s.u., which is about one-tenth of a piezo-electric constant d_{11} of quartz crystal." (Fukada, 1957, [32]).

This is a tough concept to grasp because most structures that researchers look for to be crystalline are inorganic and have a complete, uniform structure with no impurities.

The concept presented in the previous paragraph is how an organic material can also be a crystal. The author finds out that this process on how animal bone forms a crystal matrix to gain strength was being studied later on. The literature search revealed an article from 1999 on the study of how bone becomes a crystal similar to quartz ([33]).

What Fukada is doing is trying to find out different piezo-electric constants from organic materials and compare them to each other and to inorganics as well. The author also found examples of others that also tried to find piezo-constants as well. While the original work was on whale bones, other organic materials followed.

Table I. Piezoelectric constant and organic composition of mammalian hard tissues (N = number of samples; the variations are SD)

Material %	N	d (pC/N)	Matrix
Cementum	6	0.027 ± 0.018	32.1 ± 0.3
Dentine	6	0.028 ± 0.015	28.2 + 0.4
Bone	7	0.22 ± 0.036	31.2 ± 2.1

Figure 2-3: Examples of different piezo-electric constants in organic materials.

(Marino, 1989 [45])

What Marino shows us here is that not only bone but other organic materials do exhibit piezo-qualities. While these are weaker in nature compared to quartz, it still needs

to be mentioned, as our research has revealed that piezo-material is also made up of artificial organic material. It is described as artificial because it is grown.

The process of making an organic crystal involves several proteins that govern bone becoming a crystalline solid. Scheufler found the following: "Homodimeric bone morphogenetic protein-2 (BMP-2) is a member of the transforming growth factor beta (TGF-beta) superfamily that induces bone formation and regeneration, and determines important steps during early stages of embryonic development in vertebrates and non-vertebrates. BMP-2 can interact with two types of receptor chains, as well as with proteins of the extracellular matrix and several regulatory proteins. [the work] reports here the crystal structure of human BMP-2 determined by molecular replacement and refined to an R-value of 24.2 % at 2.7 A resolution." (Scheufler, 1999, [33]) This is proof that bone is a crystal but it also can be flexible as well. The gist is that there are organic materials that can become crystal as well.

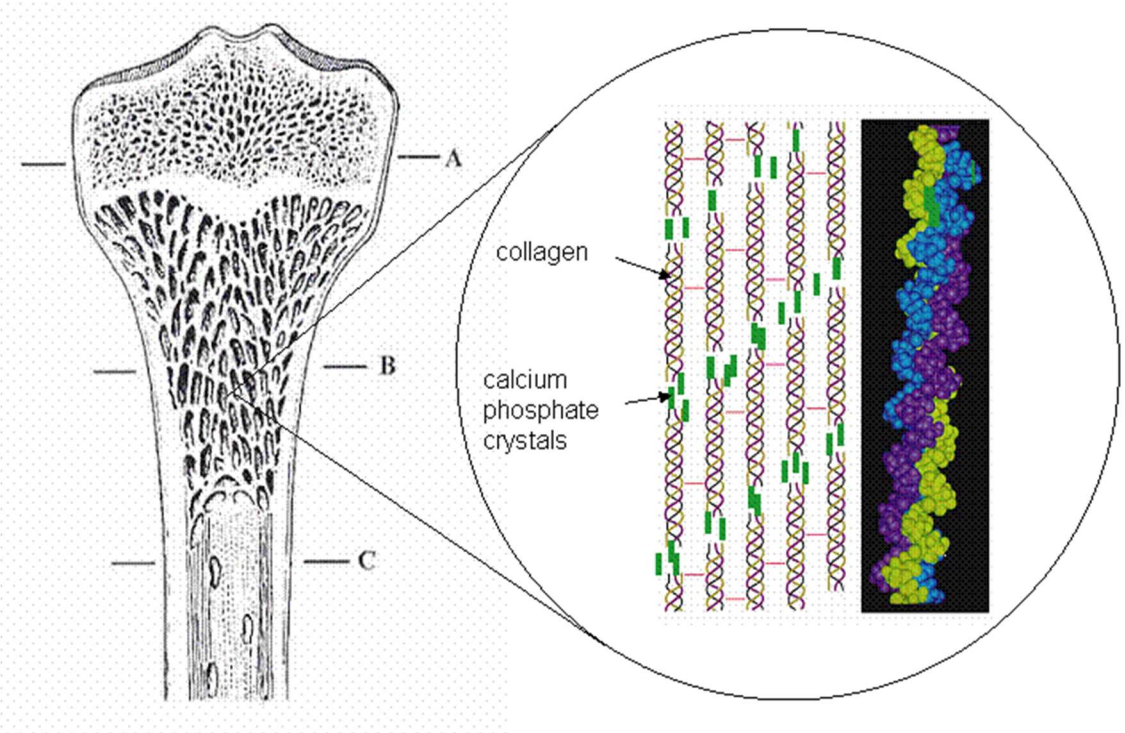

Figure 2-4: Bone as a crystalline structure showing how a piezo-material can be organic (Davies, 2012[34])

The image shown in the figure above is the crystalline structure of bone. This is important, as it shows that there are organic materials that form a crystalline structure as in-organics do. While this is an important facet of this thesis, the main focus is on trying to find a suitable piezo-electrical object to research and to understand how it is formed.

The author briefly mentions Kawai here also. This literature search unearthed a 30th anniversary paper about his discovery. "Dr. Heiji Kawai of the Kobayashi Institute of Physical Research (Tokyo) first reported his discovery of strong piezo-electricity in oriented polyvinylidene fluoride (PVDF) in 1969. After directing the Kobayashi Institute of Physical Research and Rion Co. Ltd." (Brown, 2000, [35]) This paper shows that Kawai

discovered PVDF's, which were related to Dr. Fukata's work. The article also mentions that both worked together on piezo-organics and discovered and engineered a great deal of other uses for PVDFs.

With Pierre Curie and Gabrielle Lippmann, our overview of the pre-background work is complete. Both Pierre Curie and John Harrison are the shoulders on which a lot of the later work is based on. In the next section, the author covers work by Professor Bottega and Professor Boroujerdy and others whose recent work supports this thesis. After that, the thesis covers the work of another researcher Steven Xu, who studied holes in piezo-objects. Together this represents the background work pertinent to this thesis and which provides the reader a useful overview of work done previously.

Chapter 3

Literature Review

The author found and cited several previous works dealing with studies in piezo-electric elements and the snap-through phenomenon. One of the experts in piezo-electrical devices, who did a lot of work on instability of patched plates, is professor Bottega of Rutgers University. ([4, 5]) Professor Boroujerdy of Iran ([3, 6, 7]) also did several works on the theoretics of the snap-through equations. We also found that a professor Xu ([8]) did work in this area. These are the three major individuals covered in the literature review.

A. Boroujerdy [3, 6, 7]

The literature review revealed a number of recent works, including some by Boroujerdy, M.S. His work is theoretical in relation to what this researcher is doing on a practical level. Boroujerdy proposed several equations that explain the flip effect phenomenon. The researcher validated Boroujerdy's equations with some of his own, and used the force method to validate his methods. The researcher then derived some equations to explain this, and then compared the results to the results that Boroujerdy came up with. Both derivations are very similar. See the equation derivation (Chapter 5) for more details. Some differences between this researcher's work and Boroujerdy's work that Boroujerdy deals with FGM's (Functionally graded material) while this paper deals more specifically with piezo-polymers. As previously stated, Boroujerdy's work is also theoretical while the researcher's is practical.

Boroujerdy started by deriving the equations for piezo-FGM shallow spherical shells and found that "buckling analysis is based on the equilibrium equations of shallow

spherical shell, the classic theory of Love–Kirchhoff, and the Sanders nonlinear kinematics equations. The analytical solutions are obtained for uniform external pressure, thermal loadings, and constant applied actuator voltage." (Boroujerdy, 2013, [3]) The paper explains that there is a critical temperature and a critical voltage at which the flip. Boroujerdy's work was also with spherical shells; however, an earlier model was of a conical shape.

Boroujerdy also developed the theoretical equations of the snap-through buckling equations. In his work he states, "The results show that the axisymmetric buckling of Piezo-FGM shallow clamped spherical shells under thermo-electro-mechanical loading is of snap-through type. The intensity of buckling is dependent on the geometry of the shell, value of thermo-electro-mechanical loading and type of thermal loading." (Boroujerdy, 2014, [7])

Boroujerdy and his model of the bi-material domes and the bi-material set up are also important for this thesis. The figure below gives good geometries for what this thesis's model is going to look like.

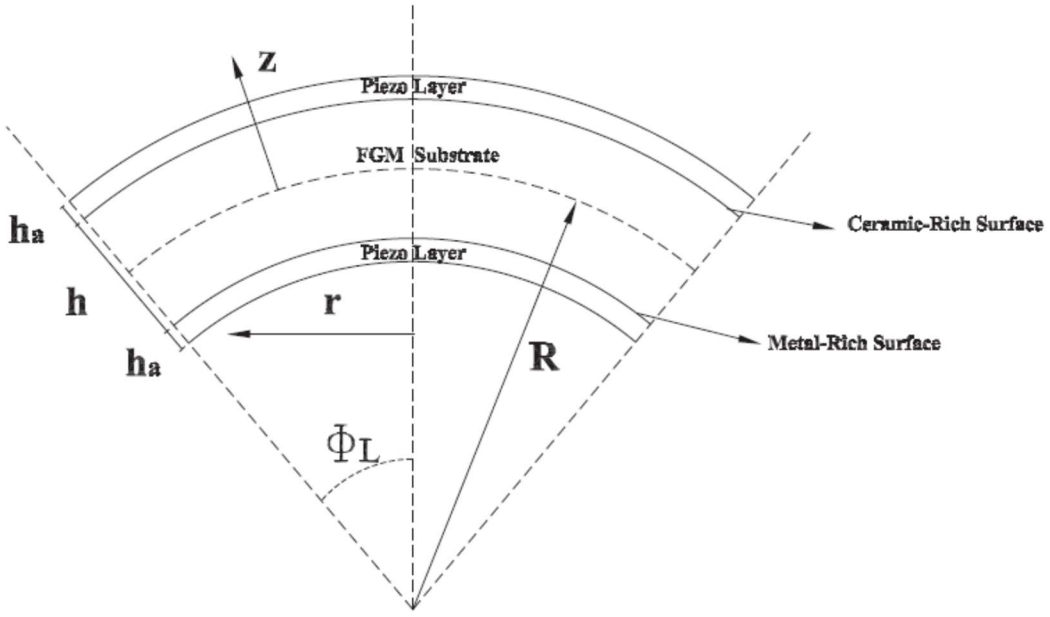

Fig. 1. Geometry of spherical shell.

Figure3-1: Geometry of spherical shell used in Boroujerdy's papers (Boroujerdy, 2014, [7])

While the above figure is close to what this work is researching, Boroujerdy performed it assuming a double piezo-layer. The present study will focus on the snap-through of a single layer piezo-element. However, this work has to look at the piezo-elements and the research involved. It was also a ceramic shape involved in Boroujerdy's research, while we are interested eventually in piezo-films. While ceramics are important to the piezo-field, the present work did not cover them because, for a switch, material that is very flexible and has a lot of ductility is required.

Boroujerdy also did some research on the critical temperature wherein he discovered the critical temperature when a shape flips from one side to the other. This is

important theoretical work, as it explains the flip-through effect and what this researcher is going to find experimentally later on.

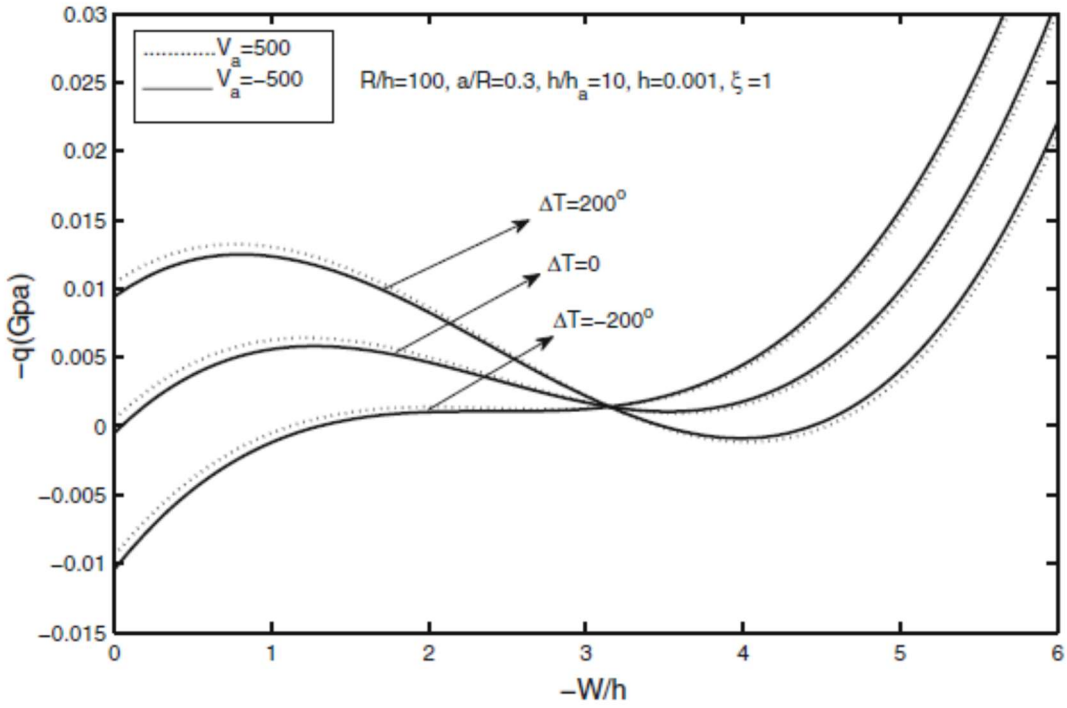

Figure 3-2: Critical temperature of the snap-through effect (Boroujerdy, 2013, [3])

This chart shows the critical temperature given a pressure and shape difference. What Boroujerdy showed here is that the snap-through effect is also dependent on the external pressure. While this is important, as external pressure does put some force into question and does effect the internal moment of the part, it will not be researched here. Boroujerdy also did do some other work with regard to just temperature versus shape size.

Boroujerdy also did some other work with regard to conical shells. This is a basis from which one can go to spherical shells.

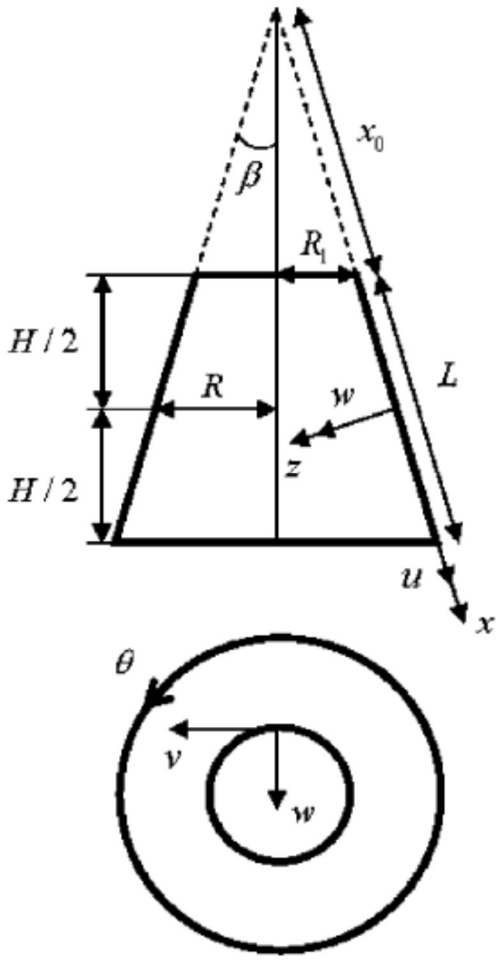

Figure 3-3: Geometry of a conical shell (Boroujerdy 2007, [6])

The geometry above is evidently similar to the spherical geometry later developed. The primary focus of Boroujerdy's work was to show that there are laws and equations that govern the buckling of several layered shapes such as shells. Boroujerdy also gets into other geometries and boundary conditions in his other works. This shape is similar to what Boroujerdy researched later.

B. Bottega [4, 5]

The literature search revealed that Professor Bottega of Rutgers University had studied a similar phenomenon of patched piezo-plates. Bottega studied what happens when a primary plate has a secondary plate of a different size patched onto it. This research was done because: "A number of investigations have been performed concerning various aspects of the integrity of patched structures. Among several issues, thermal effects such as thermally induced instability." (Bottega, 2000, [4]) This is where the researcher started to look for piezo-electrical instability, as piezo-electrical term deals with voltage, which is similar to temperature. Bottega's paper also showed that a patch is unstable and can cause a structure to change shape and buckle and flip.

One additional Bottega work focused on the flip-through effect for bi-material plates. His research is described as follows: "In each case it was predicted that the structure will deflect in one direction upon application and subsequent increases of a temperature change until a critical temperature is achieved, at which point the structure will dynamically sling to an equilibrium configuration associated with deflections in the opposite sense of the original and then deflect further in that direction as the temperature is increased." (Bottega, 2006, [5]) Bottega's paper also provided several graphical representations that were used to develop the equation for what the researcher proved later on in the work. This work by Bottega is similar to what the researcher performed, as it involved a composite structure, was on the flipping phenomenon, and was on temperature, which is similar to what the researcher did with electric current.

Bottega also used a model that is similar to Boroujerdy's, which was similar to the one that was modeled in this thesis. If the top layer that is presented in the figure below expands more slowly than the bottom layer, then the whole system becomes unstable and then flips.

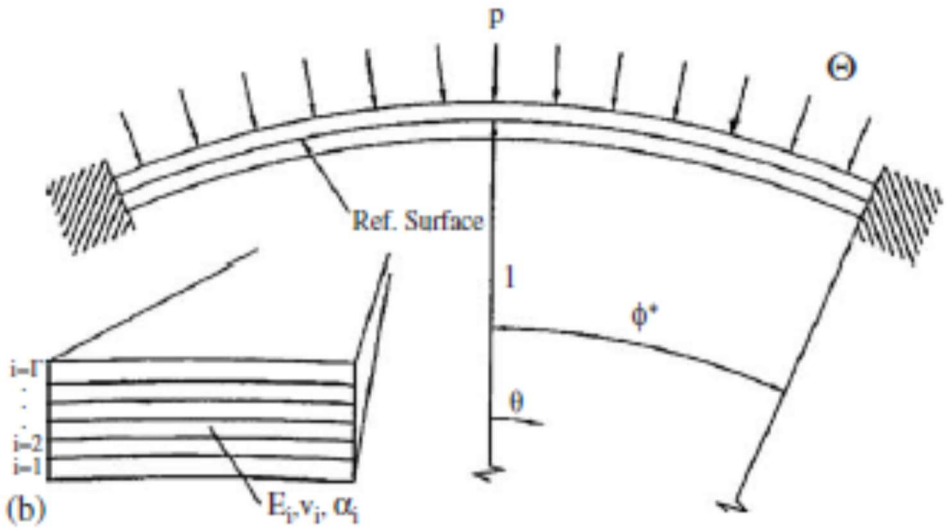

Figure 3-4: Bottega's bi-material plate similar to Boroujerdy's (Bottega, 2006, [5])

The reader can see the similarities between Boroujerdy's and Bottega's models. This is a great model for the snap-through effect. This model is also good because it shows that the ends of the system have to be rigidly connected as was found later in the research.

Bottega also had another model and equation set that included patched plates, as this was another area of his research. This is seen in Figure 3-5 below.

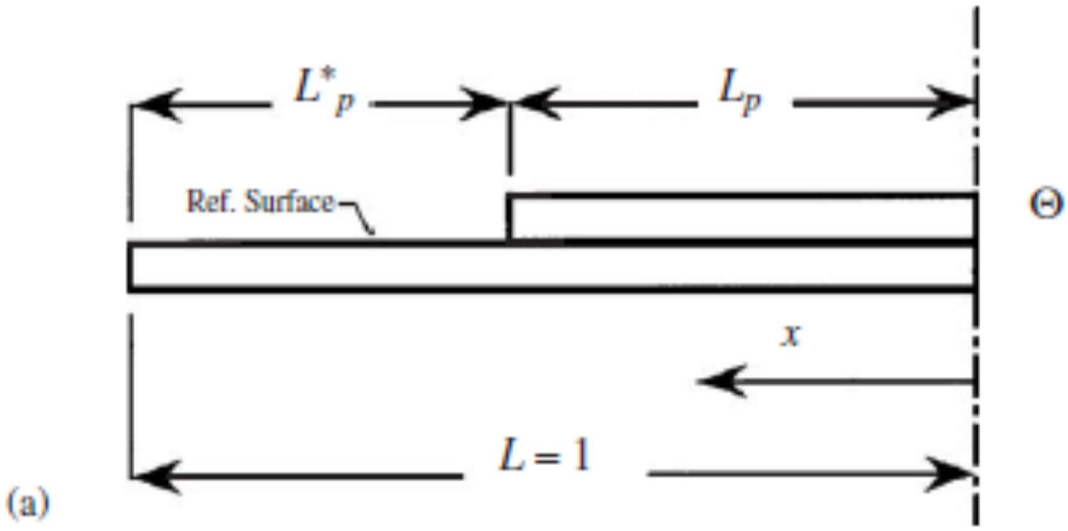

Figure 3-5: Bottega's patched flip-through buckling plate (Bottega, 2006, [5])

In this figure, Bottega has a patched plate that only covers a part of the whole plate. While this was considered at first, the researcher decided for this thesis to go with a standard plate rather than the patched plate. This was because patched plates are harder to accurately mass-produce and do not have easily definable geometry. Finally, this type of patch can become damaged due to fatigue if it gets bent too many times. This is a possible area for future research.

C. Timeshenko ([21])

To understand the flip effect, the researcher has to return to the works of Timeshenko. Timeshenko did works on shear, stress, and strain in thin-walled objects. This is the closest comparison to what the researcher is going to propose later in this thesis. Below shows the figure as to how Timeshenko broke down the stresses in a thin-walled element, which is what the present thesis focuses on.

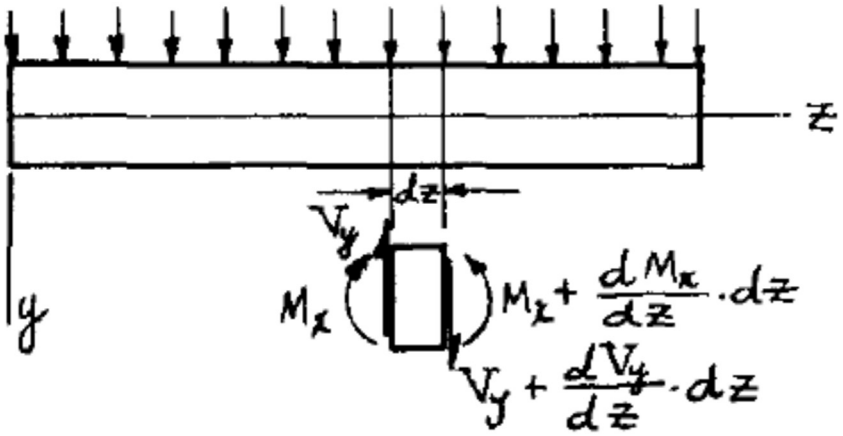

Figure 3-6: Timoshenko's bar element of stresses, (Timoshenko 1945, [21])

In this diagram, Timoshenko shows how a bar element is loaded and how he gets the internal moment. Internal moment is key to how this flip effect works, as it is an in-balance between internal moments and external forces. Later on in the thesis, energy methods will be used to come up with the governing equations. This is only the start of what Timoshenko studied.

Timoshenko also studied the thin-walled element shown below.

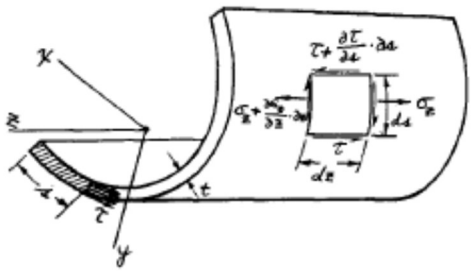

Figure 3-7: Thin walled object under axial constraints, formation of the stress model. (Timoshenko, 1945, [21])

In this figure, the reader can see the different stresses that make up an element in torsion and bending. For the purposes of this thesis, the researcher ignored any torsional effects. While there is torsion that happens on a disk, these torsional effects cancel each other out. Timoshenko lays the basic groundwork for energy methods in piezo-electrical objects.

D. Xu [8,9]

Another researcher, Professor Xu, did research on piezo-electric plates with holes in them. This research looked at the hole as a stress point. It also highlighted how the plate reacts to having a hole in the center and how this affects the stability of the plate.

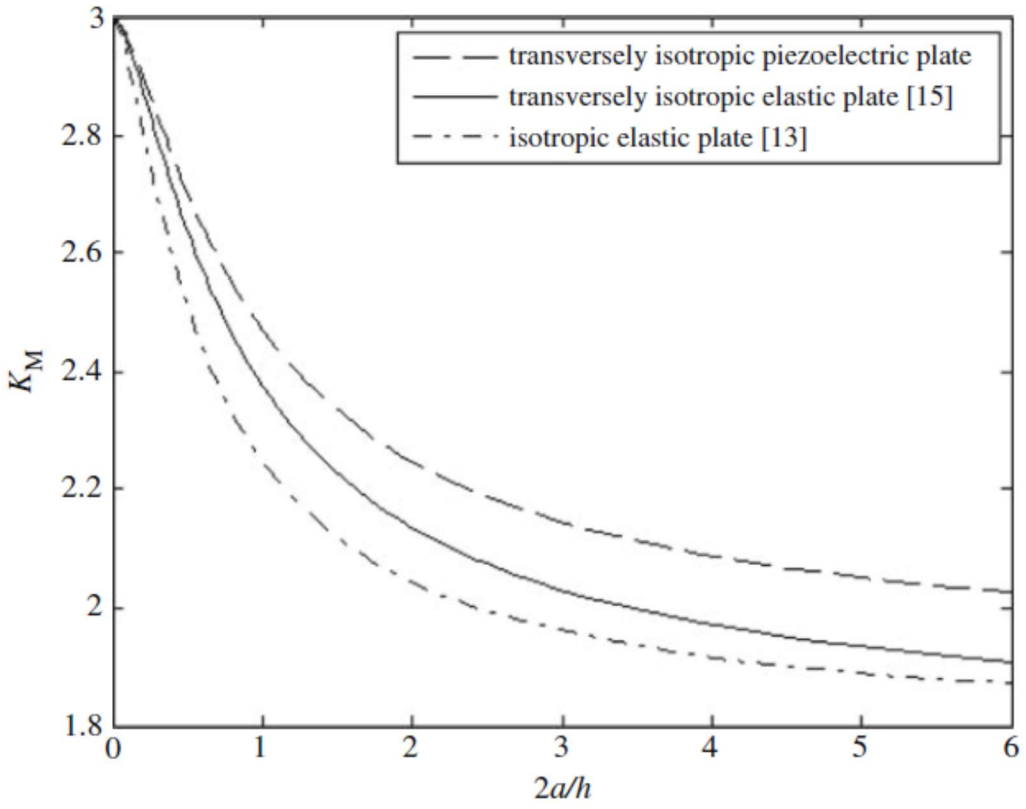

Figure 3-8: Moment concentration versus hole diameter and plate thickness (Xu, 2013, [9])

What is seen here is that the moment goes up if the hole diameter is large versus the size of the plate itself. The hole diameter experiment is also very important, as one of the most successful shapes that was found in a later section was the washer shape, which was where a lot of the pre-thesis information was concentrated. What this also shows is that, because a higher moment concentration can be achieved around holes, it can be easier for the shape to flip.

This is the extent of the findings of the literature review considered relevant to this topic. The rest of this chapter will review what is in the piezo-industry and the types of piezo-electric objects that exist. There are several types of piezo-elements that will and will not work.

E. Manufacturing of Piezo-electric Objects [13]

The next point of information before this thesis proceeds is to present the different piezo-elements and how they are used is this: how are piezo-electric elements made? Xu from the previous section defines this further: "The piezo-electric tape consists of many patterned and densely packed PZT (lead zirconate titanate) elements sandwiched between two flexible films/foils." [9] In general, most piezo-electric objects are a layer of the piezo-electric material that is coated onto another surface that does not have piezo-electric properties. This makes it very easy and inexpensive to make piezo-electric objects.

Piezo-electric elements can be home-manufactured. There is a whole step-by-step process that has been put online about this and is available through many different websites. Here is one that uses washing salts: http://www.instructables.com/id/Rochelle-Salt/ There are many other sources of these homemade piezo-electrical creations. [13] Since this is just informational, the reader can look more of these up and see how to make them. In this thesis, the researcher is showing that piezo-objects are easy to home-manufacture as long as the manufacturer knows what they are doing and follows the instructions carefully.

Chapter 4

Piezo-electric Objects

A. Types

This thesis will not get into the chemical properties of the piezo-electrical objects. Rather, this section is to differentiate between the two common types of piezo-electrical devices. This chapter will look into why one worked for the type of problem in this thesis and why the others did not. One of the main things the researcher has to do to confirm the reasons one did not work and the other did is to do a review of fixed versus pinned connections.

1. Ceramic

The first type of piezo-electric devices is a ceramic device. The ceramic device is an extremely rigid object. The lion's share of the piezo-electrical objects currently found in the industry are ceramic. These are noted below in the push button and actuator sections of this thesis. The advantages of the ceramics are that they very durable. They also can put out a lot of electrical energy for very little mechanical or heat energy put into it. The ceramic material can also take high temperatures. These are not very moldable, and custom molds for these are very expensive and take many engineering costs to make new shapes work correctly. (American Piezo, 2015, [11])

An example of a piezo-ceramic is shown below. Note that this is just an artist's rendering of one and not a picture of one.

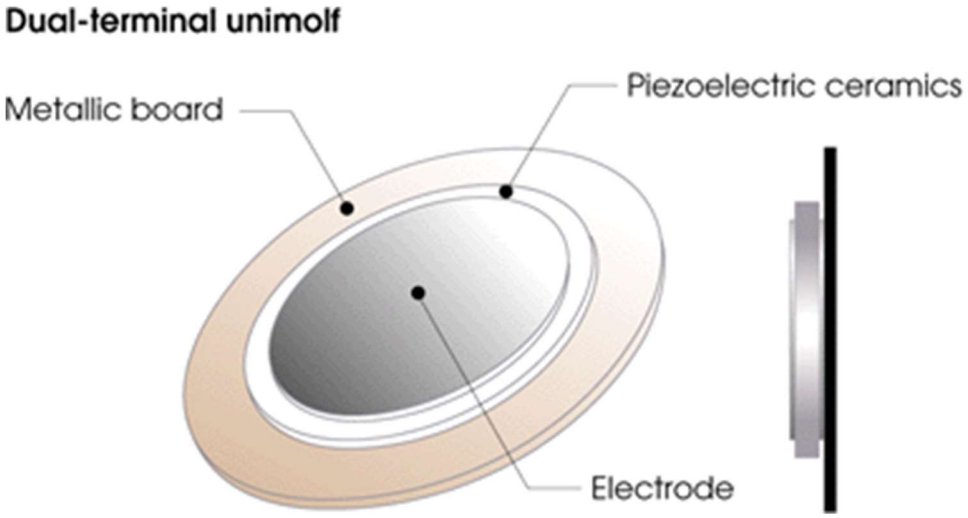

Figure 4-1: Typical setup of a piezo-ceramic (Anonymous TDK products, 2014, [20])

2. Films

The second type of material used for piezo-electric devices is a piezo-film. This is a very thin layer of flexible piezo-material. This type is used because it is very moldable and can be flexed into a number of different shapes. An example of what one looks like appears below.

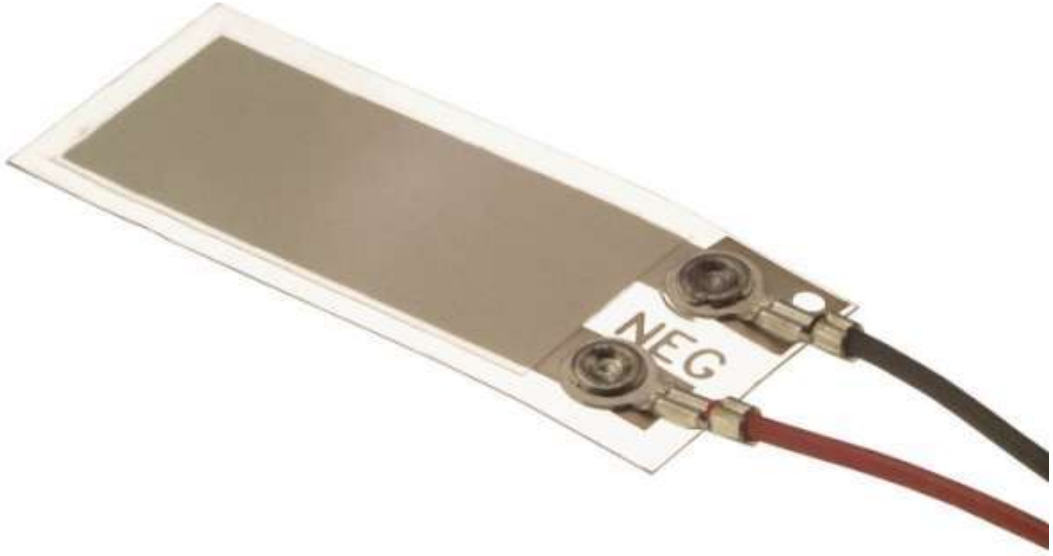

Figure 4-2: Example of piezo-film from the industry (Measurement Sensors, 2015, [17])

Piezo-films make great speaker elements as they flex back and forth easily under a small electrical charge. "Piezo-electric film is an enabling transducer technology with unique capabilities. Piezo-film produces voltage in proportion to compressive or tensile mechanical stress or strain, making it an ideal dynamic strain gage. It makes a highly reliable, low-cost vibration sensor, accelerometer or dynamic switch element. Piezo-film is also ideally suited for high fidelity transducers operating throughout the high audio (>1kHz) and ultrasonic (up to 100MHz) ranges." (Measurement Sensors, 2015, [17]) Simply put, this seller is saying that films are easy to produce, are low cost, have long life, and are very accurate. This seller is where the piezo-element came from for the experiment.

3. Composites

Piezo-electric films have also turned into piezo-electric fiber composites. "Piezo-electric fiber composites (PFCs) have attracted much attention owning to their unique structures and improved strength and toughness compared with monolithic piezo-ceramic wafers." (Lin, 2013[27]) The gist is that, if the ceramic is made into a composite fiber, it will be more flexible and more durable over many more cycles than the typical ceramic in use.

B. Applications

1. Piezo-electrical Buttons

A piezo-electrical button is a button activated either by a human element or by a lever that pushes it. First, the lever is pushed into the piezo-electrical button. With the force of the lever on the piezo-electrical button, the button is depressed. The depression of the button causes the piezo-electrical element to change shape. When the button changes shape, it builds an electrical charge in it because the piezo-element has been reshaped. Once the element starts to return to its original shape, the charge is released into the system to which it is connected. This charge goes to a device it is hooked up to that monitors this charge. Once this charge reaches the controller, it activates whatever the controller is hooked up to.

The advantages of the piezo-electric push buttons are as follows: “Minimizes production loss due to cleaning procedure, minimizes frequent replacement due to corrosion, minimizes bacteria growth potential from crevices, includes UL Certified product for industrial panel, offers custom laser engraving” (Rockwell Automation, 2015, [10]). The piezo-electrical device is often used because it can pick up a touch signal and then actuate. This avoids the replacement costs of a standard mechanical push button. It also helps with cutting down on having more moving parts which take energy to power.

Figure 4-3: Examples of typical piezo-electrical buttons (Rockwell Automation, 2015, [10])

These typically are a ceramic that moves very minimally (roughly on a scale of perhaps 10^{-4}) in relation to the size of the actual object) and gives off a great electrical charge to power whatever the button is applied to. The applications include elevators, fire exits, operation panels, and crosswalks. These are the first applications of the piezo-electrical devices that exist around us today.

The piezo-button is important for this thesis because of the fact it can be reshaped. One of the properties that has not yet been studied is whether a piezo-element can hold its own prime shape when it is activated. The prime shape is what the piezo-electric element turns into when the electric charge is put on it. This translate into, given a quantity of electricity or heatflux/cooling flux introduced into the system, the piezo-electric system is activated and alters shape.

2. <u>Actuators</u>

Actuators are thin ceramics that are fused together and that react to an electrical charge by moving back and forth. Regarding their applications: "the piezo-electric actuator is used in a variety of industrial, automotive, medical, aviation, aerospace and consumer electronics applications. Piezo-actuators are found in precision knitting machinery and braille machines. The silent drive characteristics make piezo-actuators an excellent auto focusing mechanism in microphone-equipped video cameras and mobile phones. Finally, since piezo-actuators require no lubrication to operate, they are used in cryogenic and vacuum environments." (APC international, 2015, [11]) Again, these are ceramics and provide some movement back and forth under an electrical charge. Ceramics can be only secured rigidly at one edge. An example of an actuator appears below.

Figure 4-4: Example of Piezo-electric actuator, (Courtesy Thor Labs, 2015, [22])

These were studied as part of this thesis. However, in the end the part that was obtained did not have the flexibility needed for this thesis. Additionally, to clamp these down in the three areas minimally needed to make a switch would not work. This was due to the fact that relative to the piezo-films these are very rigid and might break the ridged clamps used to clamp them down before flipping to the desired shape.

3. Speakers

A final application of piezo-devices, flexible piezo-films, is found in speakers and speaker elements. "Piezo-elements come in handy when you need to detect vibration or a knock. You can use these for tap or knock sensors quite easily by reading the voltage on the output. They can also be used for a very small audio transducer such as a buzzer." (Sparkfun Products, 2015, [16]) Flexible piezo-films are elements that can even pick up vibrations, and they can make sounds like sirens when activated. This is also the easiest of the three elements to make, since they do not require any form-fitting baking, and unlike the other two don't require precision measurements to create the proper sized element. Speaker elements are created in sheets and then cut to desired size.

Speaker elements can also be made out of crystals. There is a way to make a homemade piezo-electrical speaker.

The piezo-speaker elements are also the cheapest, compared to the other two elements. A chart below shows actual comparisons of the different prices of these elements.

Element type	Approximate price range
Button	$100 to $500 (depends on casing etc.)
Actuator	$20 to $200
Speaker	$2 to $20

Figure 4-5: List of approximate pricing of piezo-elements (Source was through phone calls or email to several manufacturers)

As can be seen, the researcher obtained this range of pricing from various websites that sell piezo-objects. In the end, it was found that the cheapest were the speaker elements, due to ease of manufacturing. This is important, since cost is always the first area that is looked at when implementing a new technology. The other plus is that these elements have ease of manufacture.

4. The Purpose

The purpose of the background was to lead the reader into the problem statement with some knowledge of said background, and to explain where many of the assumptions for the experiment came from. Alternative topics the researcher could have chosen to experiment on were reviewed, and a current overview of the industry regarding piezo-elements was included. This leads up to the question of actual switches. Can a perfect switch be made out of these elements, or is it impossible? Indeed, industry leaders the researcher talked to said it could not be manufactured.

Conclusion of Background Information

The background information leads one to this problem: can it be done in the real world or is it just theoretical mathematics? Can a piezo-electrical disk shaped object bend under the right conditions, or will it remain in the same shape? The second part is this: will it be able to hold its shape moving forward or not? Timeshenko showed in his work ([21]) about internal moments that there exists an internal moment that forces an object to keep its shape. The second part of this thesis asks: at what point will an object that goes through the flip effect return to its original shape? This question is posed because it is known that there is a new internal moment that is developed when the shape flips through.

The next section goes into derivation of the equations. After that, the rest of the thesis unfolds and goes into comparing the finite element methods to the experiments and the equations that are derived. The main goal of those is to be able finally to compare them to experimental results that the researcher obtained when he built a switch out of the piezo-films that are found in the industry. This covers the background information.

Chapter 5

Derivation of Equations

In the previous chapter, it was found that energy methods are used heavily in finding out about how these piezo-electrical disks flip. It was found that most of the background is on bi-material, multi-layered, multi variable and not a homogenous material. It was also discovered that a curved shape is used, and no plate is perfectly flat. If a strip or plate is perfectly flat, there will not be any flip effect.

The next chapter goes into deriving the equations. This mainly involves taking Harrison's ([12]) bi-metallic strip and eventually getting it to the point where this switch ends up using a disk shape. In chapters 6 and 7, it is shown how the end switch that was developed is a disk shape. For now, the reader should see it as a disk shape. Later on, it is established that the disk shape is the only one possible. This is due to geometric limitations and market availability of the other shapes.

A Type of problem

This problem is a disk problem that is in spherical coordinates. The researcher has to start defining this in the XYZ plane and then define this in spherical coordinates later on. This problem is also a symmetrical problem where the disk can be sliced in half and end up with the same half hemisphere on either side. This problem is also a linear problem. The last point to note about this problem is the deriver mathematically calculates all the other variables, plugs them in, and then solves for a critical temperature or voltage or some combination of them. A researcher can also work backwards with a critical temperature, voltage, or a combination these to obtain geometries.

The problem is also axial symmetric buckling and failure. This is important, since it shows that the failure will not require the object to try to obtain higher modes during deformation than the first mode. It is assumed that the external force will act normal to the entire surface.

This problem is also defined as a shallow shell. Shallow versus deep depends not on the thickness of the shell but the height of the dome. The thickness is described as either thick or thin, with thick rarely being used. In this case, thick is not used due to the fact there are temperature gradients that have to start being accounted for which are beyond the scope of this thesis. A few definitions exist related to the difference between a shallow and a deep spherical shell. The two reference points that Boroujerdy (ref #6, 7) uses are $\sin(\beta)\sim 0$ or $\beta \leq 20$. Anything more than this would be considered a deep spherical shell. Since testing COMSOL with a shallow and a deep shell and seeing more favorable results with a shallow shell, the shallow shell shape was chosen. Below appear the COMSOL results between a shallow and a deep spherical shell.

Figure 5-1: Typical spherical shallow shell before flipping in COMSOL.

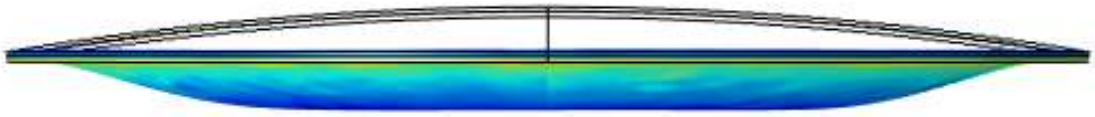

Figure 5-2: Buckled piezo-electric model note for other models the shape follows similar

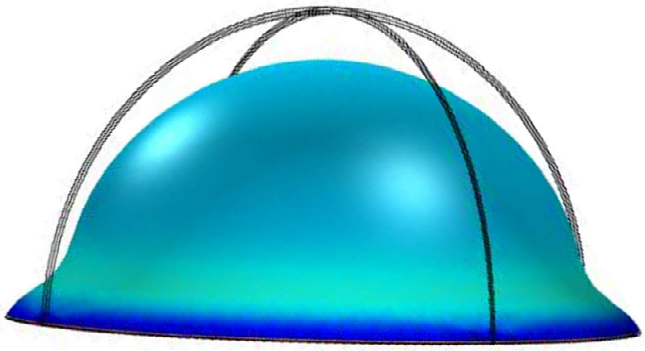

Figure 5-3: Display of the deep spherical shell angle is 90 degrees. Note the shell does not flip through but rather retracts and expands.

B Geometric Representation of the Problem

Below are a few diagrams of the subject problem for this spherical shell.

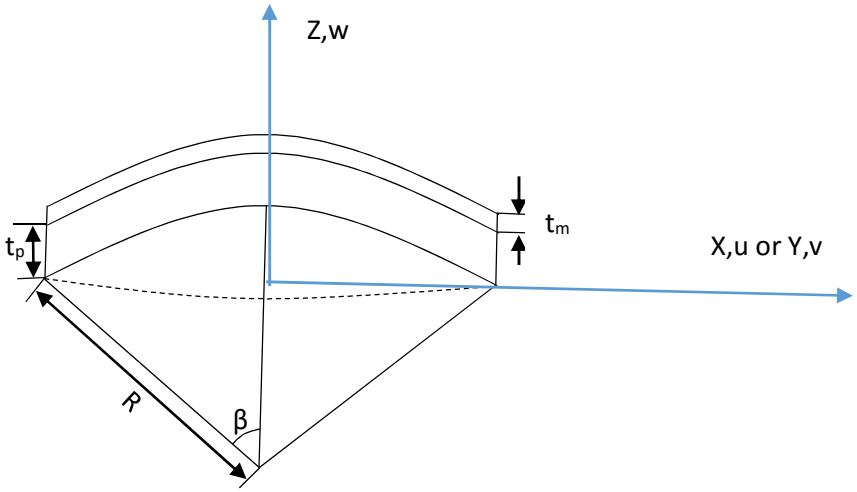

Figure 5-4: Physical representation of the spherical dome problem. Front view or side view in XZ or YZ plane

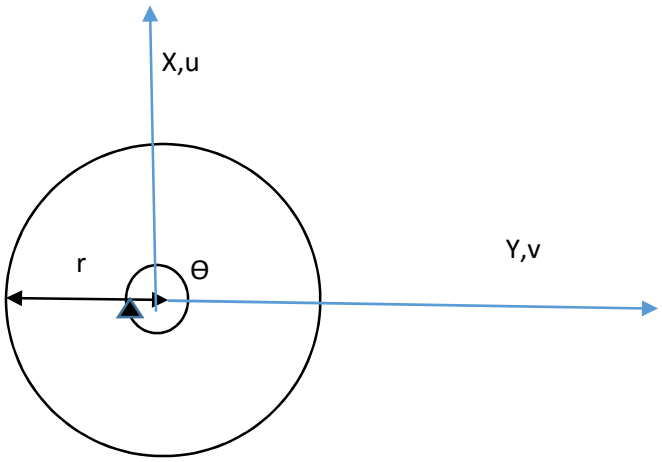

Figure 5-5: Top view of the spherical element in XY plane

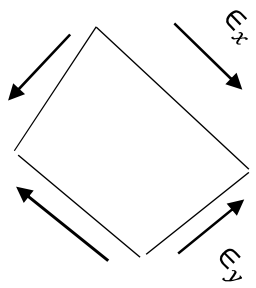

Figure 5-6: Square element showing the shear and bending stresses, shearing stress gamma is through the paper. Note this is on the hemisphere and is just an element.

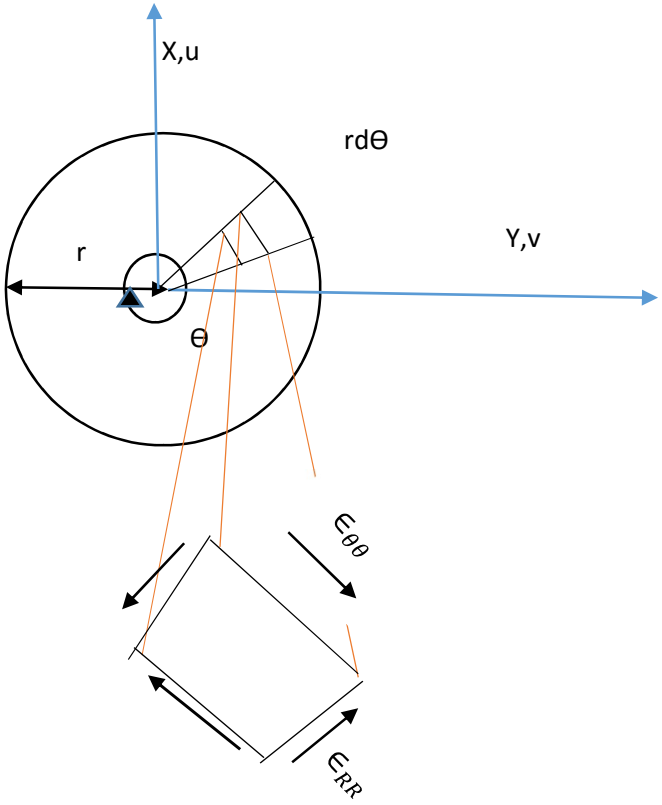

Figure 5-7: Spherical element showing the shear and bending stresses, shearing stress gamma is through the paper. Note this is on the hemisphere and is just an element.

Summary of Steps Needed to Solve for Critical Voltage or Temperature

1. Diagram the problem at hand including geometry and shape properties.
2. Define stress strain equations used for type of shape most representative (IE Sanders, basic mechanics, Euler's or other equations).
3. Define the averages or shape functions used for E, alpha and Poisson's ratios.
4. Define stiffness matrixes for a shell element.
5. Combine the stiffness matrixes with the values defined in 3. Use this to determine forces and moments in shell object.
6. Define static force equations at a certain point on the object.
7. Define stress function(s).
8. Solve these equations by filling in the forces and moments obtained in 5 and stress functions in 7.
9. Derive the shape geometric compatibility equation.
10. Simplify and then solve the differential equation.
11. Define boundary conditions including the amplitude equations (the amplitude is for the total deflection of the object) and solve for them.
12. Find the orthogonal equation and use the Garlerkin method to solve for constants.
13. Solve this equation for the variables T and V for temperature and voltage change respectively. These become the critical buckling temperature and critical buckling voltage.

C Nonlinear Equations

Sanders derived with non-linear kinematic equations for spherical shells. These are as follows. (Sanders, 1961, [52]) Additionally this is back up by (Ventsel, 2001, [54]) These are defined now and are used later in this derivation. Note that u is a deflection in the x direction, v is a deflection in the y direction, and w is a deflection in the z direction. κ is an addition to the strain to take in account the curvature of the surfaces.

The beginning equations were as follows

$$\begin{bmatrix} \epsilon_1 \\ \epsilon_2 \\ \gamma_{12} \end{bmatrix} = \begin{bmatrix} \frac{\partial u}{\partial x} + \frac{w}{R} + \frac{1}{2}\left(\frac{\partial w}{\partial x}\right)^2 \\ \frac{\partial v}{\partial y} + \frac{w}{R} + \frac{1}{2}\left(\frac{\partial w}{\partial x}\right)^2 \\ \frac{\partial u}{\partial y} + \frac{\partial v}{\partial x} + \frac{\partial w \partial w}{\partial x \partial y} \end{bmatrix} \qquad \text{(eq. 5-1)}$$

$$\begin{bmatrix} \kappa_{RR} \\ \kappa_{\theta\theta} \\ \kappa_{r\theta} \end{bmatrix} = \begin{bmatrix} \frac{\partial w^2}{\partial x^2} \\ \frac{\partial w^2}{\partial y^2} \\ \frac{\partial w^2}{\partial x \partial y} \end{bmatrix} \qquad \text{(eq. 5-2)}$$

Substitute $\partial x = \partial r, \partial y = r\ \partial\theta$

$$\begin{bmatrix} \epsilon_1 \\ \epsilon_2 \\ \gamma_{12} \end{bmatrix} = \begin{bmatrix} u\frac{\partial}{\partial r} + \frac{w}{R} + \frac{1}{2}\left(\frac{\partial w}{\partial r}\right)^2 \\ \frac{\partial v}{r\ \partial\theta} + \frac{w}{R} + \frac{1}{2}\left(\frac{\partial w}{\partial r}\right)^2 \\ \frac{\partial u}{r\ \partial\theta} + v\frac{\partial}{\partial r} + \frac{\partial w \partial w}{r \partial r\ \partial\theta} \end{bmatrix} \qquad \text{(eq. 5-3)}$$

$$\begin{bmatrix}\kappa_{RR}\\ \kappa_{\theta\theta}\\ \kappa_{r\theta}\end{bmatrix} = \begin{bmatrix} w\frac{\partial^2}{\partial r^2} \\ \frac{\partial w^2}{r^2\,\partial\theta^2} \\ \frac{\partial w^2}{r\,\partial\theta\partial r}\end{bmatrix} \qquad \text{(eq. 5-4)}$$

Perform the chain rule to the $\kappa_{\theta\theta}$ and $\kappa_{r\theta}$ as well as the first terms of $\in_{\theta\theta}$ and the $\gamma_{r\theta}$ for the final form below.

$$\begin{bmatrix}\in_{RR}\\ \in_{\theta\theta}\\ \gamma_{r\theta}\end{bmatrix} = \begin{bmatrix} u\frac{\partial}{\partial r} + \frac{w}{R} + \frac{w^2}{2}\frac{\partial}{\partial r} \\ \frac{u+v}{2}\frac{\partial}{\partial\theta} + \frac{w}{R} + \frac{w^2}{2r^2}\frac{\partial}{\partial\theta} \\ \frac{u\frac{\partial}{\partial\theta}-v}{r} + v\frac{\partial}{\partial r} + \frac{w^2}{r}\frac{\partial}{\partial\theta\partial r}\end{bmatrix} \qquad \text{(eq. 5-5)}$$

$$\begin{bmatrix}\kappa_{RR}\\ \kappa_{\theta\theta}\\ \kappa_{r\theta}\end{bmatrix} = \begin{bmatrix} w\frac{\partial^2}{\partial r^2} \\ \frac{w\partial^2}{\partial\theta^2} + \frac{w\partial}{r\partial r} \\ \frac{w\partial^2}{\partial\theta\partial r} - \frac{w\partial}{r^2\partial\theta}\end{bmatrix} \qquad \text{(eq. 5-6)}$$

Diagram of deflections

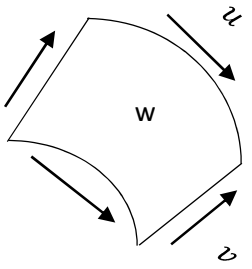

Figure 5-8: Element showing the deflection directions (Note: w is a deflection into the page as it is normal to the surface**.)**

This is an important relation, as this is a nonlinear problem and therefore traditional linear buckling problems will not work, since when the snap-through occurs it has to go into a higher mode before reaching a steady state.

The researcher also has to define some basic concepts. First is that Poisson's ratio is defined as the same at any point. For this particular problem, the researcher defines that the "north pole," when the hemispherical part of the bowl is turned down, is the furthest point on the surface from the edge. This also assumes a straight longitudinal cut is made through the hemisphere.

Below are definitions of averaged moduli of elasticity and averaged alpha values. Poisson's ratio is assumed to be the same throughout both materials and is assumed throughout the rest of this work as 0.3. This is also listed in the reference manual of the material being tested see appendix A.

$$\nu = \nu(0.3) \qquad \text{(eq. 5-7)}$$

For simplicity's sake, the focus of this thesis is on one critical point at the top of the dome (north pole). This point is critical since it is the furthest point for the clamps. It also is the point that will first start to buckle due to temperature differences. In addition, once one point buckles, additional points start to buckle due to instability of the crystalline matrix.

The researcher found that some papers use a complex shape function defined by several variables that is beyond the scope of this thesis. Since the topic of this thesis is about developing a switch with comparison to computer models and theoretical equations and not about developing shape functions for multi-layered shells, the deriver will simplify

the E and alpha terms based upon the simple law of averages. The E and the α values are of the same magnitude for this type of material and problem. Additionally, the true E and alpha values may not be known since one is not testing this composite layered disk in a lab. There also exist errors in fabrication and manufacturing. Therefore, based upon height calculations the E and alpha values are assumed below as simple averages.

$$E = E_m \frac{t_m}{t_m+t_p} + E_p \frac{t_p}{t_m+t_p} \qquad \text{(eq. 5-8)}$$

$$\alpha = \alpha_m \frac{t_m}{t_m+t_p} + \alpha_p \frac{t_p}{t_m+t_p} \qquad \text{(eq. 5-9)}$$

1 Defining Temperature Strain

To form a bridge for the reader, the researcher feels it is useful to provide the reader with a sense of where temperature strain is derived for this equation. The reader should know from basic mechanics that a basic bar element will undergo a change in length when the temperature changes. This is found in the equation below, which can be found in any undergraduate mechanics textbook (Gere, 2002, [50])

$$\Delta_l = \left(T_f - T_i\right)\alpha l \qquad \text{(eq. 5-10)}$$

For the remainder of this thesis, if there is a temperature change it will be noted as variable ω, as this is not used anywhere else.

$$\omega = \left(T_f - T_i\right) \qquad \text{(eq. 5-11)}$$

Since in this paper one is interested in strain for the next steps, one has to cancel out the length variables: the $\Delta_l, and\ l$. The strain due to temperature is then

$$\in_T = \omega\alpha \qquad \text{(eq. 5-12)}$$

This temperature strain will be used further in the derivation below.

D Stress Strain Matrix

For this equation, stress strain comes into the picture, and proper derivation of stress and strain are needed. For a simple curved piece, this is done in the following way. This is where stress strain gets averaged out and a curvature factor κ is introduced, (Gere, 2002, ref#50) backed up by (Krauthammer, 2001, ref#54)

$$\bar{\epsilon}_{rr}=\epsilon_{rr}+z\kappa_{rr} \qquad \text{(eq. 5-13)}$$

$$\bar{\epsilon}_{\theta\theta}=\epsilon_{\theta\theta}+z\kappa_{\theta\theta} \qquad \text{(eq. 5-14)}$$

$$\bar{\gamma}_{r\theta}=\gamma_{r\theta}+2z\kappa_{r\theta} \qquad \text{(eq. 5-15)}$$

The law of piezo-shells is given below, taking into account the voltage and the temperature effects. ([7]) Note that for the final term it is just the piezo-electric stress constants e_{31}, e_{32}, multiplied by the electric field which is voltage divided by the thickness of the piezo-layer. The variable capital V is not to be confused with ν for Poisson's ratio, V is an applied voltage.

$$\begin{bmatrix}\bar{\sigma}_{rr}\\ \bar{\sigma}_{\theta\theta}\\ \bar{\tau}_{\theta r}\end{bmatrix}=\begin{bmatrix}Q_{11} & Q_{12} & 0\\ Q_{21} & Q_{22} & 0\\ 0 & 0 & Q_{66}\end{bmatrix}\left\{\begin{bmatrix}\overline{\epsilon_{rr}}\\ \bar{\epsilon}_{\theta\theta}\\ \bar{\gamma}_{r\theta}\end{bmatrix}-\begin{bmatrix}\alpha\\ \alpha\\ 0\end{bmatrix}\omega\right\}-\begin{bmatrix}0 & 0 & e_{31}\\ 0 & 0 & e_{32}\\ 0 & 0 & 0\end{bmatrix}\begin{bmatrix}0\\ 0\\ V/t_m\end{bmatrix} \qquad \text{(eq. 5-16)}$$

The elastic stiffness has to be defined. (Gere, 2002, ref#49)

$$[Q]=\begin{bmatrix}\frac{E}{(1-\nu^2)} & \frac{\nu E}{(1-\nu^2)} & 0\\ \frac{\nu E}{(1-\nu^2)} & \frac{E}{(1-\nu^2)} & 0\\ 0 & 0 & \frac{E}{(1+\nu)}\end{bmatrix} \qquad \text{(eq. 5-17)}$$

The dielectric piezo-stress constants have to be defined as well. The research revealed that, in this case, stiffness is only in the piezo- or metal rich layer, and that the plastic's layer properties do not come into it, since this layer will not have the charge. The constants d_{31} and d_{32} are defined in the manual in appendix A, and they are strain constants. Note that Q_{11} , Q_{12}, and Q_{22} are defined for the piezo (M) layer only. The plastic layer does not come into the picture here.

$$e_{31} = d_{31}Q_{11} + d_{32}Q_{12} \qquad \text{(eq. 5-18)}$$

$$e_{32} = d_{31}Q_{12} + d_{32}Q_{22} \qquad \text{(eq. 5-19)}$$

$$e_{31} = d_{31}\left(\frac{E}{(1-v^2)}\right)_m + d_{32}\left(\frac{vE}{(1-v^2)}\right)_m \qquad \text{(eq. 5-20)}$$

$$e_{32} = d_{31}\left(\frac{vE}{(1-v^2)}\right)_m + d_{32}\left(\frac{E}{(1-v^2)}\right)_m \qquad \text{(eq. 5-21)}$$

$$\begin{bmatrix}\bar{\sigma}_{rr}\\ \bar{\sigma}_{\theta\theta}\\ \bar{\gamma}_{\theta r}\end{bmatrix} = \begin{bmatrix}\frac{E}{(1-v^2)} & \frac{vE}{(1-v^2)} & 0\\ \frac{vE}{(1-v^2)} & \frac{E}{(1-v^2)} & 0\\ 0 & 0 & \frac{E}{(1+v)}\end{bmatrix}\left\{\begin{bmatrix}\in_{rr}+z\kappa_{rr}\\ \in_{\theta\theta}+z\kappa_{\theta\theta}\\ \gamma_{r\theta}+2z\kappa_{r\theta}\end{bmatrix} - \begin{bmatrix}\alpha\\ \alpha\\ 0\end{bmatrix}\omega\right\} - \begin{bmatrix}0 & 0 & e_{31}\\ 0 & 0 & e_{32}\\ 0 & 0 & 0\end{bmatrix}\begin{bmatrix}0\\ 0\\ V/t_m\end{bmatrix}$$

(eq. 5-22)

Next step is to insert the terms for the piezo-stress constants. This was realized to be missing from the original papers, but has to be accounted for as only the piezo-layer "feels" the electric field; the other larger plastic layer does not have this property and acts as an insulator. This is a key factor when the researcher starts looking at electrical effects.

$$\begin{bmatrix}\bar{\sigma}_{rr}\\ \bar{\sigma}_{\theta\theta}\\ \bar{\gamma}_{\theta r}\end{bmatrix}=\begin{bmatrix}\frac{E}{(1-v^2)} & \frac{vE}{(1-v^2)} & 0\\ \frac{vE}{(1-v^2)} & \frac{E}{(1-v^2)} & 0\\ 0 & 0 & \frac{E}{(1+v)}\end{bmatrix}\left\{\begin{bmatrix}\in_{rr}+z\kappa_{rr}\\ \in_{\theta\theta}+z\kappa_{\theta\theta}\\ \gamma_{r\theta}+2z\kappa_{r\theta}\end{bmatrix}-\begin{bmatrix}\alpha\\ \alpha\\ 0\end{bmatrix}\omega\right\}-$$

$$\begin{bmatrix}0 & 0 & d_{31}\left(\frac{E}{(1-v^2)}\right)_m+d_{32}\left(\frac{vE}{(1-v^2)}\right)_m\\ 0 & 0 & d_{31}\left(\frac{vE}{(1-v^2)}\right)_m+d_{32}\left(\frac{E}{(1-v^2)}\right)_m\\ 0 & 0 & 0\end{bmatrix}\begin{bmatrix}0\\ 0\\ V/t_m\end{bmatrix} \qquad \text{(eq. 5-23)}$$

After inserting the dielectric constants, one solves the two matrix multiplications on the right side for the stresses

$$\begin{bmatrix}\bar{\sigma}_{rr}\\ \bar{\sigma}_{\theta\theta}\\ \bar{\gamma}_{\theta r}\end{bmatrix}=$$

$$\begin{bmatrix}\frac{E}{(1-v^2)}(\in_{rr}+z\kappa_{rr}-\alpha\omega)+ & \frac{vE}{(1-v^2)}(\in_{\theta\theta}+z\kappa_{\theta\theta}-\alpha\omega) & 0\\ \frac{vE}{(1-v^2)}(\in_{rr}+z\kappa_{rr}-\alpha\omega)+ & \frac{E}{(1-v^2)}(\in_{\theta\theta}+z\kappa_{\theta\theta}-\alpha\omega) & 0\\ 0 & 0 & \frac{E}{(1+v)}(\gamma_{r\theta}+2z\kappa_{r\theta}-\alpha\omega)\end{bmatrix}-$$

$$\begin{bmatrix}0 & 0 & d_{31}\left(\frac{E}{(1-v^2)}\right)_m+d_{32}\left(\frac{vE}{(1-v^2)}\right)_m\\ 0 & 0 & d_{31}\left(\frac{vE}{(1-v^2)}\right)_m+d_{32}\left(\frac{E}{(1-v^2)}\right)_m\\ 0 & 0 & 0\end{bmatrix}\begin{bmatrix}0\\ 0\\ V/t_m\end{bmatrix} \qquad \text{(eq. 5-24)}$$

$$\bar{\sigma}_{rr}=\frac{E}{(1-v^2)}(\in_{rr}+z\kappa_{rr}-\alpha\omega)+\frac{vE}{(1-v^2)}(\in_{\theta\theta}+z\kappa_{\theta\theta}-\alpha\omega)-$$

$$\left(V/t_m\right)\left(d_{31}\left(\frac{E}{(1-v^2)}\right)_m+d_{32}\left(\frac{vE}{(1-v^2)}\right)_m\right) \qquad \text{(eq. 5-25)}$$

$$\bar{\sigma}_{\theta\theta}=\frac{vE}{(1-v^2)}(\in_{rr}+z\kappa_{rr}-\alpha\omega)+\frac{E}{(1-v^2)}(\in_{\theta\theta}+z\kappa_{\theta\theta}-\alpha\omega)-$$

$$\left(V/t_m\right)\left(d_{31}\left(\frac{E}{(1-v^2)}\right)_m+d_{32}\left(\frac{vE}{(1-v^2)}\right)_m\right) \qquad \text{(eq. 5-26)}$$

$$\bar{\gamma}_{\theta r}=\frac{E}{2(1+v)}(\gamma_{r\theta}+2z\kappa_{r\theta}) \qquad \text{(eq. 5-27)}$$

Next one has to do the same for the dielectric constants. This part only deals with the piezo-layer. The moment only takes the curved part and the force only looks at the strains.

$$\begin{bmatrix}\bar{\sigma}_{rrd}\\ \bar{\sigma}_{\theta\theta d}\\ \bar{\gamma}_{\theta rd}\end{bmatrix}=\begin{bmatrix}Q_{11} & Q_{12} & 0\\ Q_{21} & Q_{22} & 0\\ 0 & 0 & Q_{66}\end{bmatrix}\begin{bmatrix}\in_{rr}+z\kappa_{rr}\\ \in_{\Theta\theta}+z\kappa_{\Theta\theta}\\ \gamma_{r\theta}+2z\kappa_{r\theta}\end{bmatrix} \qquad \text{(eq. 5-28)}$$

$$\begin{bmatrix}\bar{\sigma}_{rrd}\\ \bar{\sigma}_{\theta\theta d}\\ \bar{\gamma}_{\theta rd}\end{bmatrix}=\begin{bmatrix}\frac{E_m}{(1-v^2)} & \frac{vE_m}{(1-v^2)} & 0\\ \frac{vE_m}{(1-v^2)} & \frac{E_m}{(1-v^2)} & 0\\ 0 & 0 & \frac{E_m}{(1+v)}\end{bmatrix}\begin{bmatrix}\in_{rr}+z\kappa_{rr}\\ \in_{\Theta\theta}+z\kappa_{\Theta\theta}\\ \gamma_{r\theta}+2z\kappa_{r\theta}\end{bmatrix} \qquad \text{(eq. 5-29)}$$

$$\begin{bmatrix}\bar{\sigma}_{rrd}\\ \bar{\sigma}_{\theta\theta d}\\ \bar{\gamma}_{\theta rd}\end{bmatrix}=\begin{bmatrix}\frac{E_m(\in_{rr}+z\kappa_{rr})}{(1-v^2)}+\frac{vE_m(\in_{\Theta\theta}+z\kappa_{\Theta\theta})}{(1-v^2)}\\ \frac{vE_m(\in_{rr}+z\ \ rr)}{(1-v^2)}+\frac{E_m(\in_{\Theta\theta}+z\kappa_{\Theta\theta})}{(1-v^2)}\\ \frac{E_m(\gamma_{r\theta}+2z\kappa_{r\theta})}{(1+v)}\end{bmatrix} \qquad \text{(eq. 5-30)}$$

After defining the dielectric portion of the force and the portion that is through stress and temperature, the researcher is ready to put both together to come up with a unified force which in this case will be per unit width due to the fact that currently everything is defined by stress and the elements all have a common width element.

The force elements that are derived from combining the piezo-element to the temperature controlled element are as follows:

$$\begin{bmatrix}\bar{\sigma}_{rr}\\ \bar{\sigma}_{\theta\theta}\\ \bar{\gamma}_{\theta r}\end{bmatrix} =$$

$$\begin{bmatrix}\frac{E}{(1-v^2)}(\in_{rr}+z\kappa_{rr}-\alpha\omega)+ & \frac{vE}{(1-v^2)}(\in_{\theta\theta}+z\kappa_{\theta\theta}-\alpha\omega) & 0\\ \frac{vE}{(1-v^2)}(\in_{rr}+z\kappa_{rr}-\alpha\omega)+ & \frac{E}{(1-v^2)}(\in_{\theta\theta}+z\kappa_{\theta\theta}-\alpha\omega) & 0\\ 0 & 0 & \frac{E}{(1+v)}(\gamma_{r\theta}+2z\kappa_{r\theta}-\alpha\omega)\end{bmatrix} -$$

$$\begin{bmatrix}0 & 0 & d_{31}\left(\frac{E}{(1-v^2)}\right)_m + d_{32}\left(\frac{vE}{(1-v^2)}\right)_m\\ 0 & 0 & d_{31}\left(\frac{vE}{(1-v^2)}\right)_m + d_{32}\left(\frac{E}{(1-v^2)}\right)_m\\ 0 & 0 & 0\end{bmatrix}\begin{bmatrix}0\\ 0\\ V/t_m\end{bmatrix} + \begin{bmatrix}\frac{E_m(\in_{rr}+z\kappa_{rr})}{(1-v^2)}+\frac{vE_m(\in_{\theta\theta}+z\kappa_{\theta\theta})}{(1-v^2)}\\ \frac{vE_m(\in_{rr}+z\kappa_{rr})}{(1-v^2)}+\frac{E_m(\in_{\theta\theta}+z\kappa_{\theta\theta})}{(1-v^2)}\\ \frac{E_m(\gamma_{r\theta}+2z\kappa_{r\theta})}{(1+v)}\end{bmatrix}$$

(eq 5-31)

Note on the last matrix: the strain is only seen in force; the curvature is only seen in moment.

Therefore, the deriver ends up with the following equations for shear and bending stress

$$\bar{\sigma}_{rr} = \frac{E}{(1-v^2)}(\in_{rr}+z\kappa_{rr}-\alpha\omega)+\frac{vE}{(1-v^2)}(\in_{\theta\theta}+z\kappa_{\theta\theta}-\alpha\omega) -$$

$$\left(V/t_m\right)\left(d_{31}\left(\frac{E}{(1-v^2)}\right)_m + d_{32}\left(\frac{vE}{(1-v^2)}\right)_m\right)+\left(\frac{E_m(\in_{rr}+z\kappa_{rr})}{(1-v^2)}+\frac{vE_m(\in_{\theta\theta}+z\kappa_{\theta\theta})}{(1-v^2)}\right)$$

(eq. 5-32)

$$\bar{\sigma}_{\theta\theta} = \frac{vE}{(1-v^2)}(\in_{rr}+z\kappa_{rr}-\alpha\omega)+\frac{E}{(1-v^2)}(\in_{\theta\theta}+z\kappa_{\theta\theta}-\alpha\omega) -$$

$$\left(V/t_m\right)\left(d_{31}\left(\frac{E}{(1-v^2)}\right)_m + d_{32}\left(\frac{vE}{(1-v^2)}\right)_m\right)+\left(\frac{vE_m(\in_{rr}+z\ _{rr})}{(1-v^2)}+\frac{E_m(\in_{\theta\theta}+z\kappa_{\theta\theta})}{(1-v^2)}\right)$$

(eq. 5-33)

$$\bar{\gamma}_{\theta r}=\frac{E}{2(1+v)}(\gamma_{r\theta}+2z\kappa_{r\theta})+\frac{E_m(\gamma_{r\theta}+2z\kappa_{r\theta})}{(1+v)} \quad \text{(eq. 5-34)}$$

In order to get this to work for shears and moments, the deriver now has to take into consideration the different heights of the different layers that are being activated at those times. Therefore, the deriver has to take into consideration also the distance that the layer is acting for the moment definitions.

$$\frac{\bar{\sigma}_{rr}}{(arb)width} = (t_m + t_p)\left(\frac{E}{(1-v^2)}(\in_{rr} + z\kappa_{rr} - \alpha\omega) + \frac{vE}{(1-v^2)}(\in_{\Theta\theta} + z\kappa_{\Theta\theta} - \alpha\omega) - \left(V/t_m\right)\left(d_{31}\left(\frac{E}{(1-v^2)}\right)_m + d_{32}\left(\frac{vE}{(1-v^2)}\right)_m\right) + t_m\left(\frac{E_m(\in_{rr}+z\kappa_{rr})}{(1-v^2)} + \frac{vE_m(\in_{\Theta\theta}+z\kappa_{\Theta\theta})}{(1-v^2)}\right)\right.$$

(eq. 5-35)

$$\frac{\bar{\sigma}_{\theta\theta}}{(arb)widt} = (t_m + t_p)\left(\frac{vE}{(1-v^2)}(\in_{rr} + z\kappa_{rr} - \alpha\omega) + \frac{E}{(1-v^2)}(\in_{\Theta\theta} + z\kappa_{\Theta\theta} - \alpha\omega) - \left(V/t_m\right)\left(d_{31}\left(\frac{E}{(1-v^2)}\right)_m + d_{32}\left(\frac{vE}{(1-v^2)}\right)_m\right) + t_m\left(\frac{vE_m(\in_{rr}+z\kappa_{rr})}{(1-v^2)} + \frac{E_m(\in_{\Theta\theta}+z\ _{\Theta\theta})}{(1-v^2)}\right)\right.$$

(eq. 5-36)

$$\frac{\bar{\gamma}_{\theta r}}{(arb)width} = (t_m + t_p)\left(\frac{E}{2(1+v)}(\gamma_{r\theta} + 2z\kappa_{r\theta})\right) + t_m\left(\frac{E_m(\gamma_{r\theta}+2z\kappa_{r\theta})}{(1+v)}\right)$$

(eq. 5-37)

The deriver can now form equations for shear and moments in the spherical object.

2 Final force and moment equations

The reader should note that these are force or moment per unit length. Since the area in question covers the same width parameter, it is omitted for a unit length since this term drops out in all cases.

$$\bar{F}_{rr} = (t_m + t_p)\left(\frac{E}{(1-v^2)}(\in_{rr} + z\kappa_{rr} - \alpha\omega) + \frac{vE}{(1-v^2)}(\in_{\Theta\theta} + z\kappa_{\Theta\theta} - \alpha\omega) - \left(V/t_m\right)\left(d_{31}\left(\frac{E}{(1-v^2)}\right)_m + d_{32}\left(\frac{vE}{(1-v^2)}\right)_m\right)\right) + t_m\left(\frac{E_m(\in_{rr})}{(1-v^2)} + \frac{vE_m(\in_{\Theta\theta})}{(1-v^2)}\right) \quad \text{(eq. 5-38)}$$

$$\bar{M}_{rr} = \frac{(t_m+t_p)^2}{2}\left(\frac{E}{(1-v^2)}(\in_{rr} + z\kappa_{rr} - \alpha\omega) + \frac{vE}{(1-v^2)}(\in_{\Theta\theta} + z\kappa_{\Theta\theta} - \alpha\omega) - \left(V/t_m\right)\left(d_{31}\left(\frac{E}{(1-v^2)}\right)_m + d_{32}\left(\frac{vE}{(1-v^2)}\right)_m\right)\right) + \frac{(t_m+t_p)^2}{2}\left(\frac{E_m(\kappa_{rr})}{(1-v^2)} + \frac{vE_m(\kappa_{\Theta\theta})}{(1-v^2)}\right) \quad \text{(eq. 5-39)}$$

$$\bar{F}_{\theta\theta} = (t_m + t_p)\left(\frac{vE}{(1-v^2)}(\in_{rr} + z\kappa_{rr} - \alpha\omega) + \frac{E}{(1-v^2)}(\in_{\Theta\theta} + z\kappa_{\Theta\theta} - \alpha\omega) - \left(V/t_m\right)\left(d_{31}\left(\frac{E}{(1-v^2)}\right)_m + d_{32}\left(\frac{vE}{(1-v^2)}\right)_m\right)\right) + t_m\left(\frac{vE_m(\in_{rr})}{(1-v^2)} + \frac{E_m(\in_{\Theta\theta})}{(1-v^2)}\right) \quad \text{(eq. 5-40)}$$

$$\bar{M}_{\theta\theta} = \frac{(t_m+t_p)^2}{2}\left(\frac{vE}{(1-v^2)}(\in_{rr} + z\kappa_{rr} - \alpha\omega) + \frac{E}{(1-v^2)}(\in_{\Theta\theta} + z\kappa_{\Theta\theta} - \alpha\omega) - \left(V/t_m\right)\left(d_{31}\left(\frac{E}{(1-v^2)}\right)_m + d_{32}\left(\frac{vE}{(1-v^2)}\right)_m\right)\right) + \frac{(t_m+t_p)^2}{2}\left(\frac{vE_m(\kappa_{rr})}{(1-v^2)} + \frac{E_m(\kappa_{\Theta\theta})}{(1-v^2)}\right) \quad \text{(eq. 5-41)}$$

$$\bar{F}_{\theta r} = (t_m + t_p)\left(\frac{E}{2(1+v)}(\gamma_{r\theta} + 2z\kappa_{r\theta})\right) + t_m\left(\frac{E_m(\gamma_{r\theta})}{(1+v)}\right) \quad \text{(eq. 5-42)}$$

$$\bar{M}_{\theta r} = \frac{(t_m+t_p)^2}{2}\left(\frac{E}{2(1+v)}(\gamma_{r\theta} + 2z\kappa_{r\theta})\right) + \frac{(t_m+t_p)^2}{2}\left(\frac{E_m(2\kappa_{r\theta})}{(1+v)}\right) \quad \text{(eq. 5-43)}$$

These are the final equations. The next step is a side tract that the researcher feels is necessary now as reinforcement for later on in the derivation, i.e., that the main sequence being solved for is the temperature effects.

E Defining The Equilibrium Equations of Shallow Spherical Shells

First, one has to get a free body diagram of the forces around the edge, the forces in the center, and the moments that all act on the entire disk.

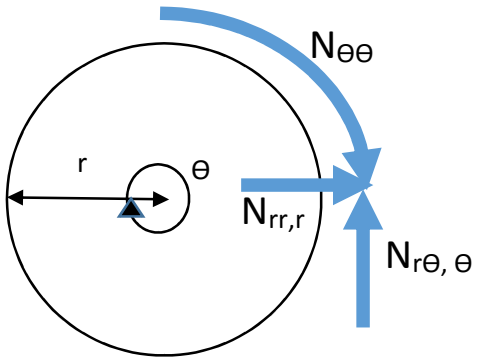

Figure 5-9: Edge forces on the disk in the XY plane (Note: q acts normal to the paper)

Next, the deriver has to put the center forces on the disk. Below are a few diagrams of the subject problem for this.

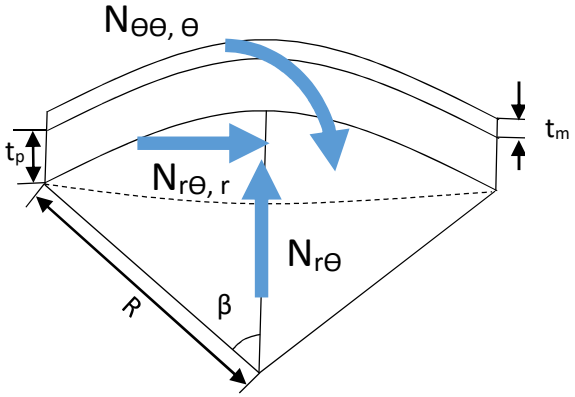

Figure 5-10: Center forces on the disk in the XZ or YX plane center and the moments that all act on the entire disk

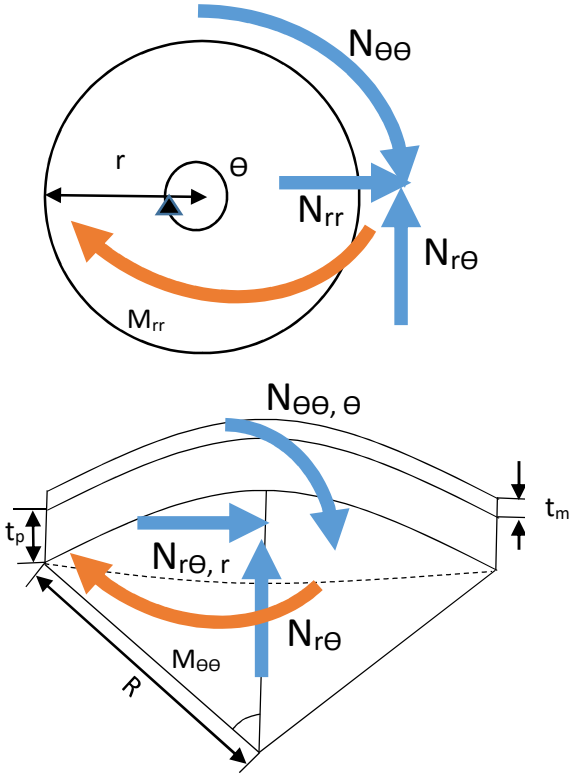

Figure 5-11: Free body diagrams showing the moments included and where they act.

For this, the researcher also has to derive the forces and the moments acting on the spherical piece.

$$F_{ij} = \int_{-t_p}^{+t_m} \sigma_{ij} dx \qquad \text{(eq. 5-44)}$$

$$M_{ij} = \int_{-t_p}^{+t_m} \sigma_{ij} x dx \qquad \text{(eq. 5-45)}$$

From these relations the sum of the forces and moments to equal zero.

For more explanation as to how these equations below are derived, please see [6].

$$(rF_{rr})\frac{\partial}{\partial r} - (F_{r\theta})\frac{\partial}{\partial \theta} - F_{\theta\theta} = 0 \qquad \text{(eq. 5-46)}$$

$$(rF_{r\theta})\frac{\partial}{\partial r} + F_{\theta\theta}\frac{\partial}{\partial \theta} + F_{r\theta}=0 \qquad \text{(eq. 5-47)}$$

$$(rM_{rr})\frac{\partial^2}{\partial r^2} + 2\left(M_{r\theta}\frac{\partial}{\partial r\partial \theta} + \frac{1}{r}M_{r\theta}\frac{\partial}{\partial \theta}\right) + \left(\frac{1}{r}\right)M_{\theta\theta}\frac{\partial^2}{\partial \theta^2} - M_{\theta\theta}\frac{\partial}{\partial r} - \left(\frac{r}{R}\right)(F_{rr} + F_{\theta\theta}) +$$

$$\left(rF_{rr}w\frac{\partial}{\partial r} + \left(\frac{1}{r}\right)F_{r\theta}w\frac{\partial}{\partial \theta}\right)\frac{\partial}{\partial r} + \left(F_{r\theta}w\frac{\partial}{\partial r} + \left(\frac{1}{r}\right)F_{\theta\theta}w\frac{\partial}{\partial \theta}\right)\frac{\partial}{\partial \theta} + qr = 0 \qquad \text{(eq. 5-48)}$$

The next step here is to get a stress function of the shallow spherical shell. This is derived by figuring out what will fit two of the three equations. What will set those equations to zero and cancel everything out. [7]

$$F_{rr} = \frac{1}{r}f\frac{\partial}{\partial r} + \frac{1}{r^2}f\frac{\partial^2}{\partial \theta^2} \qquad \text{(eq. 5-49)}$$

$$F_{\theta\theta} = f\frac{\partial^2}{\partial r^2} \qquad \text{(eq. 5-50)}$$

$$F_{r\theta} = -\left(\frac{f\frac{\partial}{\partial \theta}}{r\partial r}\right) \qquad \text{(eq. 5-51)}$$

After this, this stress function satisfies the first two equations (eq. 5-46 and 5-47). It is used in the third moment equation (eq. 5-48) at equilibrium. At this point the stress function is used to determine the critical temperature.

$$(rM_{rr})\frac{\partial^2}{\partial r^2} + 2\left(M_{r\theta}\frac{\partial}{\partial r} + \frac{1}{r}M_{r\theta}\frac{\partial}{\partial \theta}\right) + \left(\frac{1}{r}\right)M_{\theta\theta}\frac{\partial^2}{\partial \theta^2} - M_{\theta\theta}\frac{\partial}{\partial r} - \left(\frac{r}{R}\right)\left((f\frac{\partial}{\partial r} +$$

$$\frac{1}{r^2}f\frac{\partial^2}{\partial \theta^2}) + f\frac{\partial^2}{\partial r^2}\right) + \left(r\left(\frac{1}{r}f\frac{\partial}{\partial r} + \frac{1}{r^2}f\frac{\partial^2}{\partial \theta^2}\right)w\frac{\partial}{\partial r} - \left(\frac{1}{r}\right)\left(\frac{f\frac{\partial}{\partial \theta}}{r\partial r}\right)w\frac{\partial}{\partial \theta}\right)\frac{\partial}{\partial r} + \left(-\left(\frac{f\frac{\partial}{\partial \theta}}{r\partial}\right)w\frac{\partial}{\partial r} +$$

$$\left(\frac{1}{r}\right)(f\frac{\partial^2}{\partial r^2})w\frac{\partial}{\partial \theta}\right)\frac{\partial}{\partial \theta} + qr = 0 \qquad \text{(eq. 5-52)}$$

$$-(M_{rr})\frac{\partial^2}{\partial r^2} - 2\left(\frac{1}{r}\right)\left(M_{r\theta}\frac{\partial}{\partial r\partial\theta} + \frac{1}{r}M_{r\theta}\frac{\partial}{\partial\theta}\right) - \left(\frac{1}{r^2}\right)M_{\theta\theta}\frac{\partial^2}{\partial\theta^2} + \left(\frac{1}{r}\right)M_{\theta\theta}\frac{\partial}{\partial r} +$$

$$\left(\frac{1}{R}\right)\left(\left(f\frac{\partial}{\partial r} + \frac{1}{r^2}f\frac{\partial^2}{\partial\theta^2}\right) + f\frac{\partial^2}{\partial r^2}\right) - \left(\frac{1}{r}\right)wf\frac{\partial^3}{\partial r^3} - \frac{1}{r^2}wf\frac{\partial^4}{\partial r^2\partial\theta^2} + \left(\frac{1}{r^2}\right)\left(\frac{f\partial^2}{r\partial r\partial\theta}\right)w\frac{\partial^2}{\partial\theta\partial r} +$$

$$\left(\frac{f\partial^2}{r^2\partial r\partial\theta}\right)w\frac{\partial^2}{\partial r\partial\theta} - \left(\frac{1}{r^2}\right)\left(f\frac{\partial^2}{\partial r^2}\right)w\frac{\partial^2}{\partial\theta^2} - q = 0 \qquad \text{(eq. 5-53)}$$

From the above equation, the deriver collects like terms and collects terms of differentiation. The deriver also turns the moments into forces and moment arms. The equation below represents the final form after all this collection goes on of terms of the equilibrium equation.

$$\left(\frac{\frac{(t_m+t_p)^3}{2}E}{(1-v^2)} + \frac{\left(\frac{\frac{(t_m+t_p)^2}{2}E}{(1-v^2)}\right)^2}{\left(\frac{(t_m+t_p)E}{(1-v^2)}\right)}\right)€^4 w + \frac{1}{R^2}f - \left(\frac{1}{r}f\frac{\partial}{\partial r} + \frac{1}{r^2}f\frac{\partial^2}{\partial\theta^2}\right)w\frac{\partial^2}{\partial r^2} +$$

$$\frac{2}{r}\left(\frac{1}{r}f\frac{\partial}{\partial r\partial\theta} - \frac{1}{r^2}f\frac{\partial}{\partial\theta}\right)w\frac{\partial}{\partial r\partial\theta} - \frac{1}{r^2}f\frac{\partial^2}{\partial r^2}w\frac{\partial^2}{\partial\theta^2} - \frac{1}{r}f\frac{\partial^2}{\partial r^2}w\frac{dr}{dw} + \frac{2}{r^2}\left(\frac{1}{r^2}f\frac{\partial}{\partial\theta} -$$

$$\frac{1}{r}f\frac{\partial}{\partial r\partial\theta}\right)w\frac{\partial}{\partial\theta} - q = 0 \qquad \text{(eq. 5-54)}$$

F Geometric Compatibility Equation of Shallow Spherical Shells

We also need to define the geometric compatibility equation of a shallow sphere.

$$\frac{1}{r^2}\in_{rr}\frac{\partial^2}{\partial\theta^2}-\frac{1}{r}\in_{rr}\frac{\partial}{\partial r}+\frac{1}{r^2}\left(r^2\in_{\theta\theta}\frac{\partial}{\partial r}\right)\frac{\partial}{\partial r}-\frac{1}{r^2}(r\gamma_{r\theta})\frac{\partial}{\partial r\partial\theta}=\frac{€_2 w}{R}+\kappa_{r\theta}^2-\kappa_r\kappa_\theta$$

(eq. 5-55)

In order to make it easy for the reader, the researcher is going to specify the $€^4$ and the $€^2$

$$€_4=\frac{\partial^4 y}{\partial x^4}+\frac{2}{r}\frac{\partial^3 y}{\partial x^3}-\frac{1}{r^2}\frac{\partial^2 y}{\partial x^2}+\frac{1}{r^3}\frac{\partial y}{\partial x}\qquad\text{(eq. 5-56)}$$

$$€_2=-\frac{1}{r^2}\frac{\partial^2 y}{\partial x^2}+\frac{1}{r^3}\frac{\partial y}{\partial x}\qquad\text{(eq. 5-57)}$$

The researcher now needs to fill in the compatibility equation (eq. 5-55) for a shallow sphere with the equations for strain and curvature (eq. 5-3). This leads to the equation below

$$\frac{1}{r^2}\in_{rr}\frac{\partial^2}{\partial\theta^2}-\frac{1}{r}\in_{rr}\frac{\partial}{\partial r}+\frac{1}{r^2}\left(r^2\in_{\theta\theta}\frac{\partial}{\partial r}\right)\frac{\partial}{\partial r}-\frac{1}{r^2}(r\gamma_{r\theta})\frac{\partial^2}{\partial r\partial\theta}=\frac{€_2 w}{R}+\kappa_{r\theta}^2-\kappa_r\kappa_\theta$$

(eq. 5-55)

What has to happen here is that the deriver has to go back and use Sanders' equations and the original equations that were found to calculate the stresses in the hemisphere and fill those into the compatibility equation and get an equation in the form of f(stress) and w(deflection) in the z direction.

$$\frac{1}{r^2}\in_{rr}\frac{\partial^2}{\partial\theta^2}-\frac{1}{r}\in_{rr}\frac{\partial}{\partial r}+\frac{1}{r^2}\left(r^2\in_{\theta\theta}\frac{\partial}{\partial r}\right)\frac{\partial}{\partial r}-\frac{1}{r^2}(r\gamma_{r\theta})\frac{\partial}{\partial r\partial\theta}=\frac{€_2 w}{R}+\left(w\frac{\partial^2}{\partial r\partial\theta}-\frac{w\partial}{r^2\partial\theta}\right)^2-w\frac{\partial^2}{\partial r^2}\left(\frac{w\partial^2}{r^2\partial\theta^2}+\frac{w\partial}{r\partial r}\right)\text{ (eq. 5-58)}$$

The final simplified form of the equilibrium equation (eq. 5-58) for a shallow spherical shell appears below.

$$\frac{1}{\left(\frac{(t_m+t_p)E}{(1-v^2)}\right)(1-v^2)}\epsilon_4 f = \frac{\epsilon_2 w}{R} + \left(w\frac{\partial^2}{\partial r\partial\theta} - \frac{w\partial}{r^2\partial\theta}\right)^2 - w\frac{\partial^2}{\partial r^2}\left(\frac{w\partial^2}{r^2\partial\theta^2} + \frac{w\partial}{r\partial r}\right) \qquad \text{(eq. 5-59)}$$

1 Solving for w and f

The next step is to take the equilibrium equation and remove insignificant factors. Since that Θ is of a small value compared to r, the derivatives for it are removed and as a result the geometric compatibility equation is changed to

$$\frac{1}{\left(\frac{(t_m+t_p)E}{(1-v^2)}\right)(1-v^2)}\epsilon_4 f = \frac{\epsilon_2 w}{R} + \frac{\nabla^2 w}{R} - \frac{w\partial^3}{r\partial r^3} \qquad \text{(eq. 5-60)}$$

The equilibrium equation is changed to

$$\left(\frac{\frac{(t_m+t_p)^3}{2}E}{(1-v^2)} + \frac{\left(\frac{\frac{(t_m+t_p)^2}{2}E}{(1-v^2)}\right)^2}{\left(\frac{(t_m+t_p)E}{(1-v^2)}\right)}\right)\epsilon_4 w + \frac{1}{R^2}f - \left(\frac{1}{r}f\frac{\partial}{\partial r}\right)w\frac{\partial^2}{\partial r^2} - \frac{1}{r}f\frac{\partial^2}{\partial r^2}\frac{dw}{dr} - q = 0$$

(eq. 5-61)

2 Boundary Conditions

After the above equation has been formulated, the next step is to define the problem's boundary conditions. These boundary conditions are needed to solve the fourth

order and second order differential equations that we have produced. These boundaries are as follows.

$$r = 0 \xrightarrow{yields} w = W, \frac{w\partial}{\partial r} = 0, N_{rr} = finite \qquad \text{(eq. 5-62)}$$

$$r = a \xrightarrow{yields} w = W, \frac{w\partial}{\partial r} = 0, N_{rr} = N_{r0} \qquad \text{(eq. 5-63)}$$

After this, a function for W the amplitude of deflection is needed. This is as follows

$$w = W\frac{\left(a^2 - r^2\right)^2}{a^4} \qquad \text{(eq. 5-64)}$$

The next step is to substitute it into the differential equation that was derived (eq. 5-61) and plug in, solve it, and solve it for the constants.

$$f\frac{\partial}{\partial r} = \frac{\left(\frac{(t_m + t_p)E}{(1-v^2)}\right)(1-v)W}{a^4 R}\left(\frac{r^5}{6} - \frac{a^2 r^3}{2}\right) - \frac{\left(\frac{(t_m + t_p)E}{(1-v^2)}\right)(1-v)W^2}{a^8}\left(\frac{r^7}{6} - \frac{2a^2 r^5}{3} + a^4 r^3\right) +$$

$$c_1 r ln r + c_2 r + \frac{c_3}{r} \qquad \text{(eq. 5-65)}$$

The constants c_1 and c_3 equal zero since the r term cannot return a negative or be undefined since N_{r0} has a value for the buckling. Therefore, the only constant left to solve for is c_2. This constant appears below.

$$c_2 = \frac{\left(\frac{(t_m + t_p)E}{(1-v^2)}\right)(1-v)W}{3R} + \frac{\left(\frac{(t_m + t_p)E}{(1-v^2)}\right)(1-v)W^2}{2a^2} + N_{r0} \qquad \text{(eq. 5-66)}$$

Therefore, subbing in c_2 into the equation yields the following.

$$f\frac{\partial}{\partial r}=\frac{\left(\frac{(t_m+t_p)E}{(1-v^2)}\right)(1-v)W}{a^4R}\left(\frac{r^5}{6}-\frac{a^2r^3}{2}\right)-\frac{\left(\frac{(t_m+t_p)E}{(1-v^2)}\right)(1-v)W^2}{a^8}\left(\frac{r^7}{6}-\frac{2a^2r^5}{3}+a^4r^3\right)+$$

$$\frac{\left(\frac{(t_m+t_p)E}{(1-v^2)}\right)(1-v)Wr}{3R}+\frac{\left(\frac{(t_m+t_p)E}{(1-v^2)}\right)(1-v)W^2r}{2a^2}+N_{r0}r \qquad \text{(eq. 5-67)}$$

This is not the end equation, as the value for the external pressure has to be solved for. The first thing that has to be done is that this resultant has to be subbed back into the differential equation that the deriver had prior to finding constants. [7] Additionally, the residual equation is set to zero, and going via the Gerlerkin method the constants of the orthogonal equation is solved for [7].

$$q=\left(\frac{64\left(\frac{\frac{(t_m+t_p)^3}{2}E}{(1-v^2)}+\frac{\left(\frac{\frac{(t_m+t_p)^2}{2}E}{(1-v^2)}\right)^2}{\left(\frac{(t_m+t_p)E}{(1-v^2)}\right)}\right)}{a^4}+\frac{3\left(\frac{(t_m+t_p)E}{(1-v^2)}\right)(1-v^2)}{7R^2}\right)W+$$

$$\frac{1385\left(\frac{(t_m+t_p)E}{(1-v^2)}\right)(1-v^2)W^2}{693a^2R}+\frac{848\left(\frac{(t_m+t_p)E}{(1-v^2)}\right)(1-v^2)W^3}{429a^4}+\frac{40\ \ r_0W}{7a^2}+\frac{2}{R}N_{r0}r \qquad \text{(eq. 5-68)}$$

The boundary conditions must be set and N_{r0} must be solved for. Once the deriver has this result then the critical buckling temperature can be solved for. ([7]) Below is the energy gradient that has to be solved for in the equation.

$$0 = \int_0^a ru \frac{\partial}{\partial r} dr \qquad \text{(eq. 5-69)}$$

Once integrated over the area from 0 to a [7]

The deriver introduces a temperature term for term T for simplification. This T term is as follows

$$T = \omega \left(E_m \frac{t_m}{t_m + t_p} + E_p \frac{t_p}{t_m + t_p} \right) \left(\alpha_m \frac{t_m}{t_m + t_p} + \alpha_p \frac{t_p}{t_m + t_p} \right) \qquad \text{(eq. 5-70)}$$

All these terms were defined earlier on, and if the reader needs clarification, read the section on temperature again.

$$u \frac{\partial}{\partial r} = \frac{1}{\left(\left(\frac{(t_m + t_p)E}{(1-\nu^2)} \right) + t_m Q_{11}^m \right)(1-\nu^2)} \left(\frac{\partial f}{r} - \nu \frac{\partial f^2}{\partial r^2} \right) + \frac{\left(\frac{(t_m + t_p)^2}{2} E \right)}{\left(\frac{(t_m + t_p)E}{(1-\nu^2)} \right) + t_m Q_{11}^m} w - \frac{1}{2} w - \frac{w}{R} +$$

$$\frac{V_a d_{31} Q_{11}^m \left((0) for\ temp \right)}{\left(\left(\frac{(t_m + t_p)E}{(1-\nu^2)} \right) + t_m Q_{11}^m \right)(1-\nu^2)} + \frac{T((0) for\ voltage)}{\left(\frac{(t_m + t_p)E}{(1-\nu^2)} \right) + t_m Q_{11}^m} \qquad \text{(eq. 5-71)}$$

Note the notation that any term with a voltage will be a zero term for temperature and any T term will be zero when voltage is strictly applied.

$$N_{r0} = -(1+v)T - \frac{V_a d_{31} Q_{11}^m}{1-v} + W(1+v)\left(\frac{\left(\left(\frac{(t_m+t_p)E}{(1-v^2)}\right)+t_m Q_{11}^m\right)}{3R} - \frac{2\left(\frac{\frac{(t_m+t_p)^2}{2}E}{(1-v^2)}\right)}{a^2} - \frac{5\left(\frac{(t_m+t_p)E}{(1-v^2)}\right)}{36R}(1+v)\right) + \frac{W^2(1+v)}{a^2}\left(\frac{-13\left(\frac{(t_m+t_p)E}{(1-v^2)}\right)}{72}(1+v) + \frac{2\left(\left(\frac{(t_m+t_p)E}{(1-v^2)}\right)+t_m Q_{11}^m\right)}{3}\right)$$

(eq. 5-72)

This leads to the final equation for the pressure which gets set to zero as. [7]

$$q = \left(\frac{64\left(\frac{\frac{(t_m+t_p)^3}{2}E}{(1-v^2)} + \frac{\left(\frac{\frac{(t_m+t_p)^2}{2}E}{(1-v^2)}\right)^2}{\left(\frac{(t_m+t_p)E}{(1-v^2)}\right)}\right)}{a^4} + \frac{3\left(\frac{(t_m+t_p)E}{(1-v^2)}\right)(1-v^2)}{7R^2}\right)W + \frac{1385\left(\frac{(t_m+t_p)E}{(1-v^2)}\right)(1-v^2)W^2}{693a^2R} + \frac{848\left(\frac{(t_m+t_p)E}{(1-v^2)}\right)(1-v^2)W^3}{429a^4} + \frac{40W}{7a^2}\left(-(1+v)T - \frac{V_a d_{31} Q_{11}^m}{1-v} + W(1+v)\left(\frac{\left(\left(\frac{(t_m+t_p)E}{(1-v^2)}\right)+t_m Q_{11}^m\right)}{3R} - \frac{2\left(\frac{\frac{(t_m+t_p)^2}{2}E}{(1-v^2)}\right)}{a^2} - \frac{5\left(\frac{(t_m+t_p)E}{(1-v^2)}\right)}{36R}(1+v)\right) + \right.$$

$$\frac{W^2(1+v)}{a^2}\left(\frac{-13\left(\frac{(t_m+t_p)E}{(1-v^2)}\right)}{72}(1+v)+\frac{2\left(\left(\frac{(t_m+t_p)E}{(1-v^2)}\right)+t_mQ_{11}^m\right)}{3}\right)+\frac{2}{R}\left[-(1+v)T-\frac{V_ad_{31}Q_{11}^m}{1-v}+\right.$$

$$W(1+v)\left(\frac{\left(\left(\frac{(t_m+t_p)E}{(1-v^2)}\right)+h_mQ_{11}^m\right)}{3R}-\frac{2\left(\frac{\frac{(t_m+t_p)^2}{2}E}{(1-v^2)}\right)}{a^2}-\frac{5\left(\frac{(t_m+t_p)E}{(1-v^2)}\right)}{36}(1+v)\right)+$$

$$\left.\frac{W^2(1+v)}{a^2}\left(\frac{-1\ \left(\frac{(t_m+t_p)E}{(1-v^2)}\right)}{72}(1+v)+\frac{2\left(\left(\frac{(t_m+t_p)E}{(1-v^2)}\right)+t_mQ_{11}^m\right)}{3}\right)\right] \qquad \text{(eq. 5-73)}$$

This equation q gets set for zero unless the piezo-button is activated by an increase or decrease in pressure. Then the critical buckling temperature or voltage will change due to the fact that there is also a net pressure acting on the dome shape.

A simplification: the total thickness

$$t_m + t_p = t_t \quad \text{(eq. 5-74)}$$

The equation simplifies to

$$q = \left(\frac{64\left(\frac{\frac{(t_t)^3}{2}E}{(1-v^2)} + \frac{\left(\frac{\frac{(t_t)^2}{2}E}{(1-v^2)}\right)^2}{\left(\frac{(t_t)E}{(1-v^2)}\right)} \right)}{a^4} + \frac{3\left(\frac{(t_t)E}{(1-v^2)}\right)(1-v^2)}{7R^2} \right) W + \frac{1385\left(\frac{(t_t)E}{(1-v^2)}\right)(1-v^2)W^2}{693a^2R} +$$

$$\frac{848\left(\frac{(t_t)E}{(1-v^2)}\right)(1-v^2)W^3}{429a^4} - (1+v)T\left(\frac{40}{7a^2}\right) - \frac{V_a d_{31} Q_{11}^m}{1-v}\left(\frac{40W}{7a^2}\right) + \left(\frac{40}{7a^2}^2\right)(1+$$

$$v)\left(\frac{\left(\left(\frac{(t_t)E}{(1-v^2)}\right) + t_m Q_{11}^m\right)}{3R} - \frac{2\left(\frac{\frac{(t_t)^2}{2}E}{(1-v^2)}\right)}{a^2} - \frac{5\left(\frac{(t_t)E}{(1-v^2)}\right)}{36R}(1+v) \right) + \left(\frac{40}{7a^2}^3\right)\frac{(1+v)}{a^2}\left(\frac{-1\ \left(\frac{(t_t)E}{(1-v^2)}\right)}{72}(1+ \right.$$

$$\left. v) + \frac{2\left(\left(\frac{(t_t)E}{(1-v^2)}\right) + t_m Q_{11}^m\right)}{3} \right) - \frac{2(1+v)T}{R} - \frac{2V_a d_{31} Q_{11}^m}{R(1-v)} + W(1+v)\left(\frac{2}{R}\right)\left(\frac{\left(\left(\frac{(t_t)E}{(1-v^2)}\right) + h_m Q_{11}^m\right)}{3R} - \right.$$

$$\left. \frac{2\left(\frac{\frac{(t_t)^2}{2}E}{(1-v^2)}\right)}{a^2} - \frac{5\left(\frac{(t_t)E}{(1-v^2)}\right)}{36}(1+v) \right) + \frac{2W^2(1+v)}{Ra^2}\left(\frac{-13\left(\frac{(t_t)E}{(1-v^2)}\right)}{72}(1+v) + \frac{2\left(\left(\frac{(t_t)E}{(1-v^2)}\right) + t_m Q_{11}^m\right)}{3} \right)$$

(eq. 5-75)

G Calculation

A simple calculation is done to illustrate how this new piezo-electric equation works. For this only temperature is done; however, more calculations will be done in later chapters for this.

v	0.3	dimensionless	Poisson's ratio
E1	449616	PSI	plastic E
E2	290075	PSI	piezo E
d31	23	PSI/V	dielectric constant
Va	0	V	voltage applied
Q11	494083.52	PSI	stiffness constant
W(dh)	0.0156	In	deflection (in.)
a	0.0067723	In	Rsin (theta)
R	0.039	In	radius of the disk (in.)
deltaT	50	F	temperature in F
alpha1	0.0000795	1/F	plastic alpha (co-efficient of expansion)
alpha2	0.000071	1/F	piezo alpha (co-efficient of expansion)
t1	0.0078125	In	plastic layer thickness
t2	0.0043307	In	piezo-layer thickness
C	3860.0275	Constant	constant used for simplification
B	30.156465	Constant	constant used for simplification

Figure 5-12: Calculation of the deflection of the disk at ⅝ in. diameter, a temperature change of 50ºF and no voltage.

H Comparison to Boroujerdy's Methods

Professor Boroujerdy did similar work on shallow spherical shells. Boroujerdy's method was to use Sanders' equations and thin-shell theory to come up with the flip effect equations. One of the things the researcher did was take the graph below from Boroujerdy's paper, which he theoretically came up with the snap-through effect with. This is a comparison of the pressure versus a constant temperature and varying thickness on a disk.

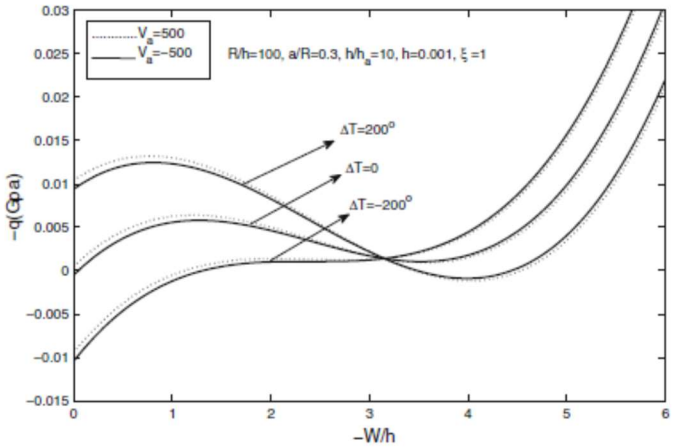

Boroujerdy's paper ([8])

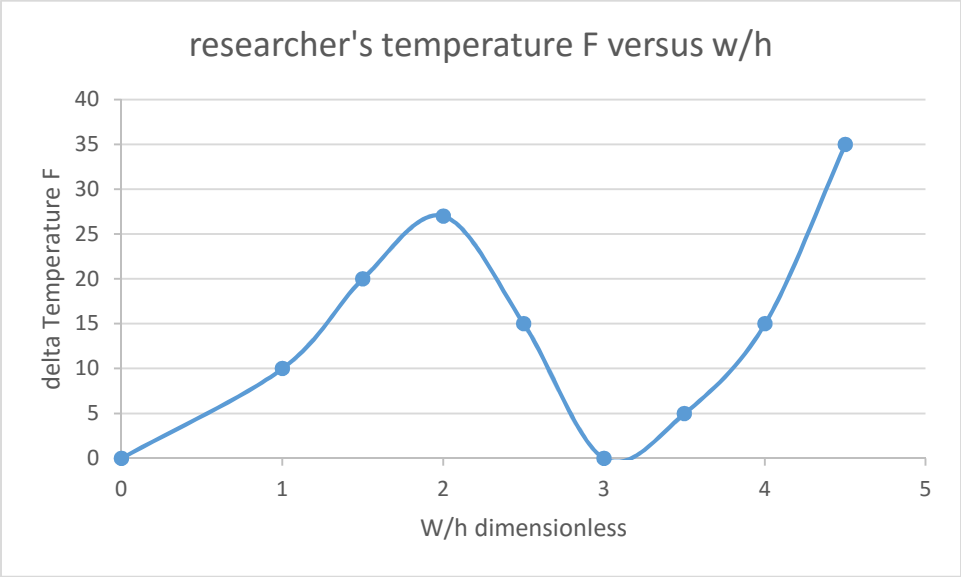

Researcher's results from the equation

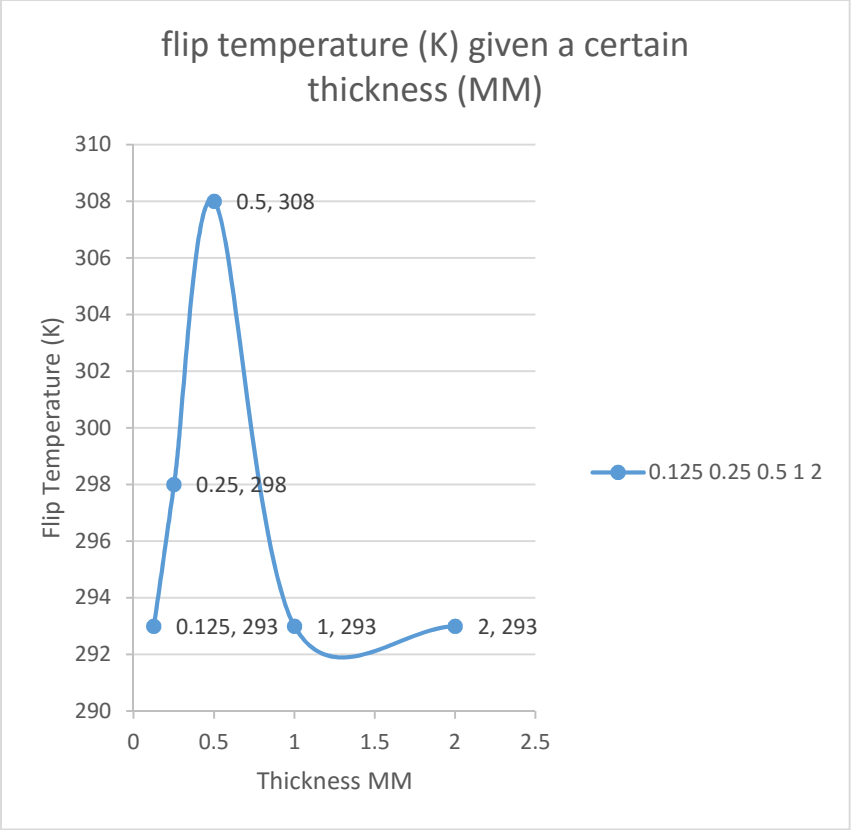

Figure 5-13: Boroujerdy's paper versus researcher's graph from finite element models.

What can be seen is that the researcher's results follow a similar trend to those of Boroujerdy. What can also be seen is that the trend-line follows a similar pattern, which is a cubic polynomial expression. In conclusion, it can be said that this equation follows closely with research that was done previously.

The model that was used by the researcher appears below. It was not possible to reproduce Boroujerdy's results since the paper was theoretical versus my practical results.

Thickness versus the flip effect (finite element methods)

thickness (mm)	mode	minimum height (x) cm	maximum height (x) cm	max stretch	minimum stretch	flip effect seen	flip temperature (K)
0.125	4	NA	NA	NA	NA (flat)	unstable	293
0.25	1	-3	9	10	2	yes	298
0.5	1	-1	8.5	10	3	yes	308
1	1	1.5	7	9	5	slight	293
2	Fund	3	5	8.5	6	no	293

Figure 5-14: Thickness versus the flip effect (finite element methods)

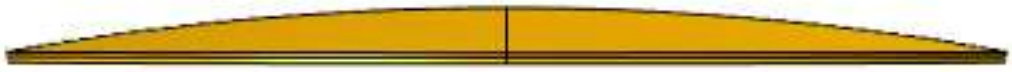

Figure 5-15: Typical spherical shallow shell before flipping in COMSOL

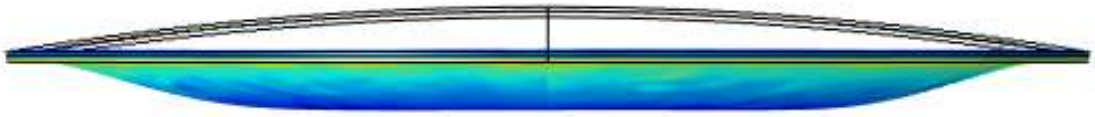

Figure 5-16: Buckled piezo-electric model (Note: for other models the shape follows similar)

Conclusions

From the results the researcher obtained above, it can be seen that the graphs are similar to the results that were obtained in the paper. From this, the thesis can move on to following the path of the energy effect. After a conceptual path of the energy is looked at, the thesis will turn to how the final shape was derived through COMSOL. Following that,

industry availability is looked at and the final shape is modified to what is currently available for building a switch.

Chapter 6

Pre-Modeling of Final Shape

The final shape to be researched for this project was selected by going over multiple objects and trying to find the easiest shape to explain while also being able to get a succinct flip on the COMSOL models. After this shape was selected, the intent was to go to the industry and see if this shape was manufactured, and if not to consider what would be a suitable alternative. This is covered in the next section of this research.

A. Bi-material strip

The original idea was to go with a bi-material strip that was seen in the pre-research. This is the shape that John Harrison selected, back at the beginning of the background research, to equalize clock movements. It was the original application of the bi-metallic strip. Refer back to the background information in chapter 2 to get more information. The bi-material strip started off as a flat piece, however during prior background research the strip with a bend was researched. The bi-material strip seen below is the first one the researcher tried.

Figure 6-1: Original shape of bi-material strip

Material Properties Inputted

E_1 = 200X10^9PA

E_2 = 69X10^9PA

T_1 = 0.1 mm

T_2 = 0.1 mm

Θ = 20 degrees

Radius = 1 M

Width = 5 MM

$T_0 = 273$ K

$T_1 = 500$ K

Given these material properties, the figure below shows the original result of the trials. Obviously after a temperature change was introduced, the final shape is below.

Figure 6-2: Shape of bi-material strip after temperature change (Note: There is a double bend in this strip showing it entered a higher mode of deformation.)

What was found in the final shape, which was able to achieve a flip effect, where the object flipped to the other side, is something in this model called a double bend. The final shape of the strip actually caused a second buckling mode to be activated. In turn, this showed the researcher that the shape was too thin, and that a thicker and more homogeneous shape was needed.

The second experiment was with electrical charge

Figure 6-3: Original shape of bi-material strip with electric charge

Material Properties Inputted

E_1 = 200X10^9PA

E_2 = 69X10^9PA

T_1 = 0.1 mm

T_2 = 0.1 mm

Θ = 20 degrees

Radius = 1 M

Width = 5 MM

V_0 = 0 Volts

V_1 = 90 Volts

Figure 6-4: Shape of strip after flip

The results were similar between the temperature change and the electrical change. The strip did have a flip effect, but ended up doing a double curve, which means that the shape reached a second higher mode.

The problem with both of these models was that there was no stability of the model, as it was showing the double bend in it meaning that the strip was too thin. It was also found that with a flat sheet a secondary flip effect happened in the transverse direction along where the strip was not clamped.

B. Circular Dome Piece

The next model had to move away from just a rectangular plate clamped at either of the shorter ends to a more stable shape. The more stable shape that was found was the disk. With the disk, however, the researcher ran into another issue that will be explained below.

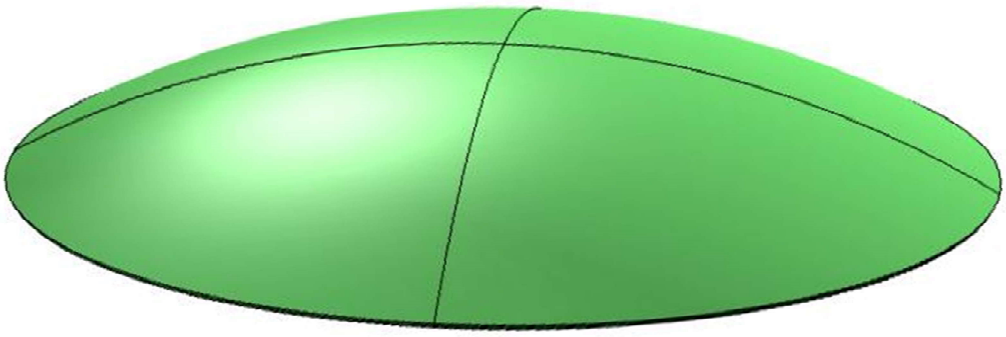

Figure 6-5: Circular dome plate model before flip

Material Properties Inputted

E_1 = 200X10^9PA

E_2 = 69X10^9PA

T_1 = 0.1 mm

T_2 = 0.1 mm

Θ = 10 degrees to 20 degrees total

Radius = 1 M

$V_0 = 0$ Volts

$V_1 = 90$ Volts

Figure 6-6: Circular dome model after flip (Note that there is still a bulge upward signaling that it is not a complete flip through.)

What can be seen from the result is that the flip did not go entirely through; it did not even reach the first mode. It was also discovered that this is not stable, as it will be forced to go back to the fundamental mode. This will not work, as for the flip effect to be achieved the shape has to buckle and go to the other side to show that a complete flip can occur.

C. Dome Shape with Top Cut off (Washer)

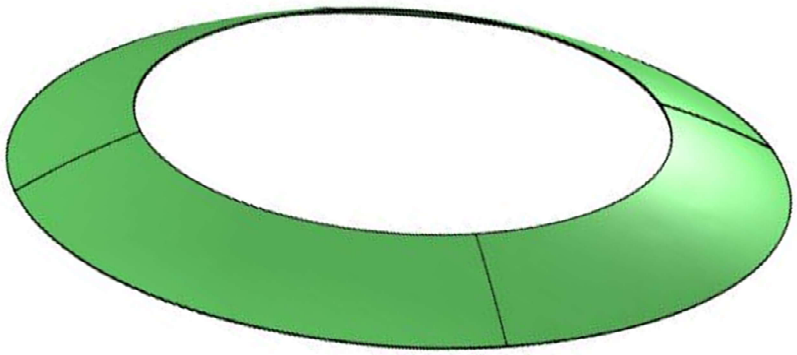

Figure 6-7: Final shape that was selected to move forward.

The next shape that was proposed was a "washer type" shape. This shape is similar to the previous shape given its stability, but with a hole cut out of the center.

Material Properties Inputted

E_1 = 200X10^9PA

E_2 = 69X10^9PA

T_1 = 0.1 mm

T_2 = 0.1 mm

Θ = 10degrees to 20 degrees total

Radius = 1 M

V_0 = 0 Volts

V_1 = 90 Volts

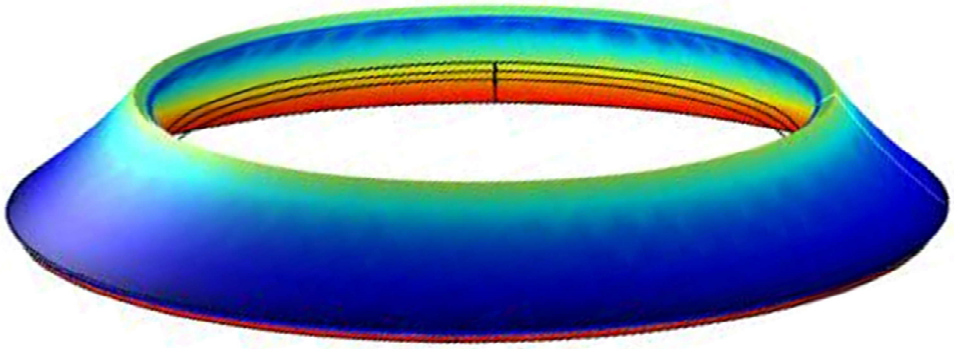

Figure 6-8: Final shape of the washer at +90 Volts (This was to show that it works.)

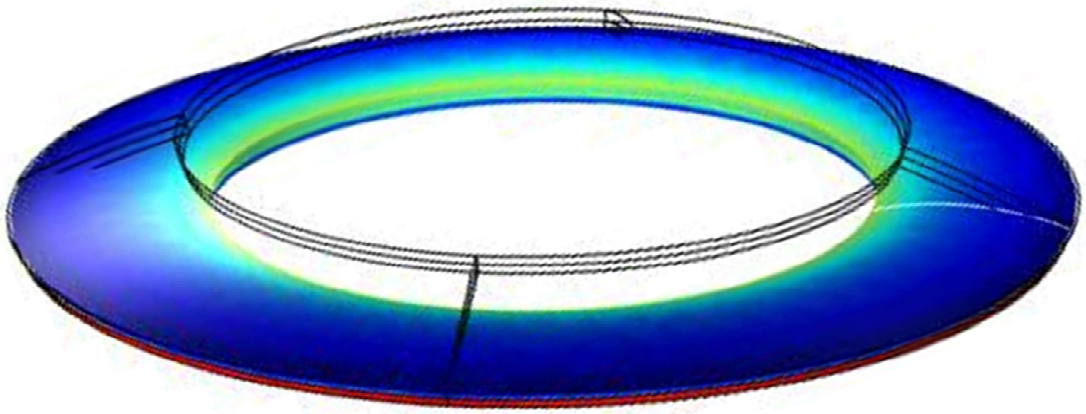

Figure 6-9: Final washer type shape at –90 volts

The fourth and final model finally had a disk that actually showed the flip effect and how it worked. The other models were not as definitive and showed that there was some instability with the results. This is the shape that was to move forward for the experiments. It was this shape that I approached the industry with, finally settling on a suitable shape with which to carry out my experiments. This researcher could then prove his point that the flip effect is achievable.

After Final Shape Achieved

After the final shape was achieved the next step was to graph out when and where a noticeable flip effect was to occur at what temperature and what it would look like given various thicknesses to see whether the flip effect would work.

Material Properties Inputted

E_1 = 200X10^9PA

E_2 = 69X10^9PA

T_1 = varies see chart

T_2 = varies see chart

L = 10 mm

Θ = 10 degrees with 20 degrees taken in the center

full rotation of model

Radius = 1 M

Thickness versus the flip effect (finite element methods)

thickness (mm)	mode	minimum height (x) cm	maximum height (x) cm	max stretch	minimum stretch	flip effect seen	flip temperature (K)
0.125	4	NA	NA	NA	NA (flat)	unstable	293
0.25	1	-3	9	10	2	yes	298
0.5	1	-1	8.5	10	3	yes	308
1	1	1.5	7	9	5	slight	293
2	Fund	3	5	8.5	6	no	293

Figure 6-10: Thickness versus the flip effect (finite element methods)

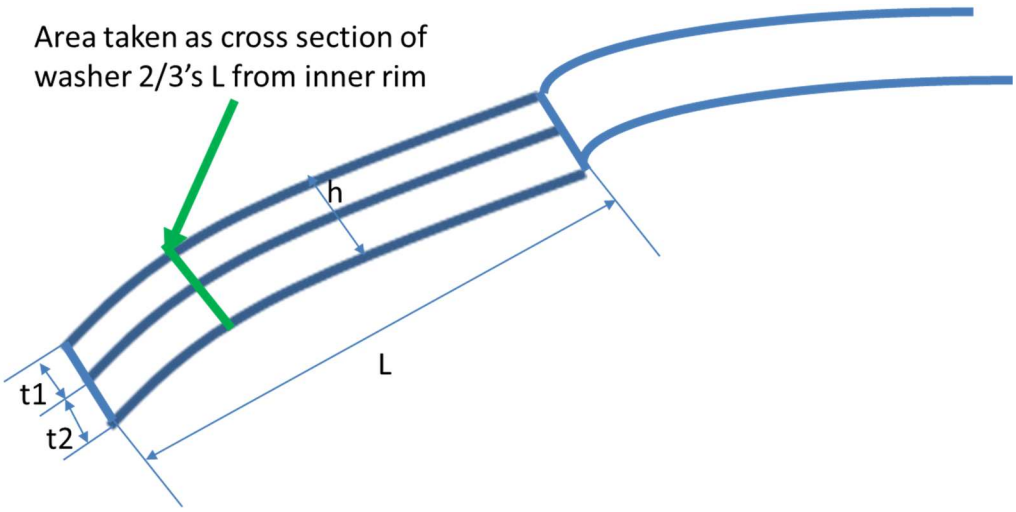

Figure 6-11: Cross section of a typical washer used in the FEM of the shape.

It was found that at a certain thickness the washer would become too thick for a noticeable flip effect to occur. What this indicated was that there was an ideal "goldilocks range" of thicknesses for this shape. Too thin and the shape would not work; too thick and the washer would not bend at all. To move forward it was required to find a suitable shape given the limitations.

Chapter 7

Industry Analysis and Input

The reason why an analysis of what is available in the industry had to be made was because a researcher has a theoretically unlimited choice in selecting piezo-electric shapes. However, there is one critical practical element for a researcher to understand. This is the fact that it takes gargantuan amounts of resources to make a series of piezo-electric shapes if they are not already available on the market, or if an entity has not already put the money up-front for constructing them. A few companies that the researcher contacted were manufacturers of piezo-electrical shapes. They stated that an experimenter would have to pay for the engineering design and simulation costs to design the shape currently prescribed in the previous section. Then the production of such a shape would require new molds which go into the factory's retooling efforts, the costs of which would be passed on to the customer.

The companies were also only willing to make the part if a researcher gave a specific order for a minimum of 1000 pieces. The final quote the researcher was given was roughly between $300K to half a million dollars to make a new piezo-shape. Therefore, since it is not financially possible for a researcher to get a new shape made, the author had to choose from manufactured shapes that existed in the industry.

It was found that disks with the tops shaved off had not yet been engineered by any firm. There were a number of disks on the market, but since this shape had not fully flipped through, it was one option. Another option that was explored was a flexible piezo-polymer

product. A third option that was also considered was just having a square for the piezo-electrical device and dealing with the rough repetitive two-way calculations later.

Piezo-disks

Researching piezo-ceramic disks, the researcher found a couple of companies that dealt in them. The main one was Piezo Systems. They had disks that had a little movement in them, but for an amount of movement that would be noticeable a one-inch disk or greater was required. The cost of one disk was impossibly high compared to the amount of material that one gets in one disk. Since the manufacturing costs of one of these disks would be extremely cost prohibitive, a different option was researched to get a better handle on the costs that are associated with these disks.

In the end, it was found that these ceramic disks were also difficult to clamp and create a good bond with. With the disk being made out of ceramic, which is a very brittle and rigid object, it was tough to design a rigid support without prematurely breaking the disk and rendering is useless. Since the design of a clamping support was also prohibitive, the decision was made not to pursue the piezo-ceramics any further than what had already been found. Instead, the conclusion that it was better to find a different piezo material and continue from there became obvious.

Piezo-film

Another option that was studied was using piezo-electric polymer films. This was a great find, because it is flexible and could be molded into a shape that would work for this thesis and experiment. The piezo-film comes in thin sheets and can be very inexpensive if mass-produced. The manufacturing of this is a lot easier, as instead of it

being manufactured individually and baked in an oven it can be coated with silver ink on a sheet and then cut to specified lengths. It also works out if there is high enough demand for these. This is also perfect due to the quick manufacturing time for them.

As a plastic, this material is a very ductile and can be easily replaced when it is broken. This bi-material object can also be very lightweight if it is made from a polymer-base sheet. The only negative to a polymer is temperature or electrical limits which have to be designed for and taken into consideration.

Piezo-electric Polymer Term

The piezo-electric polymers are known as PVDFs. They are a special class of piezo-electric elements. They first came about after it was found that whale bones and tendons exhibit a weak piezo-electric effect. Thus began the hunt for an organic (carbon based) element capable of displaying the piezo-electric properties. This discovery occurred in the 1960s. "In 1969 Kawai discovered Polarized Polyvinadilene Fluoride (or PVDF) displays a very high piezo-electric activity." (Kutz, 2015, [28]) This kick started piezo-electric polymers, which are what are used in the present thesis.

The PVDFs are manufactured in a layering process. This is a very inexpensive process compared to other manufacturing techniques: "the vinadilene fluoride monomer displays a high semi-crystalline polymer upon manufacture; this yields a high piezo-electricity content." (Kutz, 2015, [28]). This forms the betta layer for the formation of the piezo-electric element. This object is also orthotropic in nature. The chemical compound appears below, and is rather simple compared to other plastics.

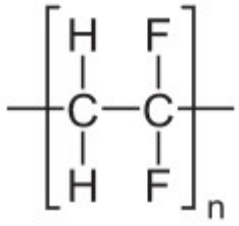

Figure 7-1: Example of a PVDF chemical compound (Plastics Europe.org, [30])

An additional discovery related to PVDFs is that their Curie point was rather low. The Curie point is actually only 103º C compared to iron, which is 770 º C. While this is rather low, there are other advantages to using PVDFs. According to a website on the industry of plastics and polymers, PVDF material is an attractive choice because it "has a very high purity and is chemically inert to most acids, aliphatic and aromatic organic compounds, chlorinated solvents, and alcohols. It is highly abrasion resistant, compared to that of polyamides, and has a low coefficient of friction. PVDF can be used within a wide range of temperatures (making it an excellent fire resistant), is unaffected by UV light and has a strong resistance to radiation. PVDF has a good capacity for thermoforming and can very easily be joined by welding." (PlasticsEurope, 2015, [30]) There is ample evidence above why these are great plastics to select for making a switch and why I went ahead and made my switch out of them.

PVDFs are also able to carry a large charge. "Large piezo-electric d33 coefficients around 600pC/N are found in corona-charged non-uniform electrets consisting of elastically "soft" (microporous polytetrafluoroethylene PTFE) and "stiff" (perfluorinated cyclobutene PFCB) polymer layers." (Neugschwandtner, 2000, [31]) This is good because then the deformation can be more pronounced and cause a larger reaction.

Most PVDFs are used in pipe lining applications. There was also this additional property information found on another website.

Properties	Repeat Unit
Glass transition temperature: -38°C.	
Melting temperature: 160° C	$C_2H_2F_2$
Amorphous density at 25° C: 1.74 g/cm^3	$-[CH_2-CF_2]-$
Crystalline density at 25° C: 2.00 g/cm^3	
Molecular weight of repeat unit: 64.03 g/mol	
Typical physical properties	

Figure 7-2: Typical properties of PVDFs (Plastics Europe.org, [30])

In conclusion, it was stated that the thesis would turn eventually to a piezo-electric polymer. The other option, piezo-ceramics, was just too cost prohibitive and broke too easily. Additionally, one has to look at what added value can be obtained. Whereas a rigid plate is expensive, a flexible plate is easy to work with and can be molded. Therefore, for the remainder of the thesis we focused strictly on the polymers.

Chapter 8

Piezo-electric Temperature Effect Experiment Switches

The original purpose of this thesis was to study the piezo-electric effect and make a near-perfect piezo-electrical switch. The term perfect has been described before in the previous section as a switch that in its form is completely shut off and does not lose energy to leakage. This thesis did take a twist, though, as information was discovered from one of the providers of the piezo-electric strips.

One of the two suppliers of piezo-materials provided a few tips on the purpose of the temperature check in the piezo-electric strips. The main tip was that the piezo-electric strip would react to temperature changes better than it would to electrical effects, and that temperature change should be looked into. The other tip was that piezo-films are the best way to get movement in a piezo-electrical object. The researcher decided to build a temperature controlled switch with a piezo-electric strip as well as an electrical one. One application of a piezo-electric temperature controlled switch is to switch on and off a device that might be subject to over-heating or freezing. This would mostly be used in motors and electrical devices in which a temperature dependent sensor with a temperature dependent switch would be critical in order to shut down a machine that might otherwise overheat.

The temperature switch is actually easy to build and can be left separate to take in temperature effects from the external environment. It would ideally be attached to a motor and be able to shut the motor off. This can happen as it is a piezo-electric material, and when a piezo-electric strip moves it does give off an electrical charge. This charge can then be used to disable the mechanical device that the switch would be connected with.

The temperature switch is assembled by pre-stressing the piezo-electric strip in a shape that is opposite to the shape that it is going to be bending into. Note that if you were going to freeze (chill) the strip, you would have to pre-stress it in the direction it would bend under temperature expansion. This is because in a clamped state the strip has to build up enough energy in it to overcome the additional internal force that the strip itself contains.

The experiments used to determine if the piezo-electric switch is possible are as follows.

1. First it has to be determined that the piezo-electric strip can bend on its own, unrestrained by any clamping device. It also has to be determined to bend enough so it can still bend when under clamped conditions.
2. The second experiment is to determine how the piezo-strip reacts to the temperature environment under a clamped, pre-stressed condition. Additionally, this experiment needs to run at all different washer sizes and different dome heights so that it can be seen how these two different variables affect the experiment.
3. The final experiment is to determine what critical temperature will be required to get the disk to return to its original state at the start of experiment 2.

A. Temperature Experiment One

Objective:

Testing the limits of the piezo-electric device without boundary conditions.

Purpose:

Experiment one was to make sure that the piezo-electric strip reacted to temperature change. The sales person that was consulted on the temperature change and electrical change of the strip did in fact claim that the strip would deform under temperature change.

Hypothesis:

Strip will react to temperature changes and change shape.

Equipment:

Piezo-electric strip

Freezer

Calipers

Steps

1. Measure and photograph strip on flat surface
2. Put strip in freezer
3. Wait 15 minutes
4. Take strip out and observe the new measurement

The experimenter found out that the piezo-strip did in fact react to a temperature change, and that it did have some shape change. Since this was the case, the thesis could continue on to the second experiment and find out more about the strip. What remained to be discovered was whether this strip would react as a standard piezo-strip and only be affected by temperature, or if other internally induced forces and stresses could shape how the strip would react. The experimenter also needed to test how the strip would maintain shape if other resisting forces were introduced.

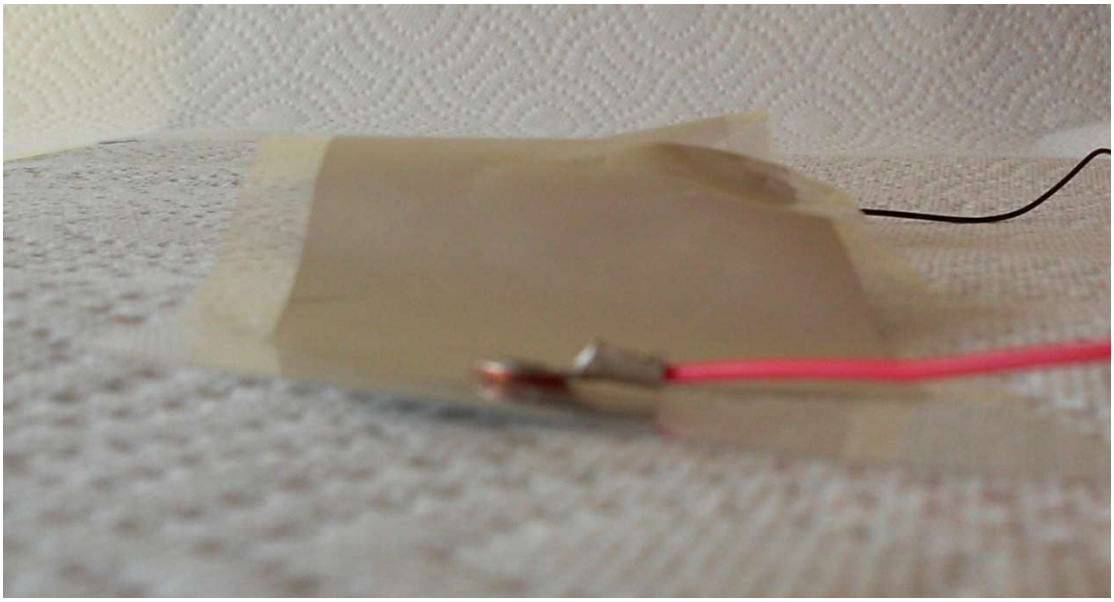

Figure 8-1: Photo of experimental strip before being put into freezer for experiment one (Notice straight edge of strip)

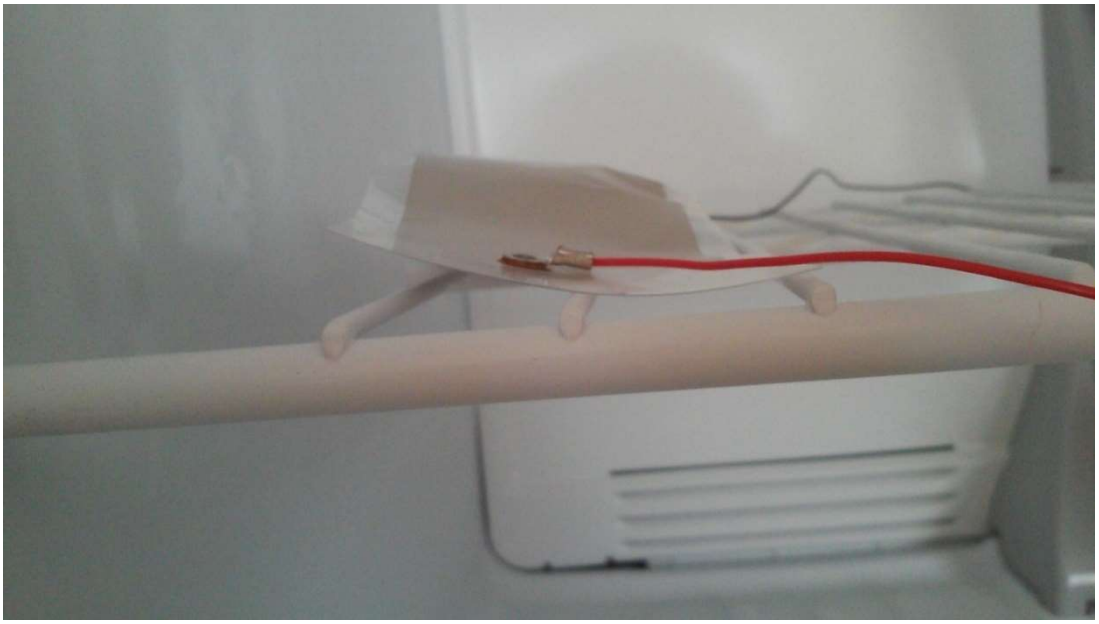

Figure 8-2: Photo of strip after being put into freezer (Notice curled up edge of strip)

From the photos above it can be observed that the strip does react to the temperature difference. For a strip that is approximately 4 cm or an inch and a half, there was a deflection of ⅜of an inch or over half a cm. Since the strip does this and reacts significantly well to temperature, the only conclusion here is to go on and do the second temperature experiment.

B. **Temperature Experiment Two**

Objective:

Freezing and analysis of the piezo-electric strip in a clamped position. Also to prove that this is of a snap-through phenomenon and not a gradual reshaping.

Purpose:

To prove that the piezo-electric strip can flip by undergoing an external change to environmental factors and remain in that position when strip is bought back to original environment

Hypothesis:

Strip will need to undergo a temperature change of roughly 50ºF to take a new shape. The strip will also stay in this position when it goes back to the regular temperature.

Assumptions:

1. Time is not factored here
2. The intensity of the cold air it is being put into is taken into consideration
3. The intensity of the temperature drop is not taken either

Equipment needed:

Clamps

2 Heavy washers (¾ inch inner diameter used)

Piezo-electric strip (Please see spec. included in appendix 1. The strip is .25 mm thick; other geometry is created by the washers.)

Freezer

Tongs

Thermometer with wire and wide temperature range (Taylor is typically a good resource for this)

Set up:

- Create a bulge in the piezo-strip so that there is a convex shape towards the negative terminal.
- Clamp it with the two washers so to keep this bulge.
- Use at least three clamps so that there is a continuous fixing of the edge and not a point fixed load.

Geometry:

The geometry of the starting shape is a convex or concave dome that is 0.25 mm thick by 15 mm in diameter. (Note that this is a prototype of switches that hopefully will be used one day as a result of this research.)

Steps:

- Measure the bulge height in the center of the dome's convexity
- Make sure the dome is clamped tight so that it forms a fixed edge

- Measure ambient (room) temperature (Note that for all experiments that ambient temperature must remain the same with little variation.)
- Measure temperature of freezer
- Measure original temperature of the piezo-electric disk
- Put piezo-strip from room temperature into freezer . Set a temperature for it to reach; in this case take it to the minimum temperature for the first disk. For additional experiments, the range was increased by ten and then was repeated, decreasing by two degrees each time for the next measurement.
- Take piezo-strip out and see that it is concave down.
- Repeat with lesser temperature ranges in intervals decreasing by ten degrees to the correct temperature where it won't flip.
- Once a temperature is reached at which the strip does not flip, work within that ten- degree range that was established to find the flipping temperature.
- Once the flipping temperature has been established for the first disk, one can easily do multiple sizes and shapes by using this as a base temperature for flipping.

*Note that the method being employed here is brute force method, since the range of temperature is very small and within a range of about 30 degrees. One way to go about this is to get the lowest temperature possible and then decrease by ten degrees each time the strip is checked. Once one reaches a point where the strip does not flip, then one knows the temperature is within that range.

- (optional) Place over a burner at at least 200ºF and watch it come back to normal shape. Warning: a piezo-strip can release sudden electricity. Be careful with this step.

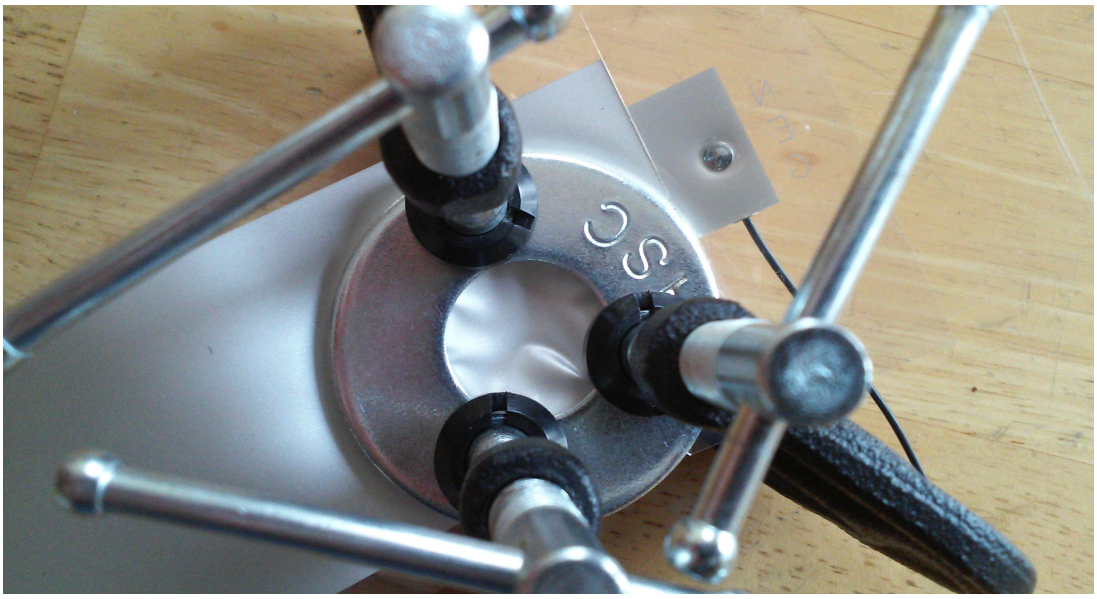

Figure 8-3: Piezo-electric strip clamped down before temperature drop (Note that it is concave down.)

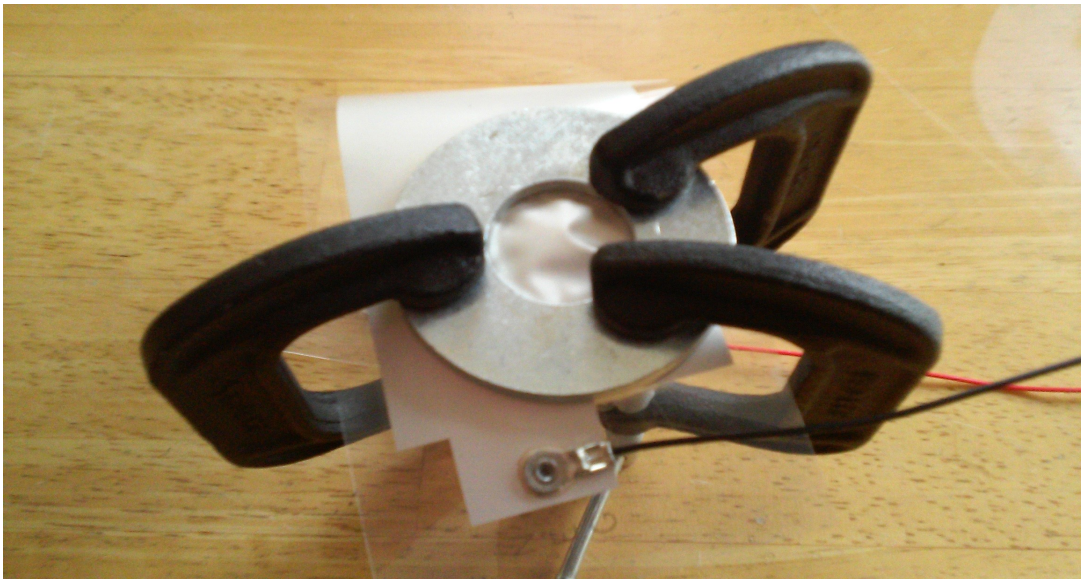

Figure 8-4: Piezo-electric strip before temperature drop–opposite side convex side

Figure 8-5: Piezo-strip after temperature drop (Note that the surface changed from convex up in Figure 8-4 to concave down.)

1. **Experimental Results**

The experiment also showed that there was a single point where the flipping point would occur.

Date: August 9, 2015

Temperature inside: 73º F

Dome height	Trial number	Change in Temperature F	Flip	Amount (inches)
-.05625 in.	1	48	yes	0.05625 in.
-.05625 in.	2	49	yes	0.05625 in.
-.05625 in.	3	50	yes	0.05625 in.
	Average	49		
-0.0625 in.	1	58	yes	0.0625 in.
-0.0625 in.	2	60	yes	0.0625 in.
-0.0625 in.	3	61	yes	0.0625 in.
	Average	60		
-0.06875 in.	1	73	yes	0.06875 in.
-0.06875 in.	2	72	yes	0.06875 in.
-0.06875 in.	3	73	yes	0.06875 in.
	Average	73		

Figure 8-6: Temperature experiment results for ¾ in. diameter washer

It was proposed later on to find out what happens if the dome height is raised (or lowered). What would be the results as to how this affects the flip-through temperature? It was found that there is a difference in the flip-through temperature, and this is stated below in the next part of this experiment.

From these results, the reader can see that there is a distinct point at which the temperature flips; similarly, the experimenter can find out where it flips in the other direction as well. It can be seen that the results are similar among the three trials. However, what one can see is that the temperature range has to increase if the shape is to flip through. This makes complete sense, and has been verified via COMSOL.

One can see that the range of experiments is similar, and while it is not exact for temperature effects, it is clear that it happens within a range. The temperature effect of the switch is off due to many reasons.

2. **Conclusion to the First Part of Experiment Two,**

From this simple experiment, we have proven that with proper clamping of the edges of a piezo-electric disk the piezo-disk will assume a new shape without being able to move back to the original shape once the disk is returned to the original temperature. Additionally, energy has to be introduced to the system before the piezo-strip can move back to the original position.

3. **Experiment Two Continued.**

It was proposed afterward to find out what would happen if we change the size of the disks that are used for clamping. The researcher continued to experiment on the polymer strip by increasing or decreasing the diameter of the washers that were used to clamp down the dome shape. The researcher also found that there is less range that one can work with if one decreases the size too much.

Date: August 9, 2015

Size of washer ring: ⅝ in.

Temperature inside: 63º F

Range (height of the dome) 0.046875 in.

Trial number	Dome height	Change in Temperature F	Flip	Amount (inches)
1	-0.046875 in.	43	yes	0.046875 in.
2	-0.046875 in.	44	yes	0.046875 in.
3	-0.046875 in.	46	yes	0.046875 in.
Average		44		
1	-0.054688 in.	60	yes	0.054688 in.
2	-0.054688 in.	63	yes	0.054688 in.
3	-0.054688 in.	66	yes	0.054688 in.
average		63		

Figure 8-7: Temperature experiment results for ⅝ in. diameter washer

Nothing else was possible for the ⅝ in. washer disks, since at a smaller dome height the disk would fall though without having any structural stability, while at a larger height the dome could not be formed.

The next trial that was done was using a 1-inch diameter ring. The same procedures as all the other experiments were followed. There was no change in using the brute force method to find the buckling temperature. The only exception here was use of

the previous data for the ¾-inch diameter washers to find out the range of starting temperatures.

Date: August 9, 2015

Temperature inside: 63 degrees F

Size of washer ring: 1 in.

Range (height of the dome): 0.05625 in.

Trial number	Change in Temperature F	Flip	Amount (inches)
1	40	yes	0.05625 in.
2	40	yes	0.05625 in.
3	40	yes	0.05625 in.
Average	40		
1	57	yes	0.078125 in.
2	55	yes	0.078125 in.
3	59	yes	0.078125 in.
Average	57		
1	81	yes	0.09375 in.
2	80	yes	0.09375 in.
3	79	yes	0.09375 in.
Average	80		

Figure 8-8: Temperature experiment results for 1-inch diameter washer

It was found that when the disk reached 1.25 inches, the shape would not hold. This is because the internal forces are not enough to hold the curvature of the disk in place. Instead, the disk needs to be stiffened, either by increasing the thickness of the material or increasing the elastic modulus of the disk. Since we are given a strip of set parameters, and since according to the manufacturer's website strips of thicker material or greater elastic modulus cannot be manufactured unless one has a minimum order and takes on great engineering costs, this result can only be achieved through COMSOL modeling.

C. Temperature Experiment Three

Objective:

This was a supplemental experiment to the first two. This experiment has the same set up as the second, but the objective was to find out the additional energy needed to force the strip back to the original position. One of the results of this experiment was shocking! After the first trial, the strip melted as the melting temperature of the polymer was reached, thereby proving that while yes, the process is reversible, it can only be done within the range that the strips are solid.

Purpose:

To find out if and how the snap-through effect can be reversed.

Hypothesis:

The strip will snap back, but at a higher temperature than where originally started.

Equipment:

Set up is the same as in the second experiment post experiment.

Additional equipment needed:

Heat source (burner)

Thermometer

Heat bath (a glass or metal (preferably glass) that can be heated up)

Tongs

The temperatures obtained were as follows.

First trial

Temperature F	Flip	Amount (inches)
163	yes	1/16 in.

Figure 8-9: Failed experiment to try to flip the polymer sheet in other direction by heating

At that point the strip permanently deformed in the bath. The deforming of the strip occurred in melting of the polymer, rendering the strip useless for future experiments. The melting point of some of the polymer strands is estimated to be around 150 degrees F at this point.

This heating process also stores energy, as when it was finally lifted from the bath after cooling, it had stored electric energy, which dissipated into the experimenter. As a result, this point was proven: that the strip can be reversed and undergo higher temperatures. However, there are limitations due to material characteristics and due to the fact that when heated the strip does store electricity that later will shock the experimenter

From this data, the reader can conclude that it takes more energy to reverse the snap-through piezo-temperature effect. This is due to what was described earlier in the thesis. Not all the energy that is being generated is being absorbed by the object. Additionally, some of the energy being created is actually going to the physical process of melting the strip, and some of the energy is going to store electricity in the strip.

D. Experiment versus Equation and COMSOL Model

At this point it has been proven that the experimental set up does work. However, it is also a good idea to show that the equations show similar if not the same results. As discussed with my advisor, an equation is only an approximate representation of what is happening in a phenomenon. Every process that has an equation has a side effect that happens that is not taken into consideration. An example of this is as follows. If one looks into the force that has to be behind a railcar given a speed and an acceleration, the general motion equations do not account for the friction in the railcar's wheels or the amount of air friction the sides of the railcar undergo. In this case, the equation provides a general idea of what is happening. While one can account for those, the equation becomes a lot longer and has more variables.

Eventually, what a researcher needs to do is determine when additional secondary effects are negligible enough to be excluded from the equation that they are forming. Presented below are the results using the equation found in the equation section of this thesis. First, the equation was used to obtain similar temperature numbers is presented.

Variable	Amount	Units	Variable name
v	0.3	dimensionless	Poisson's ratio
E_p	449616	PSI	plastic E
E_m	290075	PSI	piezo E
Ebar	392717.88	PSI	average E
d31	23	PSI/V	dielectric constant
Va	0	V	voltage applied
Q_{11}	494083.52	PSI	stiffness constant
W(dh)	0.0234375	In	deflection (in.)/2
a	0.0542651	In	Rsin (theta)
R	0.3125	In	radius of the disk (in.)
deltaT(ω)	70	F	temperature in F
α_p	0.0000795	1/F	plastic alpha (coefficient of expansion)

α_m	0.000071	1/F	piezo alpha (coefficient of expansion)
α bar	7.647E-05	1/F	average alpha value
t_p	0.0078125	In	plastic layer thickness
t_m	0.0043307	In	piezo-layer thickness
t_t	0.0121432	in	total thickness
C	5240.5008	Constant	constant used for simplification
B	31.818251	Constant	constant used for simplification

Figure 8-10: Equation input and output for disk diameter of ⅝ inches with dome height of 0.046875 in.

Variable	Amount	Units	Variable name
v	0.3	dimensionless	Poisson's ratio
E_p	449616	PSI	plastic E
E_m	290075	PSI	piezo E
Ebar	392717.88	PSI	average E
d31	23	PSI/V	dielectric constant
Va	0	V	voltage applied
Q_{11}	494083.52	PSI	stiffness constant
W(dh)	0.027344	In	deflection (in.)
a	0.0542651	In	Rsin (theta)
R	0.3125	In	radius of the disk (in.)
deltaT(ω)	80	F	temperature in F
α_p	0.0000795	1/F	plastic alpha (coefficient of expansion)
α_m	0.000071	1/F	piezo alpha (coefficient of expansion)
α bar	7.647E-05	1/F	average alpha value
t_p	0.0078125	In	plastic layer thickness
t_m	0.0043307	In	piezo-layer thickness
t_t	0.0121432	in	total thickness
C	5240.5008	Constant	constant used for simplification
B	31.818251	Constant	constant used for simplification

Figure 8-11: Equation input and output for disk diameter of ⅝ in. with dome height of 0.0546875 in.

These are the results for the ⅝-inch diameter test via the equation. Additionally, the researcher ran tests for the 1-inch diameter and the ¾-inch diameter plates. These results are presented below. The trend generally turns out to be similar to that of the experimental results.

Variable	Amount	Units	Variable name
v	0.3	dimensionless	Poisson's ratio
E_p	449616	PSI	plastic E
E_m	290075	PSI	piezo E
Ebar	392717.88	PSI	average E
d31	23	PSI/V	dielectric constant
Va	0	V	voltage applied
Q_{11}	494083.52	PSI	stiffness constant
W(dh)	0.0390625	In	deflection (in)
a	0.0868241	In	Rsin(theta)
R	0.5	In	radius of the disk (in)
deltaT(ω)	48	F	temperature in F
α_p	0.0000795	1/F	plastic alpha (co-efficient of expansion)
α_m	0.000071	1/F	piezo alpha (co-efficient of expansion)
α bar	7.647E-05	1/F	average alpha value
t_p	0.0078125	In	plastic layer thickness
t_m	0.0043307	In	piezo layer thickness
t_t	0.0121432	in	total thickness
C	5240.5008	Constant	constant used for simplification
B	31.818251	Constant	constant used for simplification

Figure 8-12: Equation input and output for disk diameter of 1 in. with dome height of 0.078125 in.

Variable	Amount	Units	Variable name
v	0.3	dimensionless	Poisson's ratio
E_p	449616	PSI	plastic E
E_m	290075	PSI	piezo E
Ebar	392717.88	PSI	average E
d31	23	PSI/V	dielectric constant
Va	0	V	voltage applied
Q_{11}	494083.52	PSI	stiffness constant
W(dh)	0.046875	In	deflection (in)
a	0.0868241	In	Rsin(theta)
R	0.5	In	radius of the disk (in)
deltaT(ω)	63	F	temperature in F
α_p	0.0000795	1/F	plastic alpha (coefficient of expansion)
α_m	0.000071	1/F	piezo alpha (coefficient of expansion)
α bar	7.647E-05	1/F	average alpha value

t_p	0.0078125	In	plastic layer thickness
t_m	0.0043307	In	piezo layer thickness
t_t	0.0121432	in	total thickness
C	5240.5008	Constant	constant used for simplification
B	31.818251	Constant	constant used for simplification

Figure 8-13: Equation input and output for disk diameter of 1 inch with Dome height of 0.09375 in.

Variable	Amount	Units	Variable name
v	0.3	dimensionless	Poisson's ratio
E_p	449616	PSI	plastic E
E_m	290075	PSI	piezo E
Ebar	392717.88	PSI	average E
d31	23	PSI/V	dielectric constant
Va	0	V	voltage applied
Q_{11}	494083.52	PSI	stiffness constant
W(dh)	0.028125	In	deflection (in)
a	0.0868241	In	Rsin(theta)
R	0.5	In	radius of the disk (in)
deltaT(ω)	32	F	temperature in F
α_p	0.0000795	1/F	plastic alpha (coefficient of expansion)
α_m	0.000071	1/F	piezo alpha (coefficient of expansion)
α bar	7.647E-05	1/F	average alpha value
t_p	0.0078125	In	plastic layer thickness
t_m	0.0043307	In	piezo layer thickness
t_t	0.0121432	in	total thickness
C	5240.5008	Constant	constant used for simplification
B	31.818251	Constant	constant used for simplification

Figure 8-14: Equation input and output for disk diameter of 1 inch with Dome height of 0.05625 in

Additional calculations were done for the ¾" diameter disk. Other disks could not be used since they were larger but the film was very flexible and could not hold a domed shape.

Variable	Amount	Units	Variable name
v	0.3	dimensionless	Poisson's ratio
E_p	449616	PSI	plastic E
E_m	290075	PSI	piezo E
Ebar	392717.88	PSI	average E
d31	23	PSI/V	dielectric constant
Va	0	V	voltage applied
Q_{11}	494083.52	PSI	stiffness constant
W(dh)	0.03125	In	deflection (in)
a	0.0651181	In	Rsin(theta)
R	0.375	In	radius of the disk (in)
deltaT(ω)	63.8	F	temperature in F
α_p	0.0000795	1/F	plastic alpha (coefficient of expansion)
α_m	0.000071	1/F	piezo alpha (coefficient of expansion)
α bar	7.647E-05	1/F	average alpha value
t_p	0.0078125	In	plastic layer thickness
t_m	0.0043307	In	piezo layer thickness
t_t	0.0121432	in	total thickness
C	5240.5008	Constant	constant used for simplification
B	31.818251	Constant	constant used for simplification

Figure 8-15: Equation input and output for disk diameter of ¾ in. with dome height of 0.0625 in.

Variable	Amount	Units	Variable name
v	0.3	dimensionless	Poisson's ratio
E_p	449616	PSI	plastic E
E_m	290075	PSI	piezo E
Ebar	392717.88	PSI	average E

d31	23	PSI/V	dielectric constant
Va	0	V	voltage applied
Q_{11}	494083.52	PSI	stiffness constant
W(dh)	0.034375	In	deflection (in)
a	0.0651181	In	Rsin(theta)
R	0.375	In	radius of the disk (in)
deltaT(ω)	72	F	temperature in F
α_p	0.0000795	1/F	plastic alpha (coefficient of expansion)
α_m	0.000071	1/F	piezo alpha (coefficient of expansion)
α bar	7.647E-05	1/F	average alpha value
t_p	0.0078125	In	plastic layer thickness
t_m	0.0043307	In	piezo layer thickness
t_t	0.0121432	in	total thickness
C	5240.5008	Constant	constant used for simplification
B	31.818251	Constant	constant used for simplification

Figure 8-16: Equation input and output for disk diameter of ¾ in. with dome height of 0.06875 in.

Variable	Amount	Units	Variable name
v	0.3	dimensionless	Poisson's ratio
E_p	449616	PSI	plastic E
E_m	290075	PSI	piezo E
Ebar	392717.8813	PSI	average E
d31	23	PSI/V	dielectric constant
Va	0	V	voltage applied
Q_{11}	494083.5165	PSI	stiffness constant
W(dh)	0.028125	In	deflection (in)
a	0.065118067	In	Rsin(theta)
R	0.375	In	radius of the disk (in)
deltaT(ω)	57	F	temperature in F
α_p	0.0000795	1/F	plastic alpha (coefficient of expansion)
α_m	0.000071	1/F	piezo alpha (coefficient of expansion)
α bar	7.64686E-05	1/F	average alpha value
t_p	0.0078125	In	plastic layer thickness
t_m	0.00433071	In	piezo layer thickness
t_t	0.01214321	in	total thickness
C	5240.500773	Constant	constant used for simplification

B	31.81825069	Constant	constant used for simplification

Figure 8-17: Equation input and output for disk diameter of ¾ in. with dome height of 0.05625 in.

The experiment was also compared to COMSOL models to make sure that the results are accurate and that the equations and the experiments are producing similar results. As will be seen below, the COMSOL models did produce similar results.

Figure 8-18: COMSOL model with .05468 in. dome height and ⅝ in. diameter ring before flip.

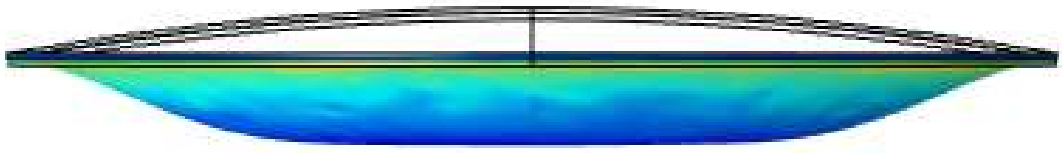

Figure 8-19: COMSOL model with .05468 in. dome height and ⅝ in. diameter ring after flip.

The modeler also ran the COMSOL model and came up with similar results after flipping. What they found was that the COMSOL model was a lot closer than the equation.

This means that the experiment is more in line with the COMSOL modeling than with the derived equation. The equation is off mainly due to averaging of elastic modulus and alpha values. Below appear all the results from the experiment versus equation versus COMSOL.

Diameter of ring: ¾ in.

Dome height (in.)	Experiment result F	COMSOL result F	Equation result F
0.05625	49	54	57
0.0625	60	63	64
0.06875	73	70	72

Figure 8-20: Summary of the ¾ in. diameter results including experiment, equation and COMSOL.

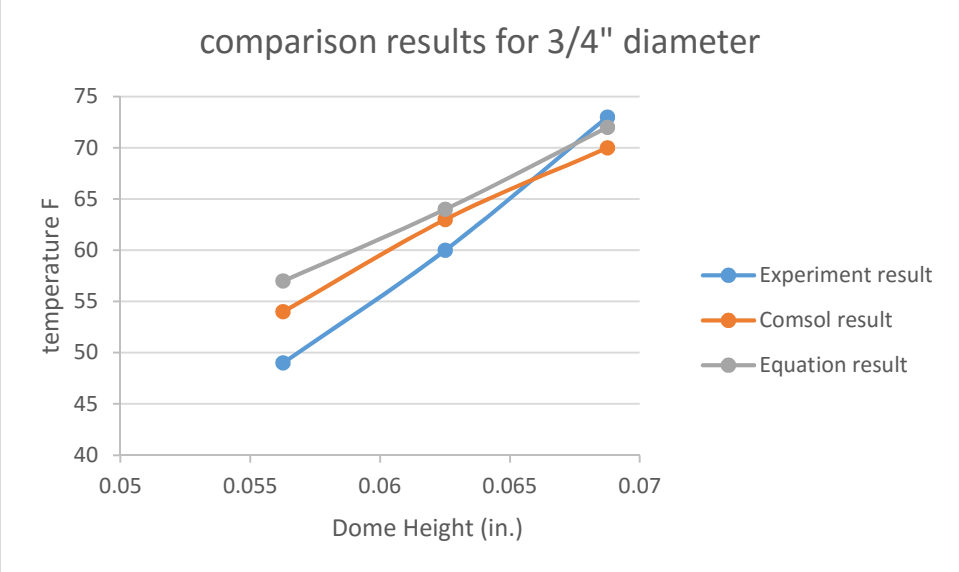

Figure 8-21: Graph of the ¾ in. diameter results

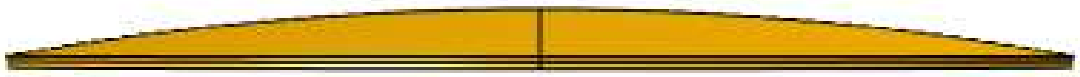

Figure 8-22: COMSOL model with .05625 in. dome height and ¾ in. diameter ring before flip

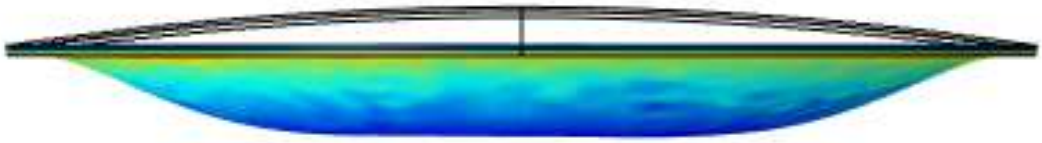

Figure 8-23: COMSOL model with .05625 in. dome height and ¾ in. diameter ring after flip

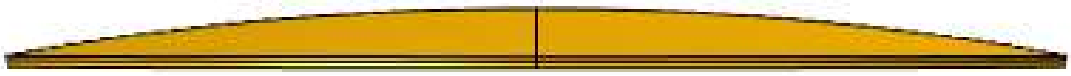

Figure 8-24: COMSOL model with .0625 in. dome height and ¾ in. diameter ring before flip

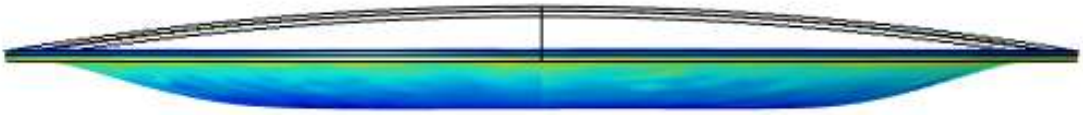

Figure 8-25: COMSOL model with .0625 in. dome height and ¾ in. diameter ring after flip

Diameter of ring: ⅝ in

Dome height (in.)	Experiment result F	COMSOL result F	Equation result F
0.046875	44	49	70
0.054688	63	57	80

Figure 8-26: Summary of the ⅝ in. diameter results

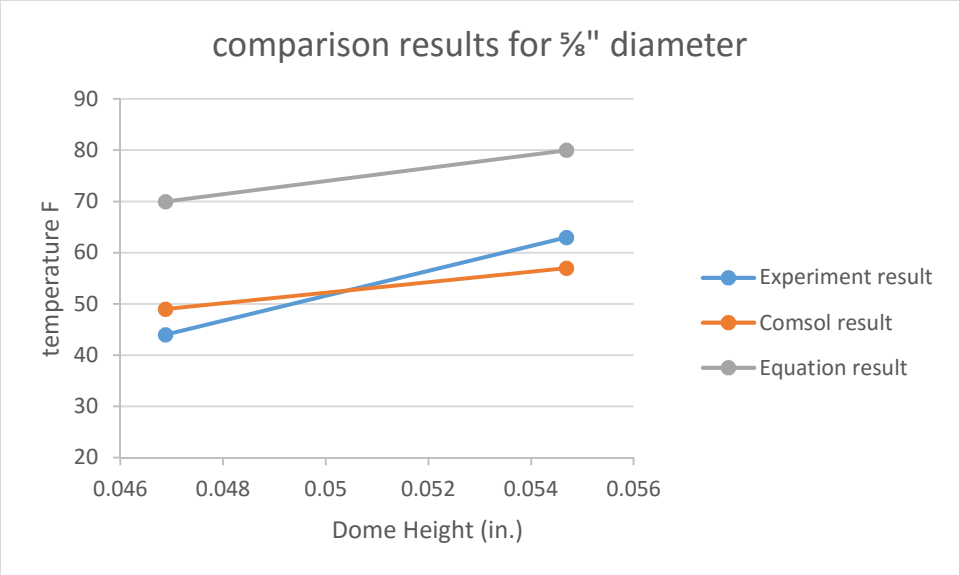

Figure 8-27: Graph of the ⅝ in. diameter results for COMSOL, equation, and experiments

Diameter of ring: 1 in.

Dome height	Experiment result F	COMSOL result F	Equation result F
0.05625	40	30	33
0.078125	57	56	48
0.09375	70	70	63

Figure 8-28: Summary of 1 in. diameter temperature results including COMSOL, experiment and equation

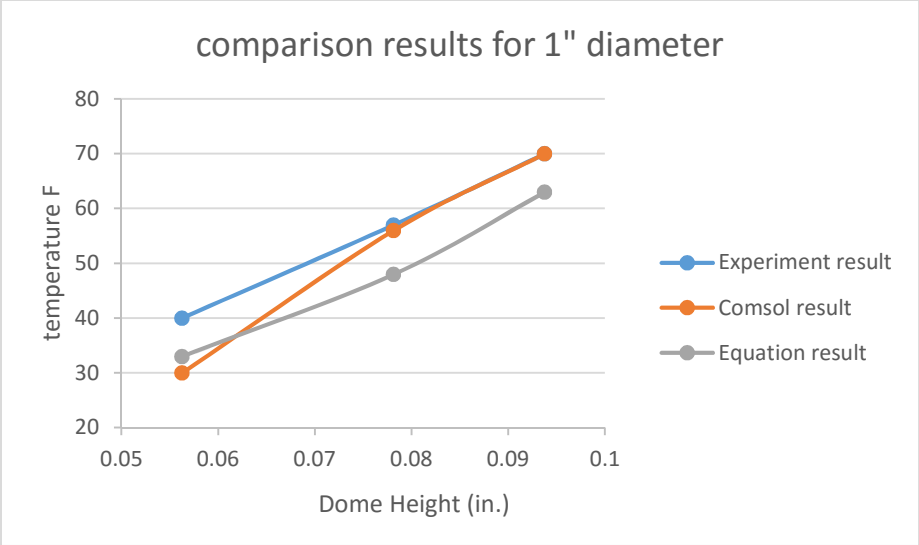

Figure 8-29: Graph of the 1 in. diameter results

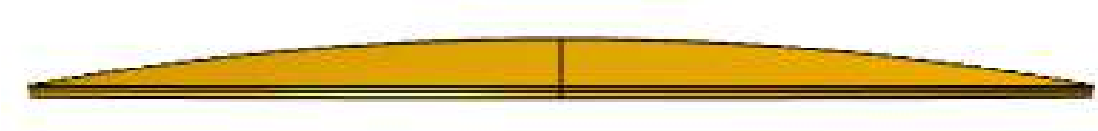

Figure 8-30: COMSOL model with 0.05625 in. dome height and 1 in. diameter ring before flip

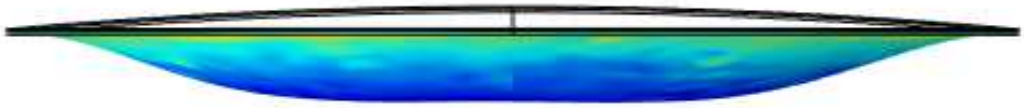

Figure 8-31: COMSOL model with 0.05625 in. dome height and 1 in. diameter ring after flip

Figure 8-32: COMSOL model with 0.078 in. dome height and 1 in. diameter ring before flip

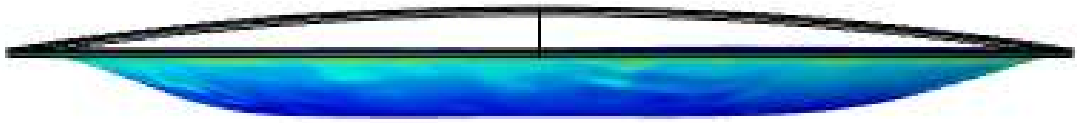

Figure 8-33: COMSOL model with 0.078 in. dome height and 1 in. diameter ring after flip

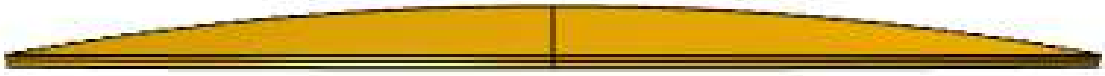

Figure 8-34: COMSOL model with 0.09375 in. dome height and 1 in. diameter ring before flip

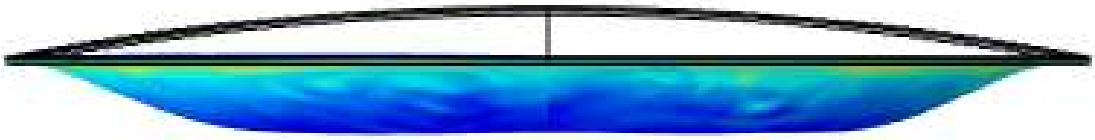

Figure 8-35: COMSOL model with 0.09375 in. dome height and 1 in. diameter ring after flip

Conclusion

From these results, we can see that COMSOL is similar to the equation. One also has to be careful about reaching a maximum temperature. If one exceeds the temperature of the material, then one ends up having a melted strip that will not be useful for the switch. One thing that was found was that this polymer melts at a low temperature. One of the

takeaways from this experiment is that the equation, COMSOL, and experiment produced very similar results for the 1 inch and ¾ inch radiuses. The ⅝ inch might be a little off because it is a smaller piece and it is harder to form a hemisphere with such a small radius.

Another key takeaway here is to experiment with more temperature resistant polymers. There are some polymers out there with higher melting temperatures. There are also some that are baked at higher temperatures, such as ABS (Acrylonitrile Butadiene Styrene) plastics. One example is the common Lego brick that melts at roughly 220º F, which is much higher than our 163º F PVDF (Lego.com, [55]). Obviously, a Lego brick cannot be used directly in this application; however, the chemical composition might be able to be modified for a stronger piezo-plastic that would be good for future experimentation.

The next chapter will focus on the electrical equations of the piezo-polymer. This will be where the researcher experiments with the other half of the equation derived in chapter 5.

Chapter 9

Piezo-electric Voltage Effect Experiment Switches

The second and the original purpose of this thesis was to study the piezo-electric effect and make a near perfect piezo-electrical switch. The term perfect has been described in the previous section as a switch that in its form is completely shut off and does not lose energy to leakage. When beginning research for this thesis, the main purpose was to study electrical switches. These were selected because the elements that the researcher was working with were primarily activated by electrical current.

The voltage switch is actually easy to build. It would ideally be attached to an electrical motor or generator in a series circuit and be able to shut the motor off. This can happen because it is a piezo-electric material, and when a piezo-electric strip moves when it is clamped it does hold its new shape. This new shape is possible through energy conservation methods and by virtue of the fact that energy cannot be created or destroyed. This shape can be used effectively to trigger a break in the line and completely turn off a piece of equipment or a voltage source.

The voltage switch is assembled by pre-stressing the piezo-electric strip into a shape that is opposite to the shape that it is going to be bending to. Note that if you were going to run a positive current through the strip, you have to pre-stress it in the direction it would bend under the opposite charge. This is because in a clamped state the strip has to build up enough electrical energy in it to overcome the additional internal force in the strip itself.

The experiments used to determine if the piezo-electric switch is possible are as follows.

1. First it has to be determined that the piezo-electric strip can bend enough on its own from an external source without any clamps. (This was done in a previous experiment on temperature by accident, it is also repeated for electricity.)
2. The second experiment is to determine how the piezo-strip reacts to the electrical charge under a clamped condition.
3. The final experiment, and the final experiment of this thesis, is to determine whether reversing the switch will be able to get the strip to return to its natural state.

A. Electrical Experiment One

Purpose:

Testing to see if strip would bend under electrical charge. Experiment 1 was to make sure that the piezo-electric strip reacted to electrical change. This information is required for other experiments to make sure they will work.

Hypothesis:

Strip will bend under electrical load

Equipment:

Strip

Piezo-electric amplifier (built for the strip)

Electrical source

Steps

1. Put the electrical ends (wires) of the strip into the positive and negative terminals of the amplifier.
2. Plug the amplifier into the outlet.
3. Oscillate the voltage to maximum for best results.
4. Observe the strip for bending.

Results:

The experiment found that the piezo-strip did in fact react to an electrical current change. A difference of 90 volts was applied to the element, which caused it to undergo

some shape change. The piezo-electric strip also worked properly by making a high-pitched sound, as this was a tweeter element. The sound is necessary since the element vibrates back and forth to create a tone. This tone is a sign that the speaker element is working in this object.

Since this experiment was successful, the researcher could continue on to the second proposed experiment and find out whether this would react similarly as a temperature change or be affected only by temperature, or if other internally induced forces and stresses could shape how this strip would react.

B. Electrical Experiment Two

Purpose:

To prove that the piezo-electric strip can flip by undergoing an external change due to environmental factors (electrical current) and remain in the flipped position when the strip is bought back to original environmental conditions

Hypothosis:

Strip will need to undergo a voltage change of roughly 90 volts to take a new shape. The strip will also stay in this position when it goes back to zero current and voltage.

Assumptions:

Time is not factored here nor is the intensity of the electrical charge as it is considered instantaneous.

Equipment needed:

Clamps (3)

2 Heavy washers (¾ inch inner diameter used)

Piezo-electric strip (Please see spec. included in appendix 1. The strip is .25 mm thick; other geometry is created by the washers.)

Piezo-electrical amplifier

Voltmeter

Set up:

- Create a bulge in the piezo-strip so that there is a convex shape towards the negative terminal.
- Clamp it with the two washers so to keep this bulge.

Geometry:

The geometry of the starting shape is a convex dome that is 0.25 mm thick

Steps:

- Measure the bulge height in the center of the domes convexity.
- Make sure the dome is clamped tight so that it forms a rigid edge.
- Hook up switch to the piezo-electric amplifier for positive current.
- Measure initial current (should be zero).
- Plug the piezo-amplifier in (turn it on).

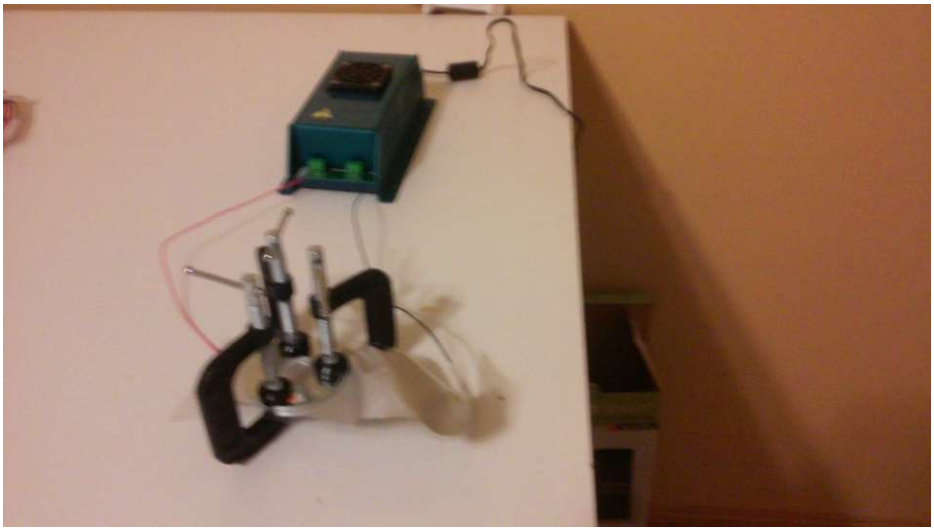

Figure 9-1: Set up of the experiment

- Wait a few minutes while the piezo-strip bends.
- Observe that piezo-strip is concave down.

Figure 9-2: Piezo-electric strip before applying a charge (voltage increase) to it

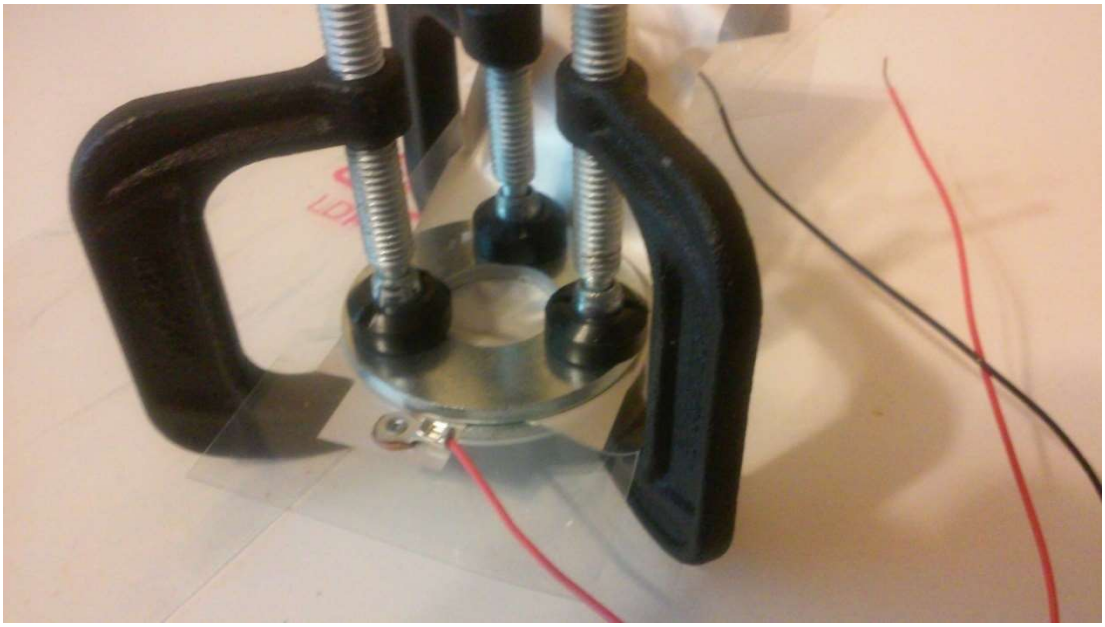

Figure 9-3: 45 degree angle of the strip before applying a charge (voltage increase) to it

Figure 9-4: close-up of figure 9-3

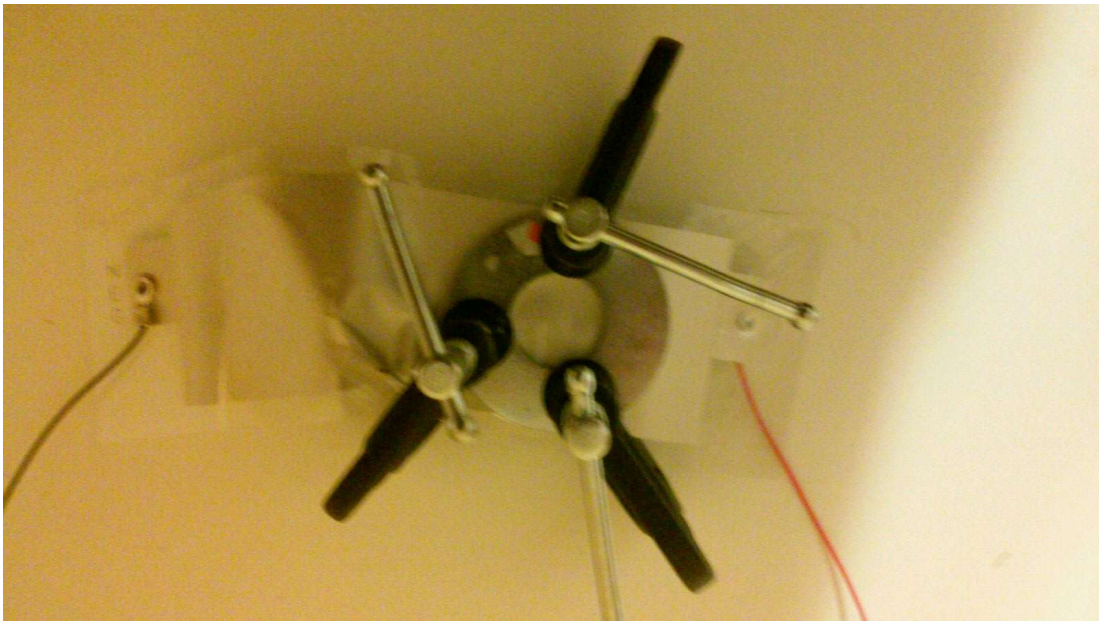

Figure 9-5: Piezo-electric strip after voltage increase

Figure 9-6: 45 degree angle of piezo-electric strip after voltage increase

Figure 9-7: Close up of Figure 9-6

The results for electrical experiments appear below.

First experiment

Date: February 13, 2015

Disk diameter: ¾”

Dome height: 0.05625 in.

Inside temperature: 63 degrees F

Outside temperature: 20 degrees F

Starting voltage: 0 volts

Assumed no ghost voltage

Trial	Voltage V	Position of dome
1	30	-0.05625 in.
2	30	-0.05625 in.
3	30	-0.05625 in.

Figure 9-8: Results for ¾ in. diameter with 0.05625 in. dome height

The researcher decided to take a short cut to reverse the piezo-electrical disk at this point. Instead of having a third experiment to do this, the second experiment is repeated with the terminals reversed. This will show what the opposite flipping voltage is. The voltage is the same. This is due to what is called a sealed system, because there are no other external factors such as loss to the air or loss through the system that exist with temperature.

Trial 2 (terminals reversed)

Date: August 23, 2015

Disk diameter ¾ in.

Inside temperature: 63 degrees F

Outside temperature: 20 degrees F

Starting voltage: 0 volts

Assumed no ghost voltage

Trial	Voltage V	Position of dome
1	-30	0.05625 in.
2	-30	0.05625 in.
3	-30	0.05625 in.

Figure 9-9: Results for ¾ in. diameter with 0.05625 in. dome height with terminals reversed

The researcher decided on increasing the dome height to find out the range and see what would happen. According to the equation, the amount of energy would have to increase so the voltage should have to increase as well.

Trials 3 and 4

Date: August 23, 2015

Disk diameter: ¾ in.

Inside temperature: 63 degrees F

Outside temperature: 80 degrees F

Starting voltage: 0 volts

Assumed no ghost voltage

Trial	Position of terminals	Voltage V	Position of dome (in.)
1	Normal	35	-0.0625
2	Normal	35	-0.0625
3	Normal	35	-0.0625
1r	Reversed	-35	0.0625
2r	Reversed	-35	0.0625
3r	Reversed	-35	0.0625

Figure 9-10: Results for ¾ in. diameter with 0.0625 in. dome height both normal and terminals reversed

As it can be seen, the voltage increases. This is caused by the increased amount of energy that has to be put into the system to get a critical buckling load, which increases the voltage required.

Trial 5

Date: August 23, 2015

Disk diameter: ¾ in.

Inside temperature: 63 degrees F

Outside temperature: 80 degrees F

Starting voltage: 0 volts

Assumed no ghost voltage

Trial	Position of terminals	Voltage V	Position of dome (in.)
1	Normal	42	-0.06875
2	Normal	42	-0.06875
3	Normal	42	-0.06875
1r	Reversed	-42	0.06875
2r	Reversed	-42	0.06875
3r	Reversed	-42	0.06875

Figure 9-11: Results for ¾ in. diameter with 0.06875 in. dome height both, normal and terminals reversed.

The researcher experimented further to find how voltage changes by changing the geometry of the disks as with the temperature experiments. Therefore, the researcher experimented with the ⅝ in. disk and the 1 in. disk. The disk sizes beyond 1 inch were not tested, since they caused the material to fall through and not be stable. As stated previously there is a certain range that one can have for these piezo-disks.

Date: August 23, 2015

Disk diameter: ⅝ in.

Inside temperature: 63 degrees F

Outside temperature: 80 degrees F

Starting voltage: 0 volts

Assumed no ghost voltage

Trial	Dome height (in.)	Voltage V	Position of terminals	Position of dome (in.)
1	0.046875	40	Normal	-0.046875
2	0.046875	40	Normal	-0.046875
3	0.046875	40	Normal	-0.046875
1r	-0.046875	-40	Reversed	0.046875
2r	-0.046875	-40	Reversed	0.046875
3r	-0.046875	-40	Reversed	0.046875
1	0.0546	45	Normal	-0.0546
2	0.0546	45	Normal	-0.0546
3	0.0546	45	Normal	-0.0546
1r	-0.0546	-45	Reversed	0.0546
2r	-0.0546	-45	Reversed	0.0546
3r	-0.0546	-45	Reversed	0.0546

Figure 9-12: Electrical experimental results for ⅝ in diameter.

As with these results, similar results were obtained with almost no variation between the trials, which was predicted. This is due to the exact flow of electricity in the switch. There is one more result for the 1-inch disk shown below.

Date: February 13, 2015

Disk diameter: 1 in.

Inside temperature: 63 degrees F

Outside temperature: 20 degrees F

Starting voltage: 0 volts

Assumed no ghost voltage

Trial	Dome height (in.)	Voltage V	Position of terminals	Position of dome (in.)
1	0.05625	20	Normal	-0.05625
2	0.05625	20	Normal	-0.05625
3	0.05625	20	Normal	-0.05625
1r	-0.05625	-20	Reversed	0.05625
2r	-0.05625	-20	Reversed	0.05625
3r	-0.05625	-20	Reversed	0.05625
1	0.078	28	Normal	-0.078
2	0.078	28	Normal	-0.078
3	0.078	28	Normal	-0.078
1r	-0.078	-28	Reversed	0.078
2r	-0.078	-28	Reversed	0.078
3r	-0.078	-28	Reversed	0.078
1	0.093	36	Normal	-0.093
2	0.093	36	Normal	-0.093
3	0.093	36	Normal	-0.093

1r	-0.093	-36	Reversed	0.093
2r	-0.093	-36	Reversed	0.093
3r	-0.093	-36	Reversed	0.093

Figure 9-13: Electrical switch results for 1 in. diameter disk

As is evident, the same pattern exists for the voltage: higher domes mean that more energy needs to be put into the switch in order for it to fall. Additionally, if the disk diameter increases, then more energy is needed to make the disk fall.

C Comparison to Equation and COMSOL

Equation calculation

Consistent with the other section, the equation needed to be calculated and compared with the results. As with the temperature portion of this project, the equation was off by some. This probably had to do with the assumptions that were made about the equation. Note that some of the secondary effects are not covered by the equation and others are approximated.

Variable	Amount	Units	Variable name
v	0.3	dimensionless	Poisson's ratio
E_p	449616	PSI	plastic E
E_m	290075	PSI	piezo E
Ebar	392717.88	PSI	average E
d31	37.04	PSI/V	dielectric constant
Va	33	V	voltage applied
Q_{11}	494083.52	PSI	stiffness constant
W(dh)	0.0234375	In	deflection (in)
a	0.0542651	In	Rsin(theta)
R	0.3125	In	radius of the disk (in)
deltaT(ω)	0	F	temperature in F
α_p	0.0000795	1/F	plastic alpha (coefficient of expansion)
α_m	0.000071	1/F	piezo alpha (coefficient of expansion)
α bar	7.647E-05	1/F	average alpha value
t_p	0.0078125	In	plastic layer thickness
t_m	0.0043307	In	piezo layer thickness
t_t	0.0121432	in	total thickness
C	5240.5008	Constant	constant used for simplification
B	31.818251	Constant	constant used for simplification

Figure 9-14: ⅝ in. diameter with dome height of 0.046875 in. equation results.

Variable	Amount	Units	Variable name
v	0.3	dimensionless	Poisson's ratio
E_p	449616	PSI	plastic E

E_m	290075	PSI	piezo E
Ebar	392717.88	PSI	average E
d31	37.04	PSI/V	dielectric constant
Va	38	V	voltage applied
Q_{11}	494083.52	PSI	stiffness constant
W(dh)	0.027344	In	deflection (in)
a	0.0542651	In	Rsin(theta)
R	0.3125	In	radius of the disk (in)
deltaT(ω)	0	F	temperature in F
α_p	0.0000795	1/F	plastic alpha (coefficient of expansion)
α_m	0.000071	1/F	piezo alpha (coefficient of expansion)
α bar	7.647E-05	1/F	average alpha value
t_p	0.0078125	In	plastic layer thickness
t_m	0.0043307	In	piezo layer thickness
t_t	0.0121432	in	total thickness
C	5240.5008	Constant	constant used for simplification
B	31.818251	Constant	constant used for simplification

Figure 9-15: ⅝ in. diameter with dome height of 0.055 in. equation results.

Variable	Amount	Units	Variable name
v	0.3	dimensionless	Poisson's ratio
E_p	449616	PSI	plastic E
E_m	290075	PSI	piezo E
Ebar	392717.8813	PSI	average E
d31	37.04	PSI/V	dielectric constant
Va	27	V	voltage applied
Q_{11}	494083.5165	PSI	stiffness constant
W(dh)	0.028125	In	deflection (in)
a	0.065118067	In	Rsin(theta)
R	0.375	In	radius of the disk (in)
deltaT(ω)	0	F	temperature in F
α_p	0.0000795	1/F	plastic alpha (coefficient of expansion)
α_m	0.000071	1/F	piezo alpha (coefficient of expansion)
α bar	7.64686E-05	1/F	average alpha value
t_p	0.0078125	In	plastic layer thickness
t_m	0.00433071	In	piezo layer thickness
t_t	0.01214321	in	total thickness
C	5240.500773	Constant	constant used for simplification

B	31.81825069	Constant	constant used for simplification

Figure 9-16: ¾ in. diameter disk with dome height of 0.05625 in.

Variable	Amount	Units	Variable name
v	0.3	dimensionless	Poisson's ratio
E_p	449616	PSI	plastic E
E_m	290075	PSI	piezo E
Ebar	392717.88	PSI	average E
d31	37.04	PSI/V	dielectric constant
Va	31	V	voltage applied
Q_{11}	494083.52	PSI	stiffness constant
W(dh)	0.03125	In	deflection (in)
a	0.0651181	In	Rsin(theta)
R	0.375	In	radius of the disk (in)
deltaT(ω)	0	F	temperature in F
α_p	0.0000795	1/F	plastic alpha (coefficient of expansion)
α_m	0.000071	1/F	piezo alpha (coefficient of expansion)
α bar	7.647E-05	1/F	average alpha value
t_p	0.0078125	In	plastic layer thickness
t_m	0.0043307	In	piezo layer thickness
t_t	0.0121432	in	total thickness
C	5240.5008	Constant	constant used for simplification
B	31.818251	Constant	constant used for simplification

Figure 9-17: ¾ in. diameter disk with dome height of 0.0625 in.

Variable	Amount	Units	Variable name
v	0.3	dimensionless	Poisson's ratio
E_p	449616	PSI	plastic E
E_m	290075	PSI	piezo E
Ebar	392717.88	PSI	average E
d31	37.04	PSI/V	dielectric constant
Va	34	V	voltage applied
Q_{11}	494083.52	PSI	stiffness constant
W(dh)	0.034375	In	deflection (in)
a	0.0651181	In	Rsin(theta)
R	0.375	In	radius of the disk (in)
deltaT(ω)	0	F	temperature in F
α_p	0.0000795	1/F	plastic alpha (coefficient of expansion)

α_m	0.000071	1/F	piezo alpha (coefficient of expansion)
α bar	7.647E-05	1/F	average alpha value
t_p	0.0078125	In	plastic layer thickness
t_m	0.0043307	In	piezo layer thickness
t_t	0.0121432	in	total thickness
C	5240.5008	Constant	constant used for simplification
B	31.818251	Constant	constant used for simplification

Figure 9-18: ¾ in. diameter disk with dome height of 0.06875 in.

Variable	Amount	Units	Variable name
v	0.3	dimensionless	Poisson's ratio
E_p	449616	PSI	plastic E
E_m	290075	PSI	piezo E
Ebar	392717.88	PSI	average E
d31	37.04	PSI/V	dielectric constant
Va	16	V	voltage applied
Q_{11}	494083.52	PSI	stiffness constant
W(dh)	0.028125	In	deflection (in)
a	0.0868241	In	Rsin(theta)
R	0.5	In	radius of the disk (in)
deltaT(ω)	0	F	temperature in F
α_p	0.0000795	1/F	plastic alpha (coefficient of expansion)
α_m	0.000071	1/F	piezo alpha (coefficient of expansion)
α bar	7.647E-05	1/F	average alpha value
t_p	0.0078125	In	plastic layer thickness
t_m	0.0043307	In	piezo layer thickness
t_t	0.0121432	in	total thickness
C	5240.5008	Constant	constant used for simplification
B	31.818251	Constant	constant used for simplification

Figure 9-19: 1 in. diameter disk with dome height of 0.05625 in.

Variable	Amount	Units	Variable name
v	0.3	dimensionless	Poisson's ratio
E_p	449616	PSI	plastic E
E_m	290075	PSI	piezo E
Ebar	392717.88	PSI	average E
d31	37.04	PSI/V	dielectric constant
Va	23	V	voltage applied

Q_{11}	494083.52	PSI	stiffness constant
W(dh)	0.0390625	In	deflection (in)
a	0.0868241	In	Rsin(theta)
R	0.5	In	radius of the disk (in)
deltaT(ω)	0	F	temperature in F
α_p	0.0000795	1/F	plastic alpha (coefficient of expansion)
α_m	0.000071	1/F	piezo alpha (coefficient of expansion)
α bar	7.647E-05	1/F	average alpha value
t_p	0.0078125	In	plastic layer thickness
t_m	0.0043307	In	piezo layer thickness
t_t	0.0121432	in	total thickness
C	5240.5008	Constant	constant used for simplification
B	31.818251	Constant	constant used for simplification

Figure 9-20: 1 in. diameter disk with dome height of 0.078 in.

Variable	Amount	Units	Variable name
v	0.3	dimensionless	Poisson's ratio
E_p	449616	PSI	plastic E
E_m	290075	PSI	piezo E
Ebar	392717.8813	PSI	average E
d31	37.04	PSI/V	dielectric constant
Va	30	V	voltage applied
Q_{11}	494083.5165	PSI	stiffness constant
W(dh)	0.046875	In	deflection (in)
a	0.086824089	In	Rsin(theta)
R	0.5	In	radius of the disk (in)
deltaT(ω)	0	F	temperature in F
α_p	0.0000795	1/F	plastic alpha (coefficient of expansion)
α_m	0.000071	1/F	piezo alpha (coefficient of expansion)
α bar	7.64686E-05	1/F	average alpha value
t_p	0.0078125	In	plastic layer thickness
t_m	0.00433071	In	piezo layer thickness
t_t	0.01214321	in	total thickness
C	5240.500773	Constant	constant used for simplification
B	31.81825069	Constant	constant used for simplification

Figure 9-21: 1 in. diameter disk with dome height of 0.094 in.

COMSOL results

The COMSOL results were a straight shot from the experiment with very little deviation. This is due to the fact that there were no differences or locations of leakage in the experiment versus actual conditions.

Figure 9-22: COMSOL model with .05468 in. dome height and ⅝ in. diameter ring before flip

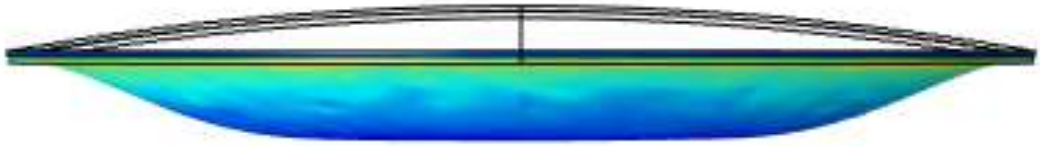

Figure 9-23: COMSOL model with .05468 in. dome height and ⅝ in. diameter ring after electrical charge is introduced over the element

Figure 9-24: COMSOL model with .05625 in. dome height and ¾ in. diameter ring before flip

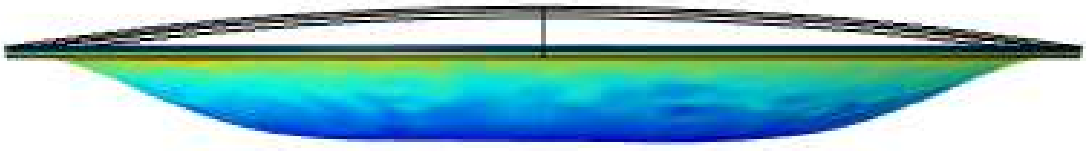

Figure 9-25: COMSOL model with .05625 in. dome height and ¾ in. diameter ring after electrical charge is introduced over the element

Figure 9-26: COMSOL model with .0625 in. dome height and ¾ in. diameter ring before flip

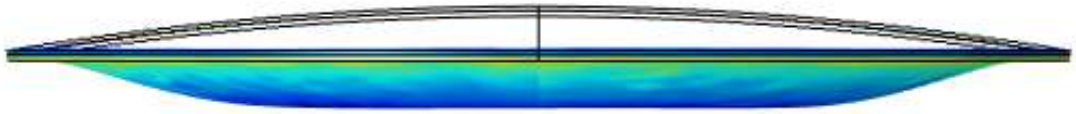

Figure 9-27: COMSOL model with .0625 in. dome height and ¾ in. diameter ring after electrical charge is introduced over the element.

Figure 9-28: COMSOL model with 0.05625 in. dome height and 1 in. diameter ring before flip

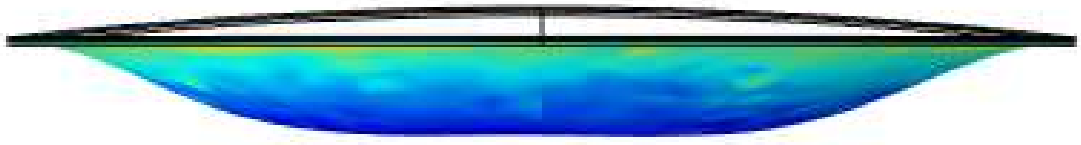

Figure 9-29: COMSOL model with 0.05625 in. dome height and 1 in. diameter ring after electrical charge is introduced over the element

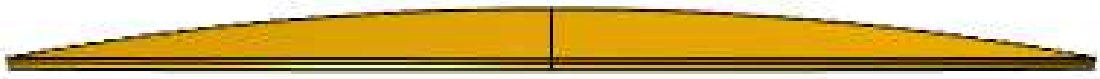

Figure 9-30: COMSOL model with 0.078 in. dome height and 1 in. diameter ring before flip

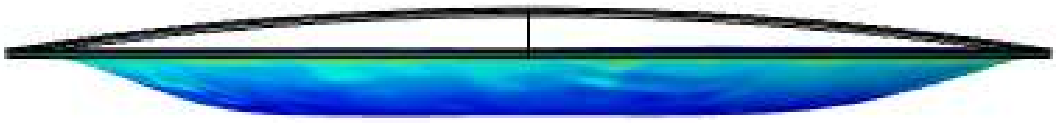

Figure 9-31: COMSOL model with 0.078 in. dome height and 1in. diameter ring after electrical charge is introduced over the element

Figure 9-32: COMSOL model with 0.09375 in. dome height and 1 in. diameter ring before flip

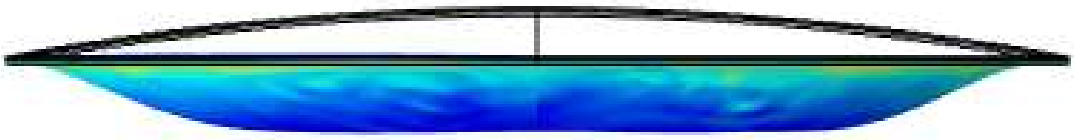

Figure 9-33: COMSOL model with 0.09375 in. dome height and 1 in. diameter ring after electrical charge is introduced over the element

Experiment	Dome position (in.)	Experiment (v)	COMSOL (V)	Equation (v)
¾ in.	0.05625	30	30	27
¾ in.	0.0625	35	35	31
¾ in.	0.06875	42	42	34
⅝ in.	0.046875	40	40	33
⅝ in.	0.054688	45	45	38
1 in.	0.05625	20	20	16
1 in.	0.078125	28	28	23
1 in.	0.09375	36	36	30

Figure 9-34: Summary of electrical results.

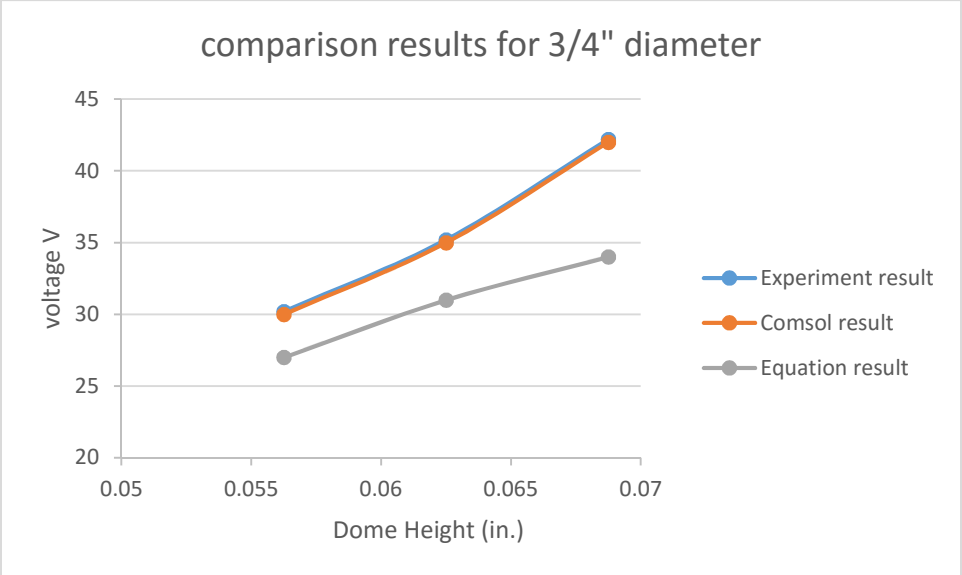

Figure 9-35: Chart of summary of results for ¾ in. disk for voltage experiments.

There was an experiment done with a ⅝ in. diameter disk that yielded the chart below.

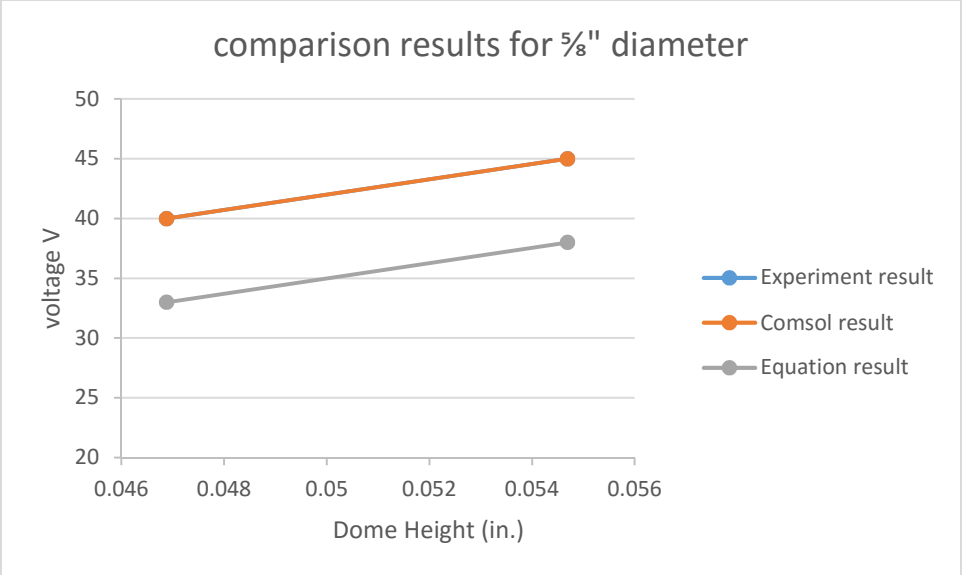

Figure 9-36: Chart of summary of results for ⅝ in. disk for voltage experiments

The last experiment that was completed was for the one-inch disk.

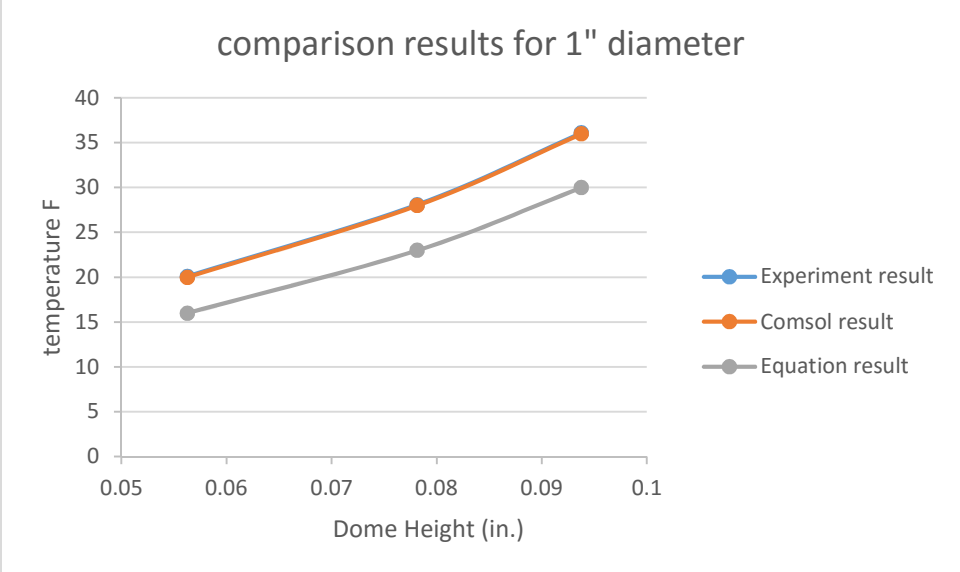

Figure 9-37: Chart of summary of results for 1-inch disk for voltage experiments

Above appeared the COMSOL models that were used (fig. 9-22 to fig. 9-33) before and after experimentation. In addition, the disk was flipped around, a negative charge applied to it, and the same exact results were obtained. It is the same model, but with electrical charge instead of temperature charges. It really resulted in the same results as the temperature with deflection. The deflections were the same, and instead of temperature changing in the external environment it was the voltage.

What can be seen from the COMSOL models is that the disk falls through after an electrical charge is applied to the model. The same result as changing the temperature is obtained.

Conclusion,

From this simple experiment we have proven that, with proper clamping of the edges of a piezo-electric disk, the piezo-disk will assume a new shape without being able to move back to its original shape after the disk is returned to the original voltage (0). Additionally, more energy (in this case electrical energy) has to be introduced to the system before the piezo-strip can move back to the original position. In the next two chapters, practical design examples will be observed to see how to apply the equation that was obtained in chapter 5 in order to design a switch to load at a certain temperature or voltage. This design work will also look into the question of the practicality of such a new device: whether is feasible, or if the current way these applications are being executed is the better alternative.

Chapter 10

Design of a Small Piezo-electrical Film Switch

In this section, the thesis going to cover one application of this newly developed technology, i.e., ways of using this piezo-film to make better switches. In this section, the researcher will present a design problem of a switch on a small scale, and evaluate how to use the given methodology to determine the appropriate size. Reasons why this problem should be looked into using this or similar technology will also be presented.

1. Sub-Small Switch for an Electronic Device

First design consideration was use of this methodology at the micro level. This is for applications with very small electronic devices currently available. The size of the plate can be several times smaller and several times thinner than what was experimented on. The piezo-electric materials can be coated in such a way that even a very thin coating is capable of being manufactured. In addition, the polymer can be very thin. One has to be sure not to go below the lower limit, thereby making a switch that cannot support itself. If there is a situation where, at rest, the external forces are greater than the internal moment, then the strip will fall into itself and never be able to support the additional temperature loading or electrical loading. Even worse, the switch would not even be able to be manufactured since these switches need to be able to hold together during the manufacturing process.

For this switch, it is assumed the limiting factor will be how much space the switch can take up. What the thesis is looking at is a small space to take the switch. It is assumed this is of microscopic proportions, and that the amount of space that we can take up is

determined by other factors such as range and thickness. Before we get into the design, we must review the background of these switches and understand why they are important.

2. Background of the Switches

Today's switches on devices are larger than they need to be. One mechanism that takes up a lot of room is the plunger operation of the actual button. The plunger is a spring that is typically made as shown here.

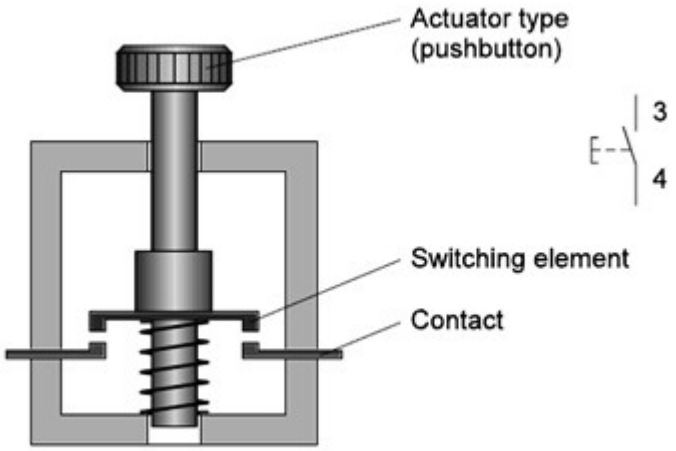

Figure 10-1: Typical push button plunger diagram. (IPEL, 2011, [37])

It can be seen that the plunger takes up the most room in the switch to make it work. This is also displayed in the photo below of the typical computer switch that is mounted to a PC. These switches are considered sub-miniature switches. The advantage of the device proposed by this thesis is that it can take the place of the switching element and can take the place of the plunger, making the switch a lot smaller than it would be with the plunger housing.

Figure 10-2: Typical small switches used for electronic technology. (3M, 2015, [36])

For this example, we are going to assume this is the power switch on a tablet that automatically turns the tablet or laptop off so it does not overheat. The beginning result is the confine of the switch; the final result is temperature range. In between, we are going to assume a thickness for the plate.

3. **Sizing of the plate diameter**

The plate diameter is going to be assumed not to be more than 2 mm or 1/16 in. This is because these devices are small that space must be considered. This particular application can go to the micro scale. Typically, a switch based on a small temperature range is not out of the ordinary. The switch would already be pre-stressed or pre-programmed to a higher temperature. One of the main things found earlier was that these switches have to be pre-molded or pre-stressed at a critical temperature.

This is important, because if the designer wanted to have an operating temperature of 200 degrees Fahrenheit but wanted the switch to kick off around 220 degrees Fahrenheit, the design temperature to pre-stress and manufacture these switches at would be 200 degrees with the switch being set off around 220. In this case, we need to know the

temperature difference we are looking for. The manufacturer would have to set the manufacturing temperature. What happens if the temperature stays below the pre-stressed temperature? Nothing will happen. The switch first would have to reach the design temperature, and then it would have to go through the range of temperature that is still considered safe. Once it reaches the unsafe temperature, it will go off.

For our purposes here, since we have most of the variables, the only variables we are looking at are the thickness and, more importantly, the deflection we are allowed. These are the two open variables that we have to move back and forth.

Thickness calculations

The thickness would have to be calculated by the equation that was found earlier by the researcher. We have to assume a size of the switch in the object. Since this has to be as small as possible, this limits the sizing. This also limits the amount that we can have the switch deflect. If we have a switch the size of a millimeter, we are allowed about ten to twenty percent for the deflection range. Any more and the switch will not flip. Any less and the switch would collapse. Therefore, we are only allowed a deflection of ten to twenty percent. We calculate the thickness in the fourth figure below.

We also had to modify the temperature range from the original 200 to 240 degrees, so instead we are operating with a 40º difference. This is necessary, because to get this to work any other way would require the disk to increase in size. Therefore:

T original – 200 degrees F

T final – 220 degrees F

This is one design for a small piezo-plate. However, one has to realize that the equation is an open form, and there is actually a range of different numbers that will work for the equation. It is known that there is a maximum allowable height for the dome due to the fact there is a difference between shallow and deep shells. In this case, the work only covers shallow shells. This is being calculated using the basic principal in chapter 5.

What was produced is a simple graph of two linear lines to show where one can get a shallow shell. This is graphed out below.

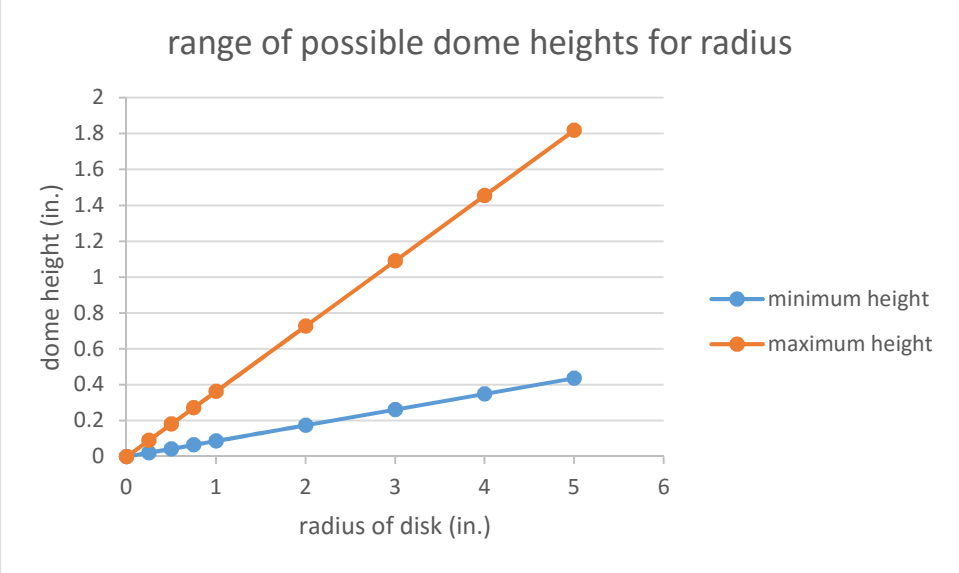

Figure 10-3: Possible shallow spherical dome heights given a radius

At this point one has to take the radius for the dome and use it to find the range of heights that can be used; in this case, it is about 1/32 in. for the radius. This is for a dome height between 0.00273 in. and 0.0114 in. The temperature ranges were found to be off, as these correspond to flip temperatures of 4464 degrees F and 5124 degrees F respectively. Therefore, the next area to look at is to make the thickness as thin as possible, remembering that there might be a point where the switch design is theoretically possible but impractical.

The next consideration was to make the thickness 10% of the original. One can change many different dimensions to get this switch to work. In this case, a decrease to 10% of the original thickness works to get the switch to work within the required space and temperature limits. This is for a dome height between 0.00273 in. and 0.0114 in. The temperature ranges were found to be off, as they correspond to flip temperatures of 5 degrees F and 20 degrees F respectively. Therefore, the highest possible dome height works for this switch. Below are the results.

Variable	value	Units	Variable name
v	0.3	dimensionless	Poisson's ratio
E_p	449616	PSI	plastic E
E_m	290075	PSI	piezo E
Ebar	392717.8813	PSI	average E
d31	23	PSI/V	dielectric constant
Va	0	V	voltage applied
Q_{11}	494083.5165	PSI	stiffness constant
W(dh)	0.001365	In	deflection (in)
a	0.005426506	In	Rsin(theta)
R	0.03125	In	radius of the disk (in)
deltaT(ω)	5	F	temperature in F
α_p	0.0000795	1/F	plastic alpha (coefficient of expansion)
α_m	0.000071	1/F	piezo alpha (coefficient of expansion)
α bar	7.64686E-05	1/F	average alpha value
t_p	0.00078125	In	plastic layer thickness
t_m	0.000433071	In	piezo layer thickness
t_t	0.001214321	in	total thickness
C	524.0500773	Constant	constant used for simplification
B	0.318182507	Constant	constant used for simplification

Figure 10-4: Input for design of a disk minimum height (small)

Variable	value	Units	Variable name
v	0.3	dimensionless	Poisson's ratio
E_p	449616	PSI	plastic E
E_m	290075	PSI	piezo E

Ebar	392717.8813	PSI	average E
d31	23	PSI/V	dielectric constant
Va	0	V	voltage applied
Q_{11}	494083.5165	PSI	stiffness constant
W(dh)	0.0057	In	deflection (in)
a	0.005426506	In	Rsin(theta)
R	0.03125	In	radius of the disk (in)
deltaT(ω)	20	F	temperature in F
α_p	0.0000795	1/F	plastic alpha (coefficient of expansion)
α_m	0.000071	1/F	piezo alpha (coefficient of expansion)
α bar	7.64686E-05	1/F	average alpha value
t_p	0.00078125	In	plastic layer thickness
t_m	0.000433071	In	piezo layer thickness
t_t	0.001214321	in	total thickness
C	524.0500773	Constant	constant used for simplification
B	0.318182507	Constant	constant used for simplification

Figure 10-5: input for design of a disk maximum height (small)

This is the design of the disk. A detailed drawing appears below.

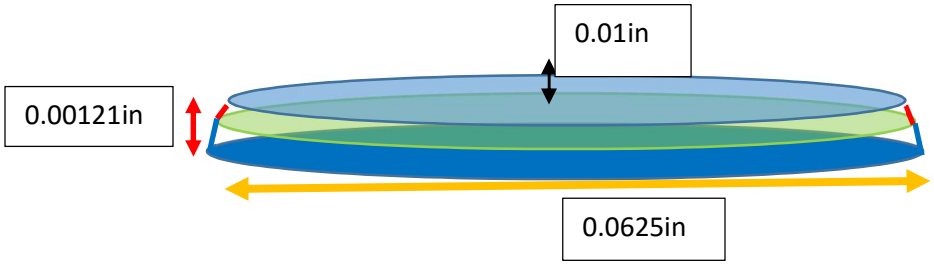

Figure 10-6: Disk to be used

Disk with cables appears below in on position

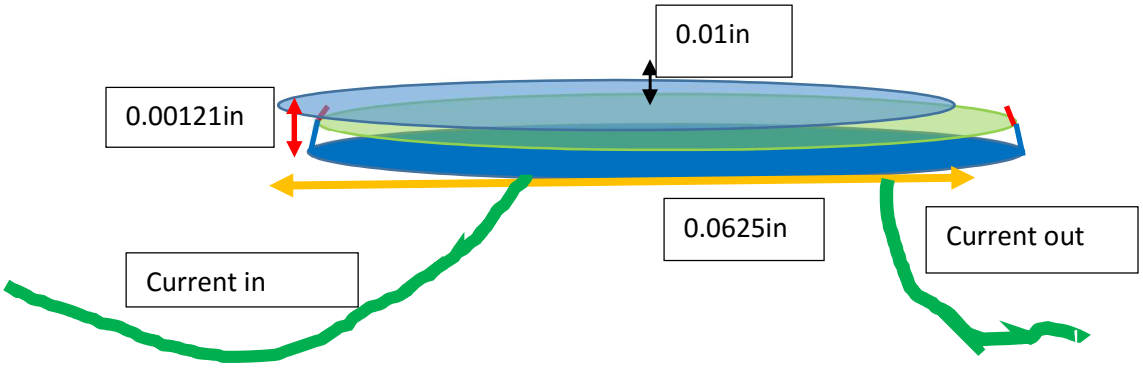

Figure 10-7: disk to be used with electric cable connected to it

Disk with cables appear below in the “on” position

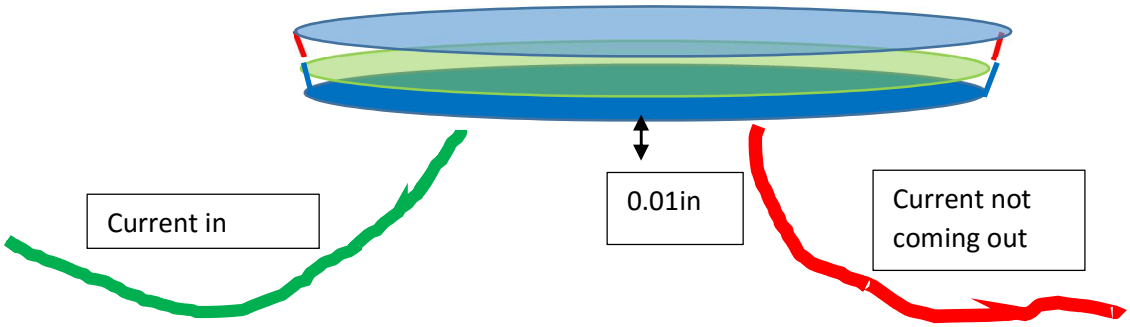

Figure 10-8: Disk to be used with electric cable connected to it (No current though, since disk was activated by overload.)

From the thickness calculation, we can get the range of temperature (or voltage we can work with). One can also size the switch based upon temperature loading needed.

The next question pertained to the cubic relationship of the line. The first thing was that the derived equation has a cubic relationship between the diameter and the depth of the dome. A simple graph of the equation taken down to the base roots of the diameter versus the dome height shows this.

Therefore the finished design of the switch is:

Diameter of disk: .078 in.

Height of dome on disk: .01 in.

Thickness of disk: .00121 in.

Thickness of plastic layer: 0.00078 in.

Thickness of piezo-layer: 0.00044 in.

T start: 200 degrees F

T end: 220 degrees F

This is one design example found for using this switch. Another design example the researcher will briefly touch upon is the design for a transformer box that is outside a residential home on the utility pole. The iterations will not be gone through in detail, but rather simplified for the reader.

Chapter 11

Design of Larger Piezo-film Switch for a Power Plant

This second design was for use at an extreme high voltage level. This would require a switch of a much greater capacity than just around 100 volts. The switch would be used in transformers for the distribution of electrical power in which levers are currently being used. For this part of the problem, the design consideration would be something of the order of KV. There is a history as to how this problem came to be, and it is still a problem for several reasons. One thing to note that this part is strictly theoretical, as the current polymer material would not be able to resist the large voltages and might melt.

Originally, switches for large electrical operations were manually operated switches similar to the "Frankenstein" type that is seen in museums. The problem with these was that an arc of electricity would form in the air if the voltages became too high.

Figure 11-1: Typical Frankenstein switch (Galco Products, [25])

A solution to these was to have the switch dipped into an oil bath and operate that way. This would also require remote operation, as with the switch is inside an oil bath you have to operate it from without. There were a few issues with this approach. First, there was the issue of obtaining an oil that would work properly and would not suddenly fail (change chemical composition). There was also an issue regarding leakage of the transformer and all the oil draining out. At that point, the transformer would be useless.

Figure 11-2: Typical transformer (photo courtesy Tectonics, [23])

The typical delivery system "for a power plant is that they use something called a CDS oil capacitor switch." (Hubbell, 2013, [23]) Such switches are designed for several

different voltages and can be used on 110V or 240V step-downs (these are the final voltages). The voltages they can handle vary widely depending on the application. The application will determine the final voltages. It was discovered later on that in order to get a power-plant type switch, other more durable and fire resistant materials would have to be looked into (higher elastic moduli and higher melting points). The application under consideration below will be for a typical 110V household switch or a circuit breaker.

This switch has a lot more options since it is not in a confined space. Some of the geometry had to be changed for this switch, as it is a higher voltage application than what is presented in this thesis.

The designer actually discovered that, when using the typical shape, there was a lot of negative energy, meaning that the switch would be too small to be used as a circuit breaker. This is obvious because if this switch were to be hit with 110 volts it would probably instantly melt due to its size. The switch the designer had to come up with would need to be much larger than the typical switch that was experimented with. Therefore, the designer had to double the thickness of the plastic layer in the switch.

The results are as follows. A switch that has a 2-inch radius is as follows. For the lowest range of height:

For a 120 V range

Variable	value	Units	Variable name
v	0.3	dimensionless	Poisson's ratio
E_p	449616	PSI	plastic E
E_m	290075	PSI	piezo E
Ebar	414993.0372	PSI	average E
d31	37.04	PSI/V	dielectric constant

Va	10	V	voltage applied
Q_{11}	494083.5165	PSI	stiffness constant
W(dh)	0.08	In	deflection (in)
a	0.347296355	In	Rsin(theta)
R	2	In	radius of the disk (in)
deltaT(ω)	0	F	temperature in F
α_p	0.0000795	1/F	plastic alpha (coefficient of expansion)
α_m	0.000071	1/F	piezo alpha (coefficient of expansion)
α bar	7.76554E-05	1/F	average alpha value
t_p	0.015625	In	plastic layer thickness
t_m	0.00433071	In	piezo layer thickness
t_t	0.01995571	in	total thickness
C	9100.528245	Constant	constant used for simplification
B	90.80375126	Constant	constant used for simplification

Figure 11-3: Input for electrical switch for low range (large)

The high range appears below

Variable	value	Units	Variable name
v	0.3	dimensionless	Poisson's ratio
E_p	449616	PSI	plastic E
E_m	290075	PSI	piezo E
Ebar	414993.0372	PSI	average E
d31	37.04	PSI/V	dielectric constant
Va	133	V	voltage applied
Q_{11}	494083.5165	PSI	stiffness constant
W(dh)	0.36	In	deflection (in)
a	0.347296355	In	Rsin(theta)
R	2	In	radius of the disk (in)
deltaT(ω)	0	F	temperature in F
α_p	0.0000795	1/F	plastic alpha (coefficient of expansion)
α_m	0.000071	1/F	piezo alpha (coefficient of expansion)
α bar	7.76554E-05	1/F	average alpha value
t_p	0.015625	In	plastic layer thickness
t_m	0.00433071	In	piezo layer thickness
t_t	0.01995571	in	total thickness
C	9100.528245	Constant	constant used for simplification
B	90.80375126	Constant	constant used for simplification

Figure 11-4: High range of voltage (Note: switch works when dome height is at a maximum.)

The resulting disk should be as in the finished design of the switch which follows.

Diameter of disk: 4 in.

Height of dome on disk- .78 in.

Thickness of disk: .02 in.

Thickness of plastic layer: 0.015625 in.

Thickness of piezo-layer: 0.00443 in.

V start 0V

V end 130V

These are the results for this disk. Making something like this would be very expensive, and it would be a non-standard part. This is just an example of what this disk can do. It is very easy to work with and to get it to work for almost any application. There is one factor behind these disks to note. The thickness of a disk has much more to do with the switch the area. However, one cannot make the disk too thick or else it will never work.

This is the design for an electrical operation. One of the key takeaways here is to study new piezo-materials that have not been found already or materials that are not currently available. A further area of research is different material properties and to

identify materials that are more heat resistant and durable. One of the other properties found with piezo-PVDFs was that they do not have the highest resistance to temperature, and instead of just melting, the plastic will deform until the original material properties are diminished or lost.

The final chapter will be the conclusion of this work and presentation of any future areas that can be studied by future researchers.

Chapter 12

Final Concluding remarks.

With the end of this thesis come the key points that were found. It was found that it is possible to have a piezo-polymeric disk act as a switch; however, one has to take a few design considerations into consideration and account for them. One has to realize that, while some problems were done using this as a design method, this is nowhere near the final work on such switches. This thesis proves that you can use piezo-electric polymers as switches using the flip-through effect, and demonstrates that you can make a switch out of a piezo-polymer. This thesis also demonstrates the limits of the piezo-polymers, and shows that the temperature that a polymer can take needs to be taken into consideration.

Experimentation Remarks

Thesis demonstrated that use of brute force is a viable option to figure out the temperature for some of the experiments. One has to be careful with brute force and make sure that the temperature of an object can be read remotely. The first thermometer for this experiment did not work, as the freezer had to be opened to read it and the results were not accurate. The second thermometer was much superior and highly accurate, as it would measure the exact temperature of the piezo-strip, the sensor being secured to the strip itself. The first thermometer used just took the temperature of the air of the freezer and not of the strip. The temperature of the strip can be very different from the temperature of the freezer.

Another lesson learned from the experimentation was that it is important to get a good experimental procedure and be ready to redo partial failures. Also research first what had gone wrong in the past with similar experiments. Just because one understands the

capabilities of experimental equipment, does not necessarily mean one knows how to apply it in an experimental setting. One also has to be able to figure out how to get the best results possible in an inexact science and be able to recreate what models show.

With regard to modeling, one has to realize exactly what one is modeling. While doing this experiment, the author found that a circular object that is pinned all around the circumference is really considered a fixed connection. This is because, unless it is for an infinitesimal length, in this case it is not the disk displays the connection as it is fixed. This is because the pinned connection one inputs gets fixed due to other adjacent segments of the circle are also acting as pins on the same plane in a different direction. These pins do not allow rotation of the pinned sections next to them since in order for the segment to rotate, adjacent segments would have to rotate around the longitudinal direction of the pin. This is physically not going to happen. As a result, a pinned connection for a disk around the entire edge is just as good as saying it is fixed. The only connection of a disk that would allow rotation is a point connection, however this is not a good connection since the representative shape is no longer a hemisphere but a 3D curved piece of plywood which would take mathematical modeling just to understand the original shape. At this point the problem is totally different than the hemisphere that was presented.

Significance of results

The results of this thesis are significant since they demonstrate that such a phenomenon does work. It also demonstrates that between the equations, COMSOL and the experiment that results were similar and followed a common trend-line in the graphs. Before there were only theoretical equations to go by and not an actual switch.

Another significant result was there was no research done with PVDH's which was an area that needed to be researched and thought out. After the discovery of a flexible material it was an area that needed attention as the researcher was examining a material with a significant deflection. With the flexible material the researcher was able to get a deflection however more deflection was desired and it showed that while it was a material that could work more deflection was needed so below is an application that could increase deflection.

Other Applications

Other applications that should be looked at with this is adding a switch on the end of a lever that will deactivate a device at the other end of the lever. With a lever device this would stretch the possibilities of this device as one would not be limited to just the deflection that can be obtained from the dome it's self but rather the deflection one could get from an entire lever moving back and forth.

Another application that one should look at is to use this switch at the microscopic scale. Everyday devices that are used get smaller and one needs switches even at the nanoscale to control these devices. One fact that was found was that these devices did not have much difference in the range of temperatures that operated this device. A developer can also look at the macroscopic scale as well and build giant switches with these however economy needs to be addressed with such a huge switch and whether or not it is cost effective given the material.

Future works

For future theses on this topic, it is suggested that future researchers go and look into developing additional polymer materials that are better heat-resistant materials. One polymer that is mentioned which has less bend but more durable is ABS plastics that LEGO blocks are made of (lego.com, [55]) Another suggestion is to look into material properties of polymer strips and investigate the design criteria that govern the material properties. In the end, focusing on the material properties first and then after approaching the sizing of the actual disk will make the design process easier.

Another area for future research is looking into other types of clamped connections. For this thesis, a monolithic non-rotational type of heavy connection was developed. This was a very rigid connection that would not allow for much flexibility of the material and might hamper the switch operation. While this is good, there is certainly room for improvement as better switches have more flexibility and a rotational edge might work better for this switch.

A third area that should be researched is fatigue life of PVDF's. While the material that was researched was very flexible even the most ductile of material have a fatigue limit where after enough of moving can cause the switch to break. A manufacturer wants to avoid material failure for as long as a warranty is valid so a fatigue life is critical to know when using this material. The type of connection used with the clamping device should be looked at as this is significant in of itself. The connection is where most fatigue occurs and some connections are more fatigue prone than others.

In the final analysis, this thesis found a new type of switch shape: a new application for a material that has existed in part for many years. Future researchers should follow the methodology of this thesis, but try to develop better materials. There are always new areas

of civil engineering that should be looked at with an eye to developing new materials. Even when one knows all the analytics, it is impossible to be completely sure that the materials utilized are optimal, because there is always a new material to be discovered and researched with.

Finis

Appendix A

Data sheets on PVDF's From Technical Manual Supplied by Manufacturer

(Note this manual is unpublished, for an updated manual write to the address on the next page)

measurement SPECIALTIES

Piezo Film Sensors

Technical Manual

Measurement Specialties, Inc.
1000 Lucas Way
Hampton, VA 23666
Tel: 757.1500
Fax: 757.766.4297
www.meas-spec.com
e-mail: piezo@meas-spec.com

P/N 1005663-1 REV E 25 March 2008

Table 1. Typical properties of piezo film

Symbol	Parameter		PVDF	Units
t	Thickness		9, 28, 52, 110	µm (micron, 10^{-6})
d_{31}	Piezo Strain Constant		23	10^{-12} $\frac{m/m}{V/m}$ or $\frac{C/m^2}{N/m^2}$
d_{33}			-33	
g_{31}	Piezo Stress constant		216	10^{-3} $\frac{V/m}{N/m^2}$ or $\frac{m/m}{C/m^2}$
g_{33}			-330	
k_{31}	Electromechanical Coupling Factor		12%	
k_t			14%	
C	Capacitance		380 for 28µm	pF/cm^2, @ 1KHz
Y	Young's Modulus		2-4	10^9 N/m^2
V_0	Speed of Sound	stretch:	1.5	10^3 m/s
		thickness:	2.2	
p	Pyroelectric Coefficient		30	10^{-6} C/m^2 °K
ε	Permittivity		106-113	10^{-12} F/m
$\varepsilon/\varepsilon_0$	Relative Permittivity		12-13	
ρ_m	Mass Density		1.78	10^3kg/m
ρ_e	Volume Resistivity		>10^{13}	Ohm meters
$R_\square$	Surface Metallization Resistivity		<3.0	Ohms/square for NiCu
$R_\square$			0.1	Ohms/square for Ag Ink
tan δ_e	Loss Tangent		0.02	@ 1KHz
	Yield Strength		45-55	10^6 N/m^2 (stretch axis)
	Temperature Range		-40 to 80...100	°C
	Water Absorption		<0.02	% H_2O
	Maximum Operating Voltage		750 (30)	V/mil(V/µm), DC, @ 25°C
	Breakdown Voltage		2000 (80)	V/mil(V/µm), DC, @ 25°C

Table 2. Comparison of piezoelectric materials

Property	Units	PVDF Film	PZT	$BaTi0_3$
Density	10^3kg/m3	1.78	7.5	5.7
Relative Permittivity	$\varepsilon/\varepsilon_0$	12	1,200	1,700
d_{31} Constant	(10^{-12})C/N	23	110	78
g_{31} Constant	(10^{-3})Vm/N	216	10	5
k_{31} Constant	% at 1 KHz	12	30	21
Acoustic Impedance	(10^6)kg/m^2-sec.	2.7	30	30

OPERATING PROPERTIES FOR A TYPICAL PIEZO FILM ELEMENT

The DT1 element is a standard piezo film configuration consisting of a 12x30 mm active area printed with silver ink electrodes on both surfaces of a 15x40 mm die-cut piezo polymer substrate.

1. **Electro-Mechanical Conversion**
   (1 direction) 23 x 10^{-12}m/V, 700 x 10^{-6}N/V
   (3 direction) -33 x 10^{-12}m/V

2. **Mechano-Electrical Conversion**
   (1 direction) 12 x 10^{-3}V per microstrain, 400 x 10^{-3}V/µm, 14.4V/N
   (3 direction) 13 x 10^{-3}V/N

3. **Pyro-Electrical Conversion**
   8V/°K (@ 25°C)

4. **Capacitance**
   1.36 x 10^{-9}F; Dissipation Factor of 0.018 @ 10 KHz; Impedance of 12 KΩ @ 10 KHz

5. **Maximum Operating Voltage**
   DC: 280 V (yields 7 µm displacement in 1 direction)
   AC: 840 V (yields 21 µm displacement in 1 direction)

6. **Maximum Applied Force (at break, 1 direction)**
   6-9 kgF (yields voltage output of 830 to 1275 V)

Bibliography

1. Betts, Johnathan. “John Harrison English Super Genius.” *Rob Ossian’s Pirate Cove*. Rob Ossian, Nov. 2012. Web. Oct. 2014.
2. Bewoor, Anand K. *Metrology & Measurement*. New York: McGraw-Hill, 2009. 497. Print.
3. Boroujerdy, M.S., and M. R.Eslami. “Nonlinear Axisymmetric Thermomechanical Response of Piezo-FGM Shallow Spherical Shells.” *Archive of Applied Mechanics* 83.12 (Dec. 2013): 1681-1693. Print
4. Karlsson, Anette M., and W. J. Bottega. “Thermo-Mechanical Response of Patched Plates.” *AIAA Journal* 38.6 (2000): 1055–1062. Print.
5. Rutgerson, S. E., and W. J. Bottega. “Thermo-elastic Buckling of Layered Shell Segments.” *International Journal of Solid Structures* 39 (2002): 4867-4887. Print.
6. Boroujerdy, M. S. “Nonlinear Thermochemical Response of Piezo-FGM Shallow Spherical Shells.” *Applied Mechanics* 83 (2013): 1681-1693. Print.
7. Boroujerdy, M. S. “Axisymmetric Snap-through Behavior of Piezo-FGM Spherical Shells under Thermo-electro-mechanical Loading.” *International Journal of Pressure Vessels and Piping* 19.26 (2014): 120-121. Print.
8. Xu, S., and W. Wang. “Response of a Piezo-electric Plate with Circular Hole.” *Acta Mechanica* 203: 3-4 (Mar. 2009). 127-135. Print.
9. X. Wang. “Non-linear buckling for the Surface Rectangular Delamination of Laminated Piezo-electric Shells.” *Applied Mathematical Modeling* 38.1 (Jan. 2014). 374-383. Print.
10. Allen-Bradley Products. “Piezoelectric Push Buttons.” Rockwell Automation. Web. March 2015. http://ab.rockwellautomation.com/Push-Buttons/Specialty/800K-Piezo-electric-Push-Buttons
11. APC International, Ltd. “Piezo Actuators: Types and Applications.” *American Piezo*. APC International, Ltd. Web. Mar. 2015. https://www.americanpiezo.com/piezo-theory/actuators.html
12. Roberts, Alice. “A True Sea Shanty: The Story behind the Longitude Prize.” *The Guardian* 17 May 2014. Print.
13. Daniels, E. M. “Rochelle Salt.” *Instructables*. Autodesk. Web. Oct. 2015. http://www.instructables.com/id/Rochelle-Salt/ Indestructables
14. Anonymous. “Marie Curie and the Science of Radioactivity.” *American Institute of Physics*. Web. May 2015.
15. Anonymous (staff engineers). “Common Shapes & Sizes of Piezoelectric Elements.” *American Piezo.* APC International, Ltd. Web. May 2015

https://www.americanpiezo.com/product-service/custom-piezo-electric-elements/shapes-sizes.html

16. Anonymous (staff engineers) under direction of Nathan Seidle. “Piezo Element.” *Sparkfun*. Sparkfun Electronics. Web. June 2015. https://www.sparkfun.com/products/10293

17. Anonymous (staff engineers). “Piezo Film Sensors.” *Measurement Specialties*. TE Connectivity Ltd. Web. May 2015

18. Anonymous. “March 1880: The Curie Brothers Discover Piezo-electricity.” APS News 23.3 (Mar. 2014). Web. Mar. 2015.

19. Lam, Jack. “Piezo-electricity.” *Chemwiki, The Dynamic Chemistry Book.* UC Davis, 2015. Web.

20. Anonymous (staff engineers). (Company out of business and URL down) http://product.tdk.com/en/techjournal/tfl/sensor_actuator/TSTSP/index.html

21. Timoshenko, Stephen P. “Theory of Bending, Torsion and Buckling of Thin-walled Members of Open Cross Section.” *Journal of the Franklin Institute* 239.5 (May 1945): 343-361. Print.

22. Anonymous (staff engineers). “PAS009 - Piezoelectric Actuator, 40 µm Travel.” *Thorlabs*. Thorlabs. 1999 to 2015. Web. Mar. 2015. https://www.thorlabs.com/thorproduct.cfm?partnumber=PAS009&gclid=CJKWrd7E8cQCFUk8gQodkZ0Aig

23. Anonymous (staff engineers). “CSD Oil Switches.” *Trinetics*. Hubbell Incorporated. Web. Mar. 2013. http://www.trinetics.com/products/capacitor-switches/capacitor-switches/oil

24. Anonymous. “Oil Switches are Single Phase Motor Operated.” *T and D World Magazine* 17 Apr. 2012. Print.

25. Anonymous (staff engineers). “The Building Blocks of Contactors.” *Galco.com*. Galco Industrial Electronics, Inc. Web. July 2015. http://www.galco.com/comp/prod/cont.htm

26. Anonymous (staff Engineers). “CSD Oil Switches.” *Trinetics*. Hubbell Incorporated. Web. Mar. 2015. http://www.trinetics.com/products/capacitor-switches/capacitor-switches/oil

27. Lin, Xiujuan, et al. “Fabrication, Characterization, And Modeling Of Piezo-electric Fiber Composites.” *Journal Of Applied Physics* 114.2 (2013). Print.

28. Myer, Kutz. “Piezo-electric Materials.” *Mechanical Engineers Handbook*. John Wiley & Sons. 2015. Volume 1. 2. 441. Print.

29. The Editors of Encyclopedia Britannica; “The Curie Point.” *Encyclopedia Brittanica Online.* Encyclopedia Brittanica, Inc. Web. 2014.

30. Anonymous. "Polyvinylidene Fluoride (PVDF)." *PlasticsEurope*. The Association of Plastics Manufacturers. Web. March 2015. http://www.plasticseurope.org/what-is-plastic/types-of-plastics-11148/engineering-plastics/pvdf.aspx

31. Neugschwandtner, G. S., et al. "Large Piezo-electric Effects In Charged, Heterogeneous Fluoropolymer Electrets." *Applied Physics A: Materials Science & Processing* 70.1 (2000). Print.

32. Fukada, Eiichi, and Iwao Yasuda. "On the Piezo-electric Effect of Bone." *Journal of the Physical Society of Japan* 12. (1957). Print.

33. Scheufler, C., Sebald, W., and M. Hülsmeyer. "Crystal Structure of Human Bone Morphogenetic Protein-2 at 2.7 A Resolution." *Journal of Molecular Biology* 287.1 (Mar. 1999): 103-115. Print.

34. Davies, E., Duer, M.J., Ashbrook, S.E., and J.M. Griffin. "Applications of NMR Crystallography to Problems in Biomineralization: Refinement of the Crystal Structure and 31P Solid-state NMR Spectral Assignment of Octacalcium Phosphate." *Journal of the American Chemical Society* 134 (2012): 12508. Print.

35. Brown, Harris. "Introduction to the Special Issue on the 30th Anniversary of the Discovery of Piezo-electric PVDF." *IEEE Transactions on Ultrasonics, Ferroelectrics, and Frequency Control* 47. 6 (Nov. 2000): 2-3. Print.

36. Staff Engineers. "3M Series Mini Push Button Switches.", *Carling Technologies*, Maretron. 2012. Web. Oct. 2015. https://www.carlingtech.com/mini-pushbutton-switches-3m-series

37. Sen, Kusal. "Module 3 : Electropneumatics." www.*nptel*.ac.in. NPtel. 2011. Web. Oct. 2015. http://nptel.ac.in/courses/112102011/electropenumatics/electropneumatics.html,

38. Scott, Chris E. "Poly(vinylidene) Fluoride." *PolymerProcessing*.com. PolymerProcessing.com. June 2001. Web. Oct. 2015. http://polymerprocessing.com/polymers/PVDF.html

39. GR8surplus. "KUHLMAN ABB HIGH VOLTAGE 7.2KV 11.4KV SINGLE PHASE POLE TRANSFORMER 15KVA NOS." *ebay.com*. eBay Inc. 1995-2016. Web. Nov. 2015. http://www.ebay.com/itm/KUHLMAN-ABB-HIGH-VOLTAGE-7-2KV-11-4KV-SINGLE-PHASE-POLE-TRANSFORMER-15KVA-NOS-/221757101581

40. Gere, James. "Axially Loaded Members." *Mechanics of Materials, 5th ed*. Pacific Grove CA: Brooks Cole, 2001. 94. Print.

41. Bedford, Anthony. "Objects in Equilibrium." *Engineering Mechanics. 3rd ed.* Upper Saddle River, NJ: Prentice Hall, 2002. 202. Print.

42. Gere, James. "Axially Loaded Members." *Mechanics of Materials, 5th ed*. Pacific Grove CA: Brooks Cole, 2001. 78. Print.

43. Serway, Raymond. “Work.” *College Physics 10th ed.* Stamford CT: Cengage Learning, 2015. 128. Print.

44. Angle, Brandon et al. “Springs”. *www.personal.psu.edu*. Penn State University. Web. Nov. 2015. http://www.personal.psu.edu/bra5060/Springs.html

45. Marino, A. A. et al. “Piezo-electricity in Cementum, Dentine and Bone.” *Archive of Oral Biology* 34.7 (1989). 507-509. Print.

46. Colwell, Catherine. “Conservation of Energy and Springs.” *Physics lab online*. Learning Xchange. 1987 to 2015. Web. http://dev.physicslab.org/document.aspx?doctype=3&filename=oscillatorymotion_springs.xml;

47. Gavin, Henri. “Strain Energy in Linear Elastic Solids.” *people.duke.edu*. Duke University. Mar. 2015. Web. http://people.duke.edu/~hpgavin/cee201/strain-energy.pdf;

48. Steward, James. “Work Equation!” *Calculus Early Transcendental 5th ed.* New York: Brooks Cole, 2002. 987. Print.

49. Gere, James. “Axially Loaded Members.” *Mechanics of Materials, 5th ed*. Pacific Grove CA: Brooks Cole, 2001. 663. Print.

50. Anonymous. “Hair Spring, Balance Spring.” *WatchTime*. Ebner Publishing International, Inc. Web. Mar. 2015. http://www.watchtime.com/reference-center/glossary/hairspring-balance-spring/

51. Author link unavailable. “Centroids of Common Shapes.” *Engineer.com*. October 20, 2006. Web.

52. Sanders, Lyell. “Nonlinear Theories for Thin Shells.” *Office of Naval Research*, *Technical Report No. 10.* Cambridge, Massachusetts: Division of Applied Physics, Harvard University. 1961

53. Reissner, E. “On the Equations of Linear Shallow Shell Theory.” Cambridge, Massachusetts: Massachusetts Institute of Technology, 1968.

54. Ventsel, E. and T. Krauthammer. “Thin Plates and Shells Theory Analysis and Applications.” New York: Marcel Dekker, 2001.

55. Anonymous; About our bricks; *Lego.com about us*; Lego.com; July 15, 2015; Web.

56. Anonymous (staff engineers); “Piezo Film Sensors”; Technical manual; Measurement Specialties, Inc.; March 2008; (unpublished)